

Durham E-Theses

Stability Studies of Porous Media Including Surface Reactions

NICOLA LOUISE SCOTT

How to cite:

SCOTT, NICOLA LOUISE (2013) *Stability Studies of Porous Media Including Surface Reactions*.
Doctoral thesis, Durham University.

Use policy

The full-text may be used and/or reproduced, and given to third parties in any format or medium, without prior permission or charge, for personal research or study, educational, or not-for-profit purposes provided that:

- a full bibliographic reference is made to the original source
- a <https://etheses.durham.ac.uk/id/eprint/9421/> is made to the metadata record in Durham E-Theses
- the full-text is not changed in any way

The full-text must not be sold in any format or medium without the formal permission of the copyright holders.

Please consult the [full Durham E-Theses policy](#) for further details.

Stability Studies of Porous Media Including Surface Reactions

Nicola Scott

A Thesis presented for the degree of
Doctor of Philosophy



Numerical Analysis
Department of Mathematical Sciences
University of Durham
England

November 2013

Dedicated to

Mum, Dad, Michael and Matthew.

Stability Studies of Porous Media Including Surface Reactions

Nicola Scott

Submitted for the degree of Doctor of Philosophy

November 2013

Abstract

We investigate the onset of thermal convection in a number of porous models, with a focus on the influence of a boundary reaction. The models that we consider are: the Darcy porous model; the Darcy model with inclusion of the Soret effect and the Brinkman model, all with an exothermic surface reaction on the lower boundary. Numerical results are presented for each of these models and we show that the Darcy and Brinkman models with a surface reaction are structurally stable. Finally we derive stability results for a vertical porous channel that is in thermal non-equilibrium.

In Chapter 2 we investigate how the parameters of an exothermic reaction on the lower boundary of a horizontal Darcy porous layer affect the linear instability boundary. We show that for low Lewis numbers stationary convection is dominant and for larger Lewis number oscillatory convection dominates. We use a non-linear analysis to find stability boundaries for this model in Chapter 3, showing how some of the reaction parameters affect this boundary. It is shown that the two boundaries do not coincide and there is a region in which sub-critical instabilities may occur. Structural stability on the reaction parameters is established for this model in Chapter 4.

The impact of including the Soret effect on the stability of the Darcy model with a surface reaction on the lower boundary is considered in Chapter 5. When stationary convection dominates we find that increasing the Soret effect increases the critical Rayleigh number that defines the instability boundary.

Chapter 6 discusses instabilities in a highly porous layer with an exothermic surface reaction on the lower boundary. The Brinkman model is used to take into account the impact of higher level derivatives of the fluid velocity. We show that this model is structurally stable on the parameters of the reaction in Chapter 7.

Finally, in Chapter 8 we analytically derive two stability results for a vertical porous channel in thermal non-equilibrium. The first is that the model is stable for any initial data provided the Rayleigh number is below a given threshold. The second is that there is stability for any Rayleigh number given restrictions on the initial data.

Declaration

The work in this thesis is based on research carried out at the University of Durham, the Department of Mathematical Sciences, the Numerical Analysis Group, England. No part of this thesis has been submitted elsewhere for any other degree or qualification and it all my own work with the exceptions of Chapters 2, 7 and 8, which contain work published in collaboration with Prof. B. Straughan in [98], [100] and [99], respectively. Chapters 3, 4, 5 and 6 contain work published in [97], [96], [95] and [94], respectively.

Copyright © 2013 Nicola L. Scott.

“The copyright of this thesis rests with the author. No quotations from it should be published without the author’s prior written consent and information derived from it should be acknowledged”.

Acknowledgements

My thanks go to my supervisor Prof. B. Straughan for the support and encouragement I have received.

Thank you to my friends, family and Matthew who have put up with me stressing over the last three years.

I would also like to acknowledge EPSRC for providing financial support for my studies and thank Imran M for preparing the LaTeX template used for this thesis.

Contents

Abstract	iii
Declaration	v
Acknowledgements	vi
1 Introduction	1
1.1 Notation and commonly used inequalities	1
1.2 The Bénard problem	2
1.3 The averaged temperature equation	5
1.4 Overview	6
2 Instability boundaries for the Darcy model with an exothermic boundary reaction	8
2.1 Basic equations	9
2.2 Steady state and perturbation equations	10
2.2.1 Perturbation equations	13
2.2.2 Perturbed boundary conditions	14
2.3 D^2 Chebyshev-tau method	15
2.4 Results	19
3 Non-linear stability bound for the Darcy problem	23
3.1 Non-linear perturbation equations	24
3.2 The energy method	25
3.3 Euler-Lagrange equations	27
3.4 Numerical method and results	29

4	Continuous dependence of the Darcy model on the reaction parameters	34
4.1	The boundary-initial value problem	35
4.2	<i>A priori</i> estimates	36
4.2.1	C bound	37
4.2.2	$\ T\ _4$ bound	37
4.2.3	$\ \mathbf{v}\ ^2$ bound	39
4.2.4	$\ \nabla\mathbf{v}\ ^2$ bound	39
4.3	Continuous dependence on the boundary reaction terms	42
5	Influence of the Soret effect on instability boundaries for the Darcy model	48
5.1	Non-dimensional linear perturbation equations	50
5.2	Numerical results and conclusions	53
6	Instability boundaries for a highly porous medium with an exothermic boundary reaction	60
6.1	Basic equations	61
6.2	Steady state and non-dimensional perturbation equations	63
6.3	Numerical results and conclusions	66
7	Continuous dependence of the Brinkman model on the reaction parameters	74
7.1	The boundary-initial value problem	74
7.2	Continuous dependence on the boundary reaction terms	76
8	Non-linear stability results for a vertical porous channel with thermal non-equilibrium	80
8.1	Basic problem	82
8.2	Non-linear energy stability; L^2 analysis	84
8.3	Non-linear stability for all Rayleigh numbers	86
8.3.1	Physical value for α	90

Contents	ix
9 Conclusions	91
9.1 Further work	93
Bibliography	94
Appendix	106
A Chebyshev-tau numerical method	106
A.1 Chebyshev polynomials	106
A.1.1 Orthogonality of the Chebyshev polynomials	107
A.2 Chebyshev boundary identities	108
A.3 The Chebyshev differentiation matrices	109
A.3.1 First differentiation matrix	110
A.3.2 Second differentiation matrix	113
A.4 Approximation of functions	114
A.5 Application of the Chebyshev-tau method to a simple system	115
B Derivation of no-slip and stress-free boundary conditions	118
B.1 No-slip boundary	119
B.2 Stress-free boundary	119

List of Figures

2.1	Variation of the instability boundary with A , for $B = 1$, $\xi = 0$, $M\phi = 1$.	21
2.2	Variation of the instability boundary with B , for $A = 0.5$, $\xi = 0$, $M\phi = 1$.	21
2.3	Variation of the instability boundary with ξ , for $A = 0.5$, $B = 0.5$, $M\phi = 1$.	22
2.4	Variation of the instability boundary with $M\phi$, for $A = 0.5$, $B = 0.5$, $\xi = 0$.	22
3.1	Linear instability (R_c) and non-linear energy stability (R_s) curves, for $A = 0.5$, $B = 0.5$.	32
3.2	Linear instability (R_c) and non-linear energy stability (R_s) curves, for $A = 0.5$, $B = 1$.	32
3.3	Linear instability (R_c) and non-linear energy stability (R_s) curves, for $A = 1$, $B = 1$.	33
5.1	Variation of the critical Rayleigh number with the Lewis number for $A = 1$, $B = 1$, $H = 1$, $\xi = 0.5$, $M\phi = 1$.	56
5.2	Variation of the critical Rayleigh number with the Soret coefficient for $A = 1$, $B = 1$, $\xi = 0.5$, $M\phi = 1$.	56
5.3	Normalised Θ eigenfunction for $A = 1$, $B = 1$, $H = 1$, $\xi = 0.5$, $Le = 0.5$, $M\phi = 1$.	58
5.4	Normalised Φ eigenfunction for $A = 1$, $B = 1$, $H = 1$, $Le = 0.5$, $\xi = 0.5$, $M\phi = 1$.	59
6.1	Variation of R_c with A , for $B = 1$, $Br = 0.5$, $\xi = 0$ and $M\phi = 1$.	67

6.2	Variation of R_c with B , for $A = 1$, $Br = 0.5$, $\xi = 0$ and $M\phi = 1$	69
6.3	Variation of R_c with ξ , for $A = 1$, $B = 1$, $Br = 0.5$ and $M\phi = 1$	69
6.4	Variation of R_c with Br , for $A = 1$, $B = 1$, $\xi = 0$ and $M\phi = 1$	70
6.5	Variation of R_c with $M\phi$, for $A = 1$, $B = 1$, $Br = 0.5$ and $\xi = 0$	70
8.1	Diagram of a vertical porous channel in thermal non-equilibrium and differentially heated on the horizontal walls.	82

List of Tables

2.1	Values of the gradients of the temperature and salt fields, β_1 and β_3 , for given reaction parameters A , B and ξ	12
2.2	Values of R_c , k_c and $\text{Im}(\sigma_1)$	20
3.1	For $A = 0.5$, $B = 0.5$, values of μ , λ , k for which the non-linear stability curve is optimised and the corresponding values of R_s . The linear instability boundary R_c is given for comparison.	31
5.1	Values of β_1 and β_3 for given reaction parameters A , B , and ξ and a Soret boundary parameter H	53
5.2	Values of R_c , k_c and $\text{Im}(\sigma_1)$ for various values of Le and S , for $A = 1$, $B = 1$, $H = 1$, $\xi = 0.5$, $M\phi = 1$	54
5.3	Values of R_c , k_c and $\text{Im}(\sigma_1)$ for various values of Le and S , for $A = 1$, $B = 1$, $\xi = 0.5$, $M\phi = 1$	55
6.1	Values of β_1 and β_3 for specified A , B and ξ	66
6.2	Values of R_c , k_c and $\text{Im}(\sigma_1)$ for varying values of Le , A , B , ξ , Br and $M\phi$	68
6.3	Values of R_c , k_c and $\text{Im}(\sigma_1)$ as $A \rightarrow 0$, for $B = 0.5$, $Br = 0.5$, $\xi = 0$, $M\phi = 1$	71
6.4	Values of R_c , k_c and $\text{Im}(\sigma_1)$ as $Br \rightarrow 0$, for $A = 0.5$, $B = 0.5$, $\xi = 0$, $M\phi = 1$	73

Chapter 1

Introduction

This thesis investigates thermal convection in porous media and in particular considers the effect of surface reactions on the stability of a horizontal layer using both the Darcy and Brinkman models for describing the evolutionary behaviour of the fluid in a saturated body. We later consider a vertical channel in which the solid and fluid may take different temperatures and derive conditions on the Rayleigh number or initial disturbances to guarantee stability.

It is well known that heating a fluid or a gas in a saturated porous medium causes it to be less dense. This means that if a horizontal layer is heated on the upper boundary then it will naturally remain stable. However, if heating occurs on the lower boundary and is sufficient to overcome the gravitational force acting vertically downwards then the system will be unstable. Any disturbance from the steady state will result in convective motion that forms periodic cells covering the horizontal plane. Examples of the shape of these cells include hexagons and two-dimensional rolls (Christopherson [17], Chandrasekhar [14]).

1.1 Notation and commonly used inequalities

Throughout this work we will use standard indicial notation and the Einstein summation convention is used for repeated indices, where Roman indices run from 1 to 3 and a comma represents differentiation. Standard vector and tensor notation is

also used, for example, the divergence of the velocity field, \mathbf{v} , is given by

$$\operatorname{div} \mathbf{v} \equiv v_{i,i} \equiv \frac{\partial v_i}{\partial x_i} \equiv \sum_{i=3}^3 \frac{\partial v_i}{\partial x_i}.$$

The Laplace operator is denoted by Δ and is defined to act on a general function ψ by

$$\Delta\psi = \psi_{,ii} = \frac{\partial^2 \psi}{\partial x^2} + \frac{\partial^2 \psi}{\partial y^2} + \frac{\partial^2 \psi}{\partial z^2}.$$

In addition to this, in Chapters 2, 5 and 6 we use the horizontal Laplace operator, Δ^* , where

$$\Delta^* \psi = \Delta\psi - \psi_{,33} = \frac{\partial^2 \psi}{\partial x^2} + \frac{\partial^2 \psi}{\partial y^2},$$

and define a new operator D by $D = d/dz$.

The standard L^2 norm and inner product are denoted by $\|\cdot\|$ and (\cdot, \cdot) , respectively, with

$$\|f\|^2 = \int_V f^2 dV \quad \text{and} \quad (f, g) = \int_V fg dV$$

where f and g are functions and V is a general periodic cell. It is sometimes necessary for us to use the more general L^p norm, for $1 < p < \infty$ where we then have

$$\|f\|_p = \left(\int_V |f|^p dV \right)^{1/p}.$$

We often refer to the arithmetic-geometric and Cauchy-Schwarz inequalities, these are given by

$$fg \leq \frac{1}{2\lambda} f^2 + \frac{\lambda}{2} g^2,$$

where $\lambda > 0$, and

$$(f, g) \leq \|f\| \|g\|,$$

respectively.

1.2 The Bénard problem

We will now use the standard Bénard problem for a Darcy porous medium to demonstrate the methods used to find stability and instability boundaries. The equations

for a horizontal layer of depth h of a Darcy porous medium, saturated by an incompressible fluid and with a gravitational force of strength g acting vertically downwards are

$$\begin{aligned} p_{,i} &= -\frac{\mu}{K}v_i - \rho_0g(1 - \alpha(T - T_0))k_i, \\ v_{i,i} &= 0, \\ T_{,t} + v_iT_{,i} &= \kappa\Delta T, \end{aligned} \tag{1.1}$$

where $\mathbf{k} = (0, 0, 1)$, $\mathbf{v} = (u, v, w)$ and the coordinate system is chosen so that the indexes 1, 2, 3 represent the x, y, z directions respectively. The boundary conditions are

$$\begin{aligned} w &= 0, \quad T = T_U \quad \text{on} \quad z = h, \\ w &= 0, \quad T = T_L \quad \text{on} \quad z = 0, \end{aligned} \tag{1.2}$$

see for example Chapter 4 of Straughan [107]. The variables \mathbf{v} , T and p are the velocity, temperature and pressure, μ and K are the dynamic viscosity and permeability, κ is the thermal diffusivity and ρ_0 is the density of the saturating fluid at the reference temperature T_0 . The parameters T_U and T_L are constants with $T_L > T_U$.

As the temperature gradient acts vertically we consider T to be dependent on z only and consider a steady state (\bar{v}_i, \bar{T}) of (1.1). From (1.1)₃ we find that \bar{T} is a linear function of z and by evaluating the steady state on the boundaries using (1.2) we see that

$$\bar{v}_i = 0, \quad \bar{T} = -\left(\frac{T_U - T_L}{h}\right)z + T_L,$$

where \bar{p} arises from solving (1.1)₁, i.e.

$$\frac{d\bar{p}}{dz} = -\rho_0g(1 - \alpha(\bar{T} - T_0)),$$

but is here not given explicitly as it is not required for the following analysis. To this steady state we now introduce small perturbations u_i , θ and π in the form

$$v_i = \bar{v}_i + u_i, \quad T = \bar{T} + \theta, \quad p = \bar{p} + \pi.$$

After also introducing the non-dimensionalisations

$$t = t^* \frac{h^2}{\kappa}, \quad u_i = u_i^* \frac{\kappa}{h}, \quad x_i = x_i^* h, \quad T = T^* \sqrt{\frac{\kappa\mu(T_L - T_U)}{g\rho_0\alpha Kh}}, \quad p = p^* \frac{\mu\kappa}{k}$$

equations (1.1) become, on dropping the asterisks,

$$\begin{aligned} 0 &= \pi_{,i} - u_i + R\theta k_i, \\ u_{i,i} &= 0, \\ \theta_{,t} + u_i\theta_{,i} &= R w + \Delta\theta, \end{aligned} \tag{1.3}$$

where $w = u_3$ and the Rayleigh number Ra is defined by $Ra(= R^2) = hg\rho_0\alpha K(T_L - T_U)/\mu\kappa$. The boundary conditions (1.2) yield for the perturbations

$$w = 0, \quad \theta = 0 \quad \text{on } z = 0, 1.$$

To find instability boundaries we linearise (1.3) by neglecting the $u_i\theta_{,i}$ term. We then rewrite the variables in the form $u_i = u_i(\mathbf{x})e^{\sigma t}$ with similar expressions for θ and π and where σ is a general eigenvalue to obtain

$$\begin{aligned} 0 &= \pi_{,i} - u_i + R\theta k_i, \\ u_{i,i} &= 0, \\ \sigma\theta &= R w + \Delta\theta. \end{aligned} \tag{1.4}$$

In general $\sigma = \sigma_R + i\eta$ and if $\sigma_R > 0$ then a perturbation of any initial size will grow and the system is unstable. The instability boundary therefore occurs when $\sigma_R = 0$. If we multiply (1.4)₁ by u_i^* and (1.4)₃ by θ^* , where $*$ represents the complex conjugate, integrate over a periodic convection cell V in which $0 < z < 1$ and the solution is periodic in x and y , and add the results we find that

$$\sigma\|\theta\|^2 = R[(w, \theta^*) + (w^*, \theta)] - \|\mathbf{u}\|^2 - \|\nabla\theta\|^2, \tag{1.5}$$

Straughan [107], Chapter 4, where $(f, g) = \int_V fg dx$, $\|\theta\|^2 = \int_V \theta\theta^* dx$ and $\|\mathbf{u}\|^2 = \int_V u_i u_i^* dx$. By considering the imaginary part of (1.5) we find that $\eta = 0$ and the eigenvalue must be real, we may therefore set $\sigma = 0$ in (1.4) to find the instability boundary. In such cases we say that exchange of stability holds.

Next we remove the pressure term in (1.4)₃ by taking the *curl* twice, where for a function ψ the i^{th} component of the *curl* is defined by $[\nabla \times \psi]_i = \epsilon_{ijk}\partial_j\psi_k$, where ϵ_{ijk} is the 3 dimensional Levi-Civita function, and retain only the third component ($i = 3$) to obtain an equation for w . From this we find that

$$\begin{aligned} 0 &= \Delta w - R\Delta^*\theta, \\ \sigma\theta &= R w + \Delta\theta, \end{aligned} \tag{1.6}$$

where Δ^* is the horizontal Laplacian. As the convection cells must cover the whole horizontal plane the solution is now assumed to be of the form $w = W(z)f(x, y)$, $\theta = \Theta(z)f(x, y)$, where $f(x, y)$ is a periodic function of the form $f(x, y) = \exp[i(px + ry)]$ that tiles the plane and $\Delta^* f = -(p^2 + r^2)f = -k^2 f$ for a wave number k .

It is now possible to eliminate θ from (1.6) and obtain

$$(D^2 - k^2)^2 W = R^2 k^2 W, \quad (1.7)$$

where $D = d/dz$. Finally we consider the boundary conditions and notice that they may be solved by the function $W = \sin(n\pi z)$. Inserting this into (1.7) we find that

$$(n^2\pi^2 - k^2)^2 \sin(n\pi z) = R^2 k^2 \sin(n\pi z),$$

and after rearranging in terms of R^2 that

$$R^2 = \frac{(n^2\pi^2 + k^2)^2}{k^2}.$$

The solution will be unstable if any of the eigenvalue modes has $\sigma_R > 0$ and so to find the value of R for which instability first occurs we must minimise over n and k . This minimum occurs for $n = 1$, $k = \pi$ and we define the corresponding minimum value of R by R_c so that $R_c^2 = 4\pi^2$.

Below this value of R this linear method does not provide any information about the stability of the system. In order to show that there is a region of stability we must use a non-linear technique. Straughan [107] uses a non-linear energy method to show that the Euler-Lagrange equations for (1.1) are the same as (1.4). This means that the stability and instability boundaries for this problem coincide and there is stability for $R < 4\pi^2$, but instability for $R > 4\pi^2$. For many models of thermal convection this is not the case and the two boundaries do not coincide, in Chapter 3 we find that this is the case for a Darcy porous medium with an exothermic reaction on the lower boundary and provide references to other examples.

1.3 The averaged temperature equation

It is possible for the solid and fluid components of a porous medium to locally be at different temperatures, termed local thermal non-equilibrium, and we consider this

to be the case in Chapter 8. However, in much of this thesis we will use an averaged temperature equation obtained from the separate fluid and solid temperature equations as follows.

In order to average the temperature of the porous medium at a given point, \mathbf{x} , we begin by considering a small volume of the porous medium, $\bar{\Omega}$, which contains this point. This volume is taken so that a typical length scale is much smaller than the overall domain, but sufficiently larger than the pore scale, Straughan [107]. The equations for the temperature field in the solid and fluid are

$$\begin{aligned} (\rho_0 c)_s \frac{\partial T}{\partial t} &= \kappa_s \Delta T, \\ (\rho_0 c)_f \left(\frac{\partial T}{\partial t} + V_i \frac{\partial T}{\partial x_i} \right) &= \kappa_f \Delta T, \end{aligned} \quad (1.8)$$

c.f. Straughan [107]. The temperature is denoted by T , s and f represent the solid and fluid, respectively, κ_s and κ_f are the thermal diffusivities, c_s is the specific heat of the solid, c_{pf} is the specific heat at constant pressure of the fluid and ρ_{0s} and ρ_{0f} are the densities. Finally, $V_i = v_i/\phi$ is the pore average velocity, where ϕ is the porosity and v_i is the average fluid velocity at the point \mathbf{x} .

We now multiply the fluid temperature equation (1.8)₂ by ϕ and the solid temperature equation (1.8)₁ by $(1 - \phi)$. After adding the results we find

$$[(1 - \phi)(\rho_0 c)_s + \phi(\rho_0 c)_f] \frac{\partial T}{\partial t} + \phi(\rho_0 c)_f V_i \frac{\partial T}{\partial x_i} = [(1 - \phi)\kappa_s + \phi\kappa_f] \Delta T. \quad (1.9)$$

We denote $(\rho_0 c)_m = (1 - \phi)(\rho_0 c)_s + \phi(\rho_0 c)_f$ and $k_m = (1 - \phi)\kappa_s + \phi\kappa_f$ and may then rewrite (1.9) as

$$(\rho_0 c)_m \frac{\partial T}{\partial t} + (\rho_0 c)_f v_i \frac{\partial T}{\partial x_i} = k_m \Delta T. \quad (1.10)$$

Finally, dividing (1.10) by $(\rho_0 c)_f$ we find the averaged temperature field equation to be

$$\frac{1}{M} \frac{\partial T}{\partial t} + v_i \frac{\partial T}{\partial x_i} = \kappa \Delta T,$$

where $M = (\rho_0 c)_f / (\rho_0 c)_m$ and $\kappa = k_m / (\rho_0 c)_f$.

1.4 Overview

In Chapter 2 we develop the equations for a horizontal layer of a Darcy porous medium with an exothermic reaction on the lower boundary. We find linear in-

stability bounds and discuss the dependence of these on the reaction parameters. Chapter 3 then uses a non-linear energy technique to obtain an optimum stability boundary for this model. We compare the results and show that, although sub-critical instabilities may occur, the technique is useful. We demonstrate that the model depends continuously on the reaction parameters in Chapter 4. The impact of including the Soret effect on the instability boundary is considered in Chapter 5.

For a porous medium of high porosity higher order velocity terms become important and it necessary to replace the Darcy equation with the Brinkman equation, c.f. Rajagopal [88]. It is to this case that we turn our attention in Chapters 6 and 7, first developing instability boundaries and then demonstrating that the new model is continuously dependent on the reaction parameters.

In the final chapter we turn our attention to the problem of a vertical porous channel in which the solid and fluid may take different temperature profiles. We use a non-linear method to obtain conditions on the Rayleigh number such that the model is stable given any initial disturbance from the steady state and then conditions on the magnitude of the initial disturbance to gain stability for any Rayleigh number.

Chapter 2

Instability boundaries for the Darcy model with an exothermic boundary reaction

The following three chapters investigate the stability of a horizontal layer of a Darcy porous medium with an exothermic reaction on the lower boundary. In this chapter we find linear instability boundaries, we subsequently use the energy method to derive a stability bound, before demonstrating that the model is continuously dependent on the reaction parameters.

Recently, there have been many studies of convection driven by chemical reactions in porous media. Examples of such works include those of McKay [62] who investigates the effect of chemical reactions on instabilities in a viscous fluid overlaying a porous layer, Rahman & Al-Lawatia [87] and Mahdy [57] who study the influence of high order reactions, as well as Malashetty and Biradar [59] and Nguyen *et al* [68] who discuss how chemical reactions affect double-diffusive convection in an anisotropic porous layer and flow in an anisotropic porous cylinder, respectively.

There are many environmental applications to understanding the impact of chemical reactions on convection. Some interesting articles which discuss these applications are those of Andres & Cardoso [3], which links chemical reactions to the storage of carbon dioxide, and Eltayeb *et al.* [22, 23], which consider phase changes in convection at the Earth's inner core.

The particular motivation for this study is an article by Postelnicu [84] in which he considered a Darcy porous layer with an exothermic reaction on the lower wall acting as the driving force behind convective instability. In his paper it was assumed that exchange of stabilities holds, i.e. that the eigenvalues, σ_j of the problem are all real and that it is possible to set $\sigma_j = 0$ to find the instability boundary. It is not obvious that this assumption should hold and no justification was given. We therefore investigate the model from the basic equations.

2.1 Basic equations

We consider the porous layer to have a vertical depth h and be infinite in the x and y coordinates. It is saturated by an incompressible, viscous fluid that has the reactant dissolved in it. The reactant concentration, temperature, velocity, pressure and density are denoted by C , T , \mathbf{v} , p and ρ , respectively. Assuming Darcy's Law we have

$$\nabla p = -\frac{\mu}{K}\mathbf{v} - \rho g\mathbf{k}, \quad (2.1)$$

where μ is the dynamic viscosity, K is the permeability of the porous medium, $\mathbf{k} = (0, 0, 1)$ and g is gravity, which acts vertically downward. We employ the Boussinesq approximation by assuming that the density remains constant in every term except the body force. We then choose a density that takes the form used by Postelnicu [84], this is linear in temperature, but independent of the reactant concentration and may be written as

$$\rho = \rho_0(1 - \alpha(T - T_0)), \quad (2.2)$$

where α is the coefficient of thermal expansion and ρ_0 is the reference density at the reference temperature T_0 .

By inserting the density (2.2) into equation (2.1) we find that the momentum equation is

$$p_{,i} = -\frac{\mu}{K}v_i - \rho_0 g(1 - \alpha(T - T_0))k_i, \quad (2.3)$$

and as the fluid is incompressible we have

$$v_{i,i} = 0. \quad (2.4)$$

From the conservation of temperature and reactant concentration we find the equations, see for example Straughan [107],

$$\begin{aligned}\frac{1}{M}T_{,t} + v_i T_{,i} &= \kappa \Delta T, \\ \phi C_{,t} + v_i C_{,i} &= \phi k_c \Delta C,\end{aligned}\tag{2.5}$$

where $M = (\rho_0 c_p)_f / (\rho_0 c)_m$ with $(\rho_0 c)_m = \phi(\rho_0 c_p)_f + (1 - \phi)(\rho c)_s$, $\kappa = k_m / (\rho_0 c_p)_f$ is the thermal diffusivity of the porous medium, where $k_m = \kappa_s(1 - \phi) + \kappa_f \phi$, c_p is the specific heat of the fluid at constant temperature, k_c is the diffusivity of the reactant, c_s is the specific heat of the solid, the subscripts s and f represent the solid and fluid respectively and ϕ is the porosity of the medium.

On the upper wall we impose standard boundary conditions; the temperature and reactant concentration are held fixed and there is no mass flux across the wall, giving the conditions

$$T = T_U, \quad C = C_U, \quad v_i n_i = v_3 = 0, \quad \text{on } z = h.\tag{2.6}$$

The interesting boundary condition occurs on the lower wall, where an exothermic reaction converts the reactant into an inert product. The activation energy of this reaction is E , R^* signifies the universal gas constant, k_0 is a rate constant, Q is the heat released from the reaction and k_T is the rate at which heat is conducted away from the boundary. We again assume that there is no mass flux across the boundary and find the conditions

$$\begin{aligned}k_T \frac{\partial T}{\partial z} &= -Q k_0 C \exp\left(-\frac{E}{R^* T}\right), \\ \phi k_c \frac{\partial C}{\partial z} &= k_0 C \exp\left(-\frac{E}{R^* T}\right),\end{aligned}\tag{2.7}$$

$$v_i n_i = v_3 = 0 \quad \text{on } z = 0.$$

2.2 Steady state and perturbation equations

We now begin a linear analysis by non-dimensionalising the variables in equations (2.3), (2.4) and (2.5) and boundary conditions (2.6) and (2.7) by

$$\begin{aligned}x_i &= h x_i^*, \quad t = \frac{h^2}{\kappa M} t^*, \quad v_i = \frac{\kappa}{h} v_i^*, \\ C &= C_U C^*, \quad T = T_U T^*, \quad p = \frac{\kappa \mu}{K} p^*.\end{aligned}\tag{2.8}$$

After dropping the asterisks we find

$$\begin{aligned}
p_{,i} &= v_i - \frac{Kh}{\kappa\mu}\rho_0(1 - \alpha T_U(T - T_0))gk_i, \\
v_{i,i} &= 0, \\
T_{,t} + v_i T_{,i} &= \Delta T, \\
M\phi C_{,t} + v_i C_{,i} &= \frac{1}{Le}\Delta C,
\end{aligned} \tag{2.9}$$

with

$$T = 1, \quad C = 1, \quad v_3 = 0, \quad \text{on } z = 1 \tag{2.10}$$

and

$$\begin{aligned}
\frac{\partial T}{\partial z} &= -AC \exp\left(\frac{-\xi}{T}\right), \\
\frac{\partial C}{\partial z} &= BC \exp\left(\frac{-\xi}{T}\right), \\
v_3 &= 0 \quad \text{on } z = 0.
\end{aligned} \tag{2.11}$$

Here $Le = \kappa/\phi k_c$ is the Lewis number and

$$A = \frac{Qhk_0C_U}{T_Uk_T}, \quad B = \frac{k_0h}{\phi k_c}, \quad \xi = \frac{E}{R^*T_U}.$$

We now consider a steady state, $(\bar{\mathbf{v}}, \bar{T}, \bar{C}, \bar{p})$, where the fluid velocity is zero and the temperature and concentration fields remain constant, i.e. $\mathbf{v} = 0$, $T_{,t} = 0$ and $C_{,t} = 0$. As gravity acts vertically downwards and the medium is assumed to be infinite in the horizontal directions the boundary conditions induce temperature and concentration fields that are functions of the vertical position only. Using (2.9)₁, (2.9)₃ and (2.9)₄ we now find that

$$\begin{aligned}
\bar{p}_{,i} &= -\frac{Kh}{\kappa\mu}\rho_0(1 - \alpha T_U(\bar{T} - T_0))gk_i, \\
\bar{T} &= \beta_1 z + \beta_2, \\
\bar{C} &= \beta_3 z + \beta_4,
\end{aligned}$$

where β_1 , β_2 , β_3 and β_4 are constants. The exothermic reaction on the lower wall releases heat and consumes the reactant so we expect β_1 to be negative and β_3 to be positive. Evaluating this steady state on the boundaries we find

$$\begin{aligned}
\beta_1 + \beta_2 &= 1, \\
\beta_3 + \beta_4 &= 1,
\end{aligned}$$

and

$$\beta_1 = -A\beta_4 \exp\left(\frac{-\xi}{\beta_2}\right),$$

$$\beta_3 = B\beta_4 \exp\left(\frac{-\xi}{\beta_2}\right).$$

The values of A , B and ξ are chosen to coincide with those used by Postelnicu [84] and a selection of the values for β_1 and β_3 are given in Table 2.1. As expected, we

Table 2.1: Values of the gradients of the temperature and salt fields, β_1 and β_3 , for given reaction parameters A , B and ξ .

A	B	ξ	β_1	β_3
0.5	1	0	-0.25000	0.50000
1	1	0	-0.50000	0.50000
5	1	0	-2.50000	0.50000
0.5	0.5	0	-0.33333	0.33333
0.5	1	0	-0.25000	0.50000
0.5	5	0	-0.08333	0.83333
0.5	0.5	0	-0.33333	0.33333
0.5	0.5	0.15	-0.30836	0.30836
0.5	0.5	0.5	-0.25109	0.25109

see that $\beta_1 < 0$ and $\beta_3 > 0$. If A is increased, say by lowering the temperature on the upper wall or considering a reaction that releases greater heat, we would expect the resulting system to be less stable. We further believe this to be the case as we see from Table 2.1 that increasing A creates a greater temperature gradient. Increasing B creates a weaker destabilising temperature field and a stronger destabilising salt field, however the density was chosen to be dependent on only the temperature and so we expect the temperature field to dominate and the overall effect to be stabilising. If ξ is increased we notice that both the salt and the temperature fields become weaker and the change should be stabilising.

Although it is not possible to physically achieve $\xi = 0$ we may approach this value by choosing T_U to be large and E to be small. We will therefore assume that the reaction is well catalysed and hence that E , the activation energy, is low.

2.2.1 Perturbation equations

Small perturbations u_i, θ, γ, π to the steady state are now introduced to (2.9), where

$$\begin{aligned} v_i &= \bar{v}_i + u_i, & T &= \bar{T} + \theta, \\ C &= \bar{C} + \gamma, & p &= \bar{p} + \pi. \end{aligned} \quad (2.12)$$

After subtracting the steady state and introducing the non-dimensionalisations (2.8), equations (2.9) become

$$\begin{aligned} \pi_{,i} &= u_i + R\theta k_i, \\ u_{i,i} &= 0, \\ \theta_{,t} + \beta_1 w + u_i \theta_{,i} &= \Delta \theta, \\ M\phi \gamma_{,t} + \beta_3 w + u_i \gamma_{,i} &= \frac{1}{Le} \Delta \gamma, \end{aligned} \quad (2.13)$$

where $w = u_3$ and the Rayleigh number is defined by

$$R = \frac{Kh\rho_0\alpha T_U g}{\kappa\mu}.$$

Note that we now use R in a different manner to that of Chapter 1. The terms $u_i \theta_{,i}$ and $u_i \gamma_{,i}$ are the product of two small perturbations and are therefore neglected to linearise (2.13). To remove the pressure term in (2.13)₁ we twice take the curl and consider only the third component (i=3) to obtain

$$\begin{aligned} \theta_{,t} + \beta_1 w &= \Delta \theta, \\ M\phi \gamma_{,t} + \beta_3 w &= \frac{1}{Le} \Delta \gamma, \\ \Delta w - R\Delta^* \theta &= 0. \end{aligned} \quad (2.14)$$

The solutions we wish to find are time dependent and horizontally periodic so, using standard linear analysis, we expand w, θ and γ in the Fourier form

$$\begin{aligned} w &= \sum_{j=1}^{\infty} e^{\sigma_j t} f_j(x, y) W_j(z), \\ \theta &= \sum_{j=1}^{\infty} e^{\sigma_j t} f_j(x, y) \Theta_j(z), \\ \gamma &= \sum_{j=1}^{\infty} e^{\sigma_j t} f_j(x, y) \Phi_j(z), \end{aligned} \quad (2.15)$$

where f_j is some function of the form $f_j(x, y) = \exp[i(px + ry)]$ such that $\Delta^* f_j = -(p^2 + r^2)f_j = -k^2 f_j$ for a wave number k , and σ_j is the associated eigenvalue. If the real part of any σ_j is positive then instabilities will occur. We therefore consider a general eigenvalue of the system, σ , and finally obtain the equations

$$\begin{aligned} 0 &= (D^2 - k^2)W + Rk^2\Theta, \\ \sigma\Theta + \beta_1 W &= (D^2 - k^2)\Theta, \\ M\phi\sigma\Phi + \beta_3 W &= \frac{1}{Le}(D^2 - k^2)\Phi. \end{aligned} \tag{2.16}$$

2.2.2 Perturbed boundary conditions

We will now derive linearised perturbation boundary conditions by first introducing the perturbations (2.12) to (2.10) and (2.11) to find

$$\bar{T} + \theta = 1, \quad \bar{C} + \gamma = 1, \quad v_3 + w = 0, \quad \text{on } z = 1 \tag{2.17}$$

and

$$\begin{aligned} \frac{\partial(\bar{T} + \theta)}{\partial z} &= -A(\bar{C} + \gamma) \exp\left(\frac{-\xi}{\bar{T} + \theta}\right), \\ \frac{\partial(\bar{C} + \gamma)}{\partial z} &= B(\bar{C} + \gamma) \exp\left(\frac{-\xi}{\bar{T} + \theta}\right), \\ v_3 + w &= 0 \quad \text{on } z = 0. \end{aligned} \tag{2.18}$$

The steady state boundary conditions may now be subtracted from (2.17) and (2.18) to yield

$$\theta = 0, \quad \gamma = 0, \quad w = 0, \quad \text{on } z = 1$$

and

$$\begin{aligned} \frac{\partial\theta}{\partial z} &= -A\beta_4 \left[\exp\left(\frac{-\xi}{\beta_2 + \theta}\right) - \exp\left(\frac{-\xi}{\beta_2}\right) \right] - A\gamma \exp\left(\frac{-\xi}{\beta_2 + \theta}\right), \\ \frac{\partial\gamma}{\partial z} &= B\beta_4 \left[\exp\left(\frac{-\xi}{\beta_2 + \theta}\right) - \exp\left(\frac{-\xi}{\beta_2}\right) \right] + B\gamma \exp\left(\frac{-\xi}{\beta_2 + \theta}\right), \\ w &= 0 \quad \text{on } z = 0. \end{aligned} \tag{2.19}$$

Using a Taylor series expansion about $\theta = 0$ we find, that

$$\frac{-\xi}{\beta_2 + \theta} = \frac{-\xi}{\beta_2} + \theta \frac{\xi}{\beta_2^2} + O(\theta^2)$$

and hence, after neglecting the $O(\theta^2)$ terms,

$$\exp\left(\frac{-\xi}{\beta_2 + \theta}\right) = 1 + \left(\frac{-\xi}{\beta_2} + \theta\frac{\xi}{\beta_2^2}\right) + \frac{1}{2}\left(\frac{-\xi}{\beta_2} + \theta\frac{\xi}{\beta_2^2}\right)^2 + \frac{1}{6}\left(\frac{-\xi}{\beta_2} + \theta\frac{\xi}{\beta_2^2}\right)^3 + \dots$$

After linearising this becomes

$$\begin{aligned} \exp\left(\frac{-\xi}{\beta_2 + \theta}\right) &= \left(1 - \frac{\xi}{\beta_2} + \frac{\xi^2}{2\beta_2^2} - \frac{\xi^3}{6\beta_2^3} + \dots\right) + \theta\frac{\xi}{\beta_2^2}\left(1 - \frac{\xi}{\beta_2} + \frac{\xi^2}{2\beta_2^2} - \frac{\xi^3}{6\beta_2^3} + \dots\right) \\ &= \exp\left(\frac{-\xi}{\beta_2}\right) + \theta\frac{\xi}{\beta_2^2}\exp\left(\frac{-\xi}{\beta_2}\right). \end{aligned}$$

After inserting this into (2.19) and employing the Fourier transformations (2.15) the boundary conditions are given by

$$W = \Theta = \Phi = 0, \quad \text{on } z = 1, \quad (2.20)$$

and

$$\begin{aligned} W &= 0, \\ \frac{d\Theta}{dz} &= -A\frac{\beta_4\xi}{\beta_2^2}\exp\left(\frac{-\xi}{\beta_2}\right)\Theta - A\exp\left(\frac{-\xi}{\beta_2}\right)\Phi, \\ \frac{d\Phi}{dz} &= B\frac{\beta_4\xi}{\beta_2^2}\exp\left(\frac{-\xi}{\beta_2}\right)\Theta + B\exp\left(\frac{-\xi}{\beta_2}\right)\Phi \quad \text{on } z = 0. \end{aligned} \quad (2.21)$$

2.3 D^2 Chebyshev-tau method

In this section we will describe the numerical method used to calculate the critical Rayleigh number, R_c . This is the minimum value of R for which the real part of the eigenvalue, σ , become positive and it defines the instability boundary. In this thesis we will use the D and D^2 Chebyshev-Tau techniques to transform the models into a form that may be solved numerically and these methods are described in detail in Appendix A.

We will now show how the D^2 method may be applied to our current problem in order to write (2.16), (2.20) and (2.21) in the form

$$\mathbf{A}\mathbf{p} = \sigma\mathbf{B}\mathbf{p} \quad (2.22)$$

where \mathbf{A} and \mathbf{B} are matrices and \mathbf{p} is a vector. Once in this form we will use the QZ algorithm, c.f. Moler & Stewart [65], to find the eigenvalues, σ_i , then vary the wave number, k , in order to minimise R and find R_c .

Chebyshev polynomials are defined over the domain $\hat{z} \in [-1, 1]$ and so we must first transform the domain of our equations from $z \in [0, 1]$. To do this we use the transformation $\hat{z} = 2z - 1$ and (2.16) become

$$\begin{aligned} 0 &= (4D^2 - k^2)W(\hat{z}) + Rk^2\Theta(\hat{z}), \\ \sigma\Theta(\hat{z}) + \beta_1W(\hat{z}) &= (4D^2 - k^2)\Theta(\hat{z}), \\ M\phi\sigma\Phi(\hat{z}) + \beta_3W(\hat{z}) &= \frac{1}{Le}(4D^2 - k^2)\Phi(\hat{z}). \end{aligned} \quad (2.23)$$

We now expand the variables W , Θ and Φ as an infinite sum of Chebyshev polynomials, where T_n is the Chebyshev polynomial of n^{th} degree, so that

$$W(\hat{z}) = \sum_{n=0}^{\infty} W_n T_n(\hat{z}), \quad \Theta(\hat{z}) = \sum_{n=0}^{\infty} \Theta_n T_n(\hat{z}), \quad \Phi(\hat{z}) = \sum_{n=0}^{\infty} \Phi_n T_n(\hat{z}).$$

One may show that for suitably large N there is only a small margin of error between the variables W , Θ , Φ and truncated functions

$$\hat{W}(z) = \sum_{n=0}^N \hat{W}_n T_n(\hat{z}), \quad \hat{\Theta}(\hat{z}) = \sum_{n=0}^N \hat{\Theta}_n T_n(\hat{z}), \quad \hat{\Phi}(\hat{z}) = \sum_{n=0}^N \hat{\Phi}_n T_n(\hat{z}).$$

Typically we take $N = 30$ or $N = 40$. We proceed with the new functions, \hat{W} , $\hat{\Theta}$, $\hat{\Phi}$, and drop the $\hat{\cdot}$ symbols. Inserting these into (2.23) we find

$$\begin{aligned} (4D^2 - k^2)W(\hat{z}) + Rk^2\Theta(\hat{z}) &= \tau_1 T_{N-1}(\hat{z}) + \tau_2 T_N(\hat{z}), \\ \sigma\Theta(\hat{z}) + \beta_1W(\hat{z}) - (4D^2 - k^2)\Theta(\hat{z}) &= \tau_3 T_{N-1}(\hat{z}) + \tau_4 T_N(\hat{z}), \\ M\phi\sigma\Phi(\hat{z}) + \beta_3W(\hat{z}) - \frac{1}{Le}(4D^2 - k^2)\Phi(\hat{z}) &= \tau_5 T_{N-1}(\hat{z}) + \tau_6 T_N(\hat{z}), \end{aligned} \quad (2.24)$$

where τ_i are the approximation errors. Multiplying each equation in (2.24) by T_k where $k = 0, 1, \dots, N - 2$ we obtain $3N - 3$ equations that are functions of $3N + 3$ unknowns and the τ_i are removed due to the orthogonality of the Chebyshev functions.

We are now in a position to formulate the problem in the form (2.22). A vector \mathbf{p} is formed from the unknowns by $\mathbf{p} = (W_0, W_1, \dots, W_N, \Theta_0, \Theta_1, \dots, \Theta_N, \Phi_0, \Phi_1, \dots, \Phi_N)^T$ and then the equations obtained by multiplying (2.24) by T_N are constructed into two matrices \mathbf{A} and \mathbf{B} , of dimension $(3N + 3) \times (3N + 3)$. The resulting matrices

are

$$\mathbf{A} = \begin{pmatrix} 4\mathbf{D}^2 - k^2\mathbf{I} & Rk^2\mathbf{I} & \mathbf{0} \\ BC1 & 0, \dots, 0 & 0, \dots, 0 \\ BC2 & 0, \dots, 0 & 0, \dots, 0 \\ -\beta_1\mathbf{I} & 4\mathbf{D}^2 - k^2\mathbf{I} & \mathbf{0} \\ 0, \dots, 0 & BC1 & 0, \dots, 0 \\ 0, \dots, 0 & BC3 & BC4 \\ -\beta_3\mathbf{I} & \mathbf{0} & \frac{1}{Le}(4\mathbf{D}^2 - k^2\mathbf{I}) \\ 0, \dots, 0 & 0, \dots, 0 & BC1 \\ 0, \dots, 0 & BC5 & BC6 \end{pmatrix},$$

where \mathbf{I} is the identity matrix of dimension $(N-1) \times (N+1)$, \mathbf{D}^2 is the Chebyshev second-differentiation matrix of dimension $(N-1) \times (N+1)$, see Dongarra *et al* [20], and BC1-BC6 represent the boundary conditions, and

$$\mathbf{B} = \begin{pmatrix} \mathbf{0} & \mathbf{0} & \mathbf{0} \\ 0, \dots, 0 & 0, \dots, 0 & 0, \dots, 0 \\ 0, \dots, 0 & 0, \dots, 0 & 0, \dots, 0 \\ \mathbf{0} & \mathbf{I} & \mathbf{0} \\ 0, \dots, 0 & 0, \dots, 0 & 0, \dots, 0 \\ 0, \dots, 0 & 0, \dots, 0 & 0, \dots, 0 \\ \mathbf{0} & \mathbf{0} & M\phi\mathbf{I} \\ 0, \dots, 0 & 0, \dots, 0 & 0, \dots, 0 \\ 0, \dots, 0 & 0, \dots, 0 & 0, \dots, 0 \end{pmatrix}.$$

To obtain the conditions BC1-BC6 we use the identities

$$T_n(\pm 1) = (\pm 1)^n,$$

$$T'_n(\pm 1) = (\pm 1)^{n+1}n^2,$$

where the derivation of these are explained in Appendix A.2. Using these identities on the boundary conditions (2.20) and (2.21) we find the simple boundary conditions are

$$W(1) = \sum_{n=0}^N W_n = 0, \quad \Theta(1) = \sum_{n=0}^N \Theta_n = 0,$$

$$\Phi(1) = \sum_{n=0}^N \Phi_n = 0, \quad W(-1) = \sum_{n=0}^N (-1)^n W_n = 0$$

and the mixed boundary conditions are

$$\begin{aligned} \Theta'(-1) + A \frac{\beta_4 \xi}{\beta_2^2} \exp\left(\frac{-\xi}{\beta_2}\right) \Theta(-1) + A \exp\left(\frac{-\xi}{\beta_2}\right) \Phi(-1) \\ = \sum_{n=0}^N (-1)^n \left[-n^2 \Theta_n + A \frac{\beta_4 \xi}{\beta_2^2} \exp\left(\frac{-\xi}{\beta_2}\right) \Theta_n + A \exp\left(\frac{-\xi}{\beta_2}\right) \Phi_n \right] = 0, \\ \Phi'(-1) - B \frac{\beta_4 \xi}{\beta_2^2} \exp\left(\frac{-\xi}{\beta_2}\right) \Theta(-1) - B \exp\left(\frac{-\xi}{\beta_2}\right) \Phi(-1) \\ = \sum_{n=0}^N (-1)^n \left[-n^2 \Phi_n - B \frac{\beta_4 \xi}{\beta_2^2} \exp\left(\frac{-\xi}{\beta_2}\right) \Theta_n - B \exp\left(\frac{-\xi}{\beta_2}\right) \Phi_n \right] = 0. \end{aligned}$$

From these we find that BC1-BC6 in matrix \mathbf{A} are given by

$$BC1 = (1, 1, \dots, 1),$$

$$BC2 = (1, -1, \dots, 1, -1),$$

$$BC3 = \left(\frac{\hat{A}\beta_4\xi}{2\beta_2^2}, 1 - \frac{\hat{A}\beta_4\xi}{2\beta_2^2}, -4 + \frac{\hat{A}\beta_4\xi}{2\beta_2^2}, 9 - \frac{\hat{A}\beta_4\xi}{2\beta_2^2}, \dots, (-1)^N \left((N-1)^2 - \frac{\hat{A}\beta_4\xi}{2\beta_2^2} \right) \right),$$

$$BC4 = \frac{\hat{A}}{2} (1, -1, 1, \dots, -1),$$

$$BC5 = \frac{\hat{B}\beta_4\xi}{2\beta_2^2} (-1, 1, -1, \dots, 1),$$

$$BC6 = \left(-\frac{\hat{B}}{2}, 1 + \frac{\hat{B}}{2}, -\left(4 + \frac{\hat{B}}{2}\right), \dots, (-1)^N \left((N-1)^2 + \frac{\hat{B}}{2} \right) \right),$$

where

$$\hat{A} = A \exp\left(\frac{-\xi}{\beta_2}\right), \quad \hat{B} = B \exp\left(\frac{-\xi}{\beta_2}\right).$$

It is well-known that if the matrices in an equation of the form (2.22) are symmetric then the eigenvalues are real. We note that for our current problem matrices \mathbf{A} and \mathbf{B} are not symmetric and hence we do not expect the eigenvalues to be real.

We now choose a small starting value for k and calculate the eigenvalues of the matrix problem using the QZ algorithm by calling subroutine F02BJF from the NAG library. When doing this we also vary the value of N to check whether spurious eigenvalues occur. For this problem we found that none occur. If any one of the true eigenvalues has a positive real part then the system is unstable and so we order the eigenvalues in terms of the real part. The secant method is then used to find the value of R for which $\text{Re}(\sigma_1) = 0$, where σ_1 is the eigenvalue with the greatest real part. Next, we increase k in small increments and use a golden section search to

find R_c , which is the minimum value of R for which $\text{Re}(\sigma_1) = 0$ for some k . When doing this we must take care as there are often two minimums in R as we increase k , one occurs for $\text{Im}(\sigma_1) = 0$ and the other for $\text{Im}(\sigma_1) \neq 0$, R_c is the smaller of these two values. The value of k for which we find R_c is now defined as the critical wave number, k_c .

2.4 Results

We wish to examine how the reaction affects the critical Rayleigh number and so vary the values of A , B and ξ in turn, keeping each of the other parameters constant. We will also examine the effect of the parameter $M\phi$ on R_c . A selection of the values of R_c , k_c and $\text{Im}(\sigma_1)$ obtained are given in Table 2.2. We see from the table that for certain parameter values the imaginary part of σ_1 is not equal to zero. This means that, as expected, the exchange of stability does not hold. In cases where $\text{Im}(\sigma_1) = 0$ stationary convection is dominant and when $\text{Im}(\sigma_1) \neq 0$ oscillatory convection dominates.

Figures 2.1-2.4 show how increasing the values of A , B , ξ or $M\phi$ changes the value of R_c . In each figure we see that as the Lewis number is increased from $Le = 0$ the critical Rayleigh number initially increases and from the values in Table 2.2 that stationary convection is dominant here. At a value of Le , say Le_c , the curve reaches a peak and as we increase Le further R_c decreases. On this side of the peak we find oscillatory convection.

In Section 2.2 we discussed that increasing A is expected to increase R_c and increasing B or ξ to decrease R_c . Figures 2.1, 2.2 and 2.3 and Table 2.2 show that this is indeed the case.

When $\xi = 0$, if A is increased by a factor of n , R_c decreases by a factor of n . This is because β_3 is unaffected by increasing A and thus the salt gradient is unchanged, however β_1 is multiplied by a factor of n and is hence n times more destabilising.

In Figure 2.4 we notice that when stationary convection dominates the value of $M\phi$ has no impact on R_c . This should be expected as in (2.16), (2.20) and (2.21) $M\phi$ only occurs multiplied by the eigenvalue and at the onset of stationary convection

Table 2.2: Values of R_c , k_c and $\text{Im}(\sigma_1)$.

			$Le = 0.1$			$Le = 1$			$Le = 5$			$Le = 10$			
A	B	ξ	$M\phi$	R_c	k_c	$\text{Im}(\sigma_1)$									
0.5	1	0	1	109.651	2.351	0.000	121.075	2.598	0.000	122.310	2.290	-2.676	108.047	2.216	-2.616
1	1	0	1	54.825	2.351	0.000	60.538	2.598	0.000	61.155	2.298	2.676	54.023	2.216	2.616
5	1	0	1	10.965	2.351	0.000	12.108	2.598	0.000	12.231	2.285	2.674	10.805	2.216	2.616
0.5	0.5	0	1	81.847	2.342	0.000	86.836	2.490	0.000	93.145	2.298	-1.792	83.160	2.248	1.982
0.5	1	0	1	109.651	2.351	0.000	121.075	2.598	0.000	122.310	2.285	-2.674	108.047	2.216	-2.616
0.5	5	0	1	333.918	2.373	0.000	417.313	2.908	0.000	372.832	2.308	-4.855	322.772	2.200	4.502
0.5	0.5	0	1	81.847	2.342	0.000	86.836	2.490	0.000	93.145	2.298	-1.792	83.160	2.248	1.982
0.5	0.5	0.15	1	88.093	2.332	0.000	93.037	2.469	0.000	100.593	2.292	1.650	89.891	2.243	1.884
0.5	0.5	0.5	1	107.170	2.310	0.000	112.016	2.410	0.000	123.395	2.280	1.293	110.549	2.235	1.652
			$Le = 1$			$Le = 5$			$Le = 10$			$Le = 100$			
0.5	0.5	0	1	86.836	2.490	0.000	93.145	2.298	-1.792	83.160	2.248	-1.982	73.484	2.181	-1.339
0.5	0.5	0	0.5	86.836	2.490	0.000	107.753	2.309	-1.789	89.462	2.244	2.815	70.954	2.122	1.964
0.5	0.5	0	0.25	86.836	2.490	0.000	107.263	3.134	0.000	102.436	2.241	-3.863	68.136	2.046	2.845

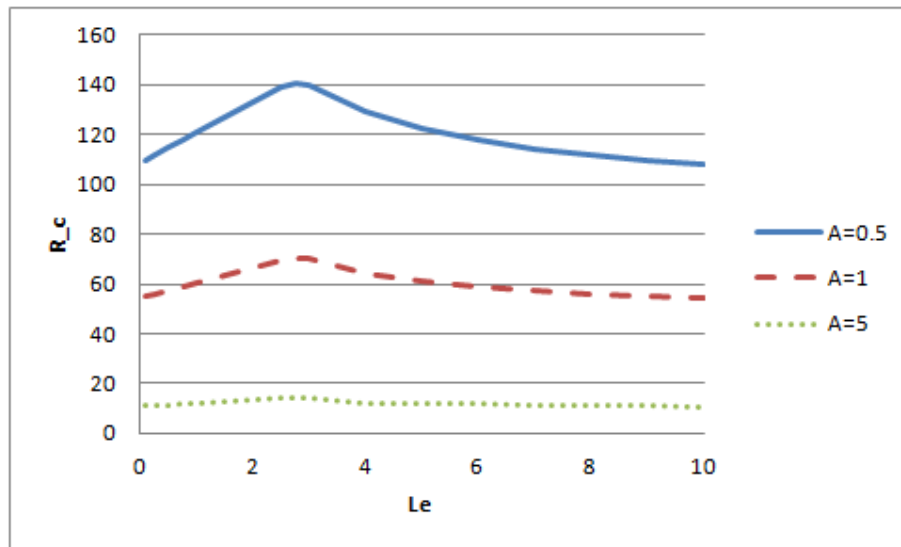


Figure 2.1: Variation of the instability boundary with A , for $B = 1$, $\xi = 0$, $M\phi = 1$.

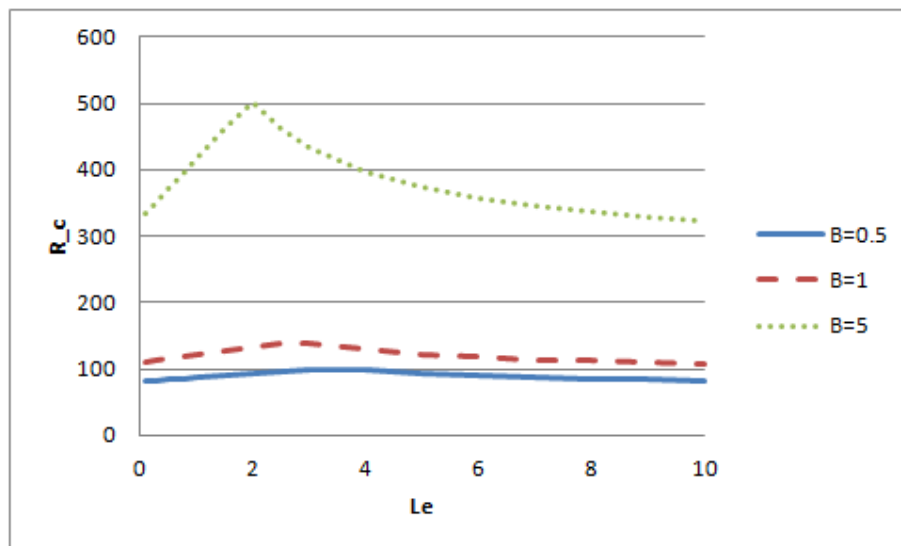


Figure 2.2: Variation of the instability boundary with B , for $A = 0.5$, $\xi = 0$, $M\phi = 1$.

$\sigma = 0$.

We here reiterate that the linear method used in this chapter only finds values of R_c above which we find instability and provides no information about the stability or instability below this boundary. In Chapter 3 we use a non-linear energy method to find a stability boundary.

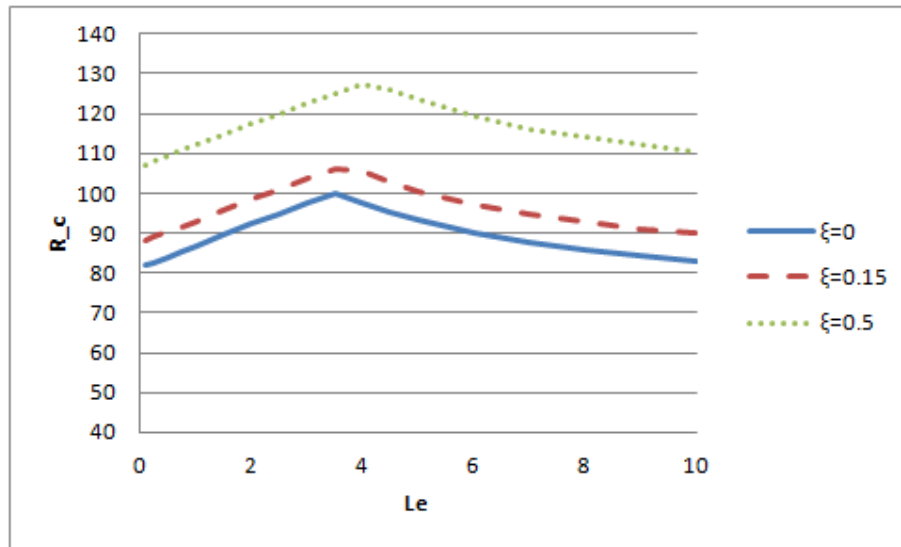


Figure 2.3: Variation of the instability boundary with ξ , for $A = 0.5$, $B = 0.5$, $M\phi = 1$.

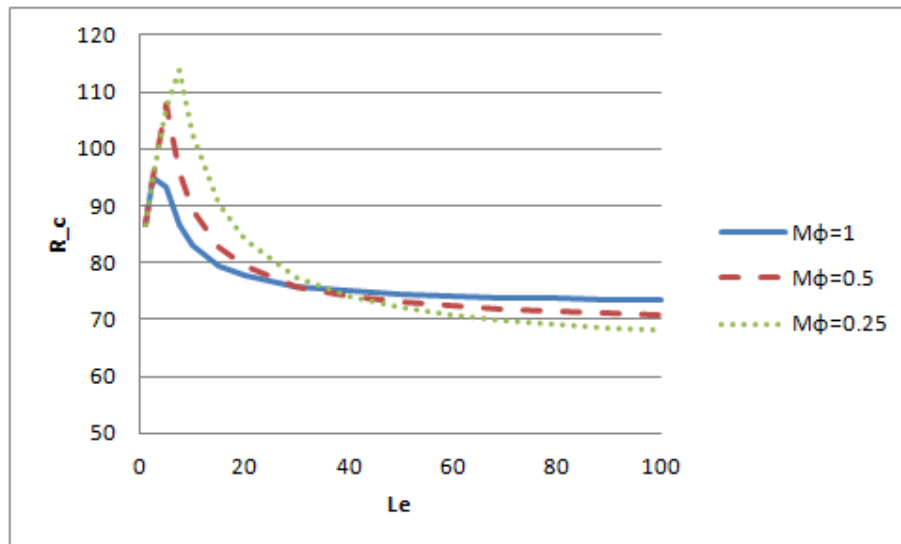


Figure 2.4: Variation of the instability boundary with $M\phi$, for $A = 0.5$, $B = 0.5$, $\xi = 0$.

Chapter 3

Non-linear stability bound for the Darcy problem

In the previous chapter we used a linear method to find instability boundaries for a horizontal layer of a Darcy porous medium with an exothermic reaction on the lower boundary. The method used provides no information about the stability or instability below these boundaries. It is possible to show that some systems are stable for all Rayleigh numbers below the boundary, for example the standard Bénard problem for a Darcy porous medium, Chapter 4 of Straughan [105], a micropolar fluid layer heated below, Ahmadi [1], or the standard Bénard problem in a fluid Joseph [40,41]. However, this is often not the case and instabilities are found to occur below this boundary, these are termed sub-critical instabilities. Some examples of systems in which such sub-critical instabilities are found include a rotating fluid, Veronis [119] and internal heating problems, Joseph & Carmi [42], Joseph & Shir [43].

To find regions of stability we must use non-linear methods; for example the variational methods used by Mulone & Rionero [67] and Hill *et al* [35] and for non-constant boundary conditions by Capone & Rionero [11]. A particularly relevant example is that of McTaggart & Straughan [63], which uses an energy technique to develop stability thresholds for a fluid with a reaction on the lower boundary. Between the stability and instability boundaries, neither the linear nor non-linear methods provide information about the stability, instead the equations must be solved using a three-dimensional computation. In some instances it is found that

non-linear stability bounds obtained are far below the linear instability bounds and the region of unknown stability is large.

In this chapter we will use a fully non-linear energy method to find an instability bound for the problem considered in Chapter 2. We will optimise this boundary and show that for moderate Lewis numbers it is reasonably near the instability boundary, but falls away for larger Le .

3.1 Non-linear perturbation equations

We begin the analysis by presenting the fully non-linear, non-dimensional perturbation equations for the problem derived in Chapter 2 as

$$\begin{aligned}\pi_{,i} &= u_i + R\theta k_i, \\ u_{i,i} &= 0, \\ \theta_{,t} + \beta_1 w + u_i \theta_{,i} &= \Delta\theta, \\ M\phi\gamma_{,t} + \beta_3 w + u_i \gamma_{,i} &= \frac{1}{Le}\Delta\gamma,\end{aligned}\tag{3.1}$$

and the non-linear, non-dimensional perturbation boundary conditions as

$$\theta = 0, \quad \gamma = 0, \quad w = 0, \quad \text{on } z = 1$$

and

$$\begin{aligned}\frac{\partial\theta}{\partial z} &= -A\beta_4 \left[\exp\left(\frac{-\xi}{\beta_2 + \theta}\right) - \exp\left(\frac{-\xi}{\beta_2}\right) \right] - A\gamma \exp\left(\frac{-\xi}{\beta_2 + \theta}\right), \\ \frac{\partial\gamma}{\partial z} &= B\beta_4 \left[\exp\left(\frac{-\xi}{\beta_2 + \theta}\right) - \exp\left(\frac{-\xi}{\beta_2}\right) \right] + B\gamma \exp\left(\frac{-\xi}{\beta_2 + \theta}\right), \\ w &= 0 \quad \text{on } z = 0.\end{aligned}$$

The non-dimensional variables u_i , θ and ϕ are perturbations in the fluid velocity, temperature and reactant concentration, respectively, and $w = u_3$. The Rayleigh number, R , and the parameters Le , $M\phi$, A , B and ξ are as defined in Chapter 2 and values of the coefficients β_1 , β_2 , β_3 and β_4 for given values of A , B and ξ are given in Table 2.1.

In Chapter 2 we discuss how the values of A , B , ξ and $M\hat{\phi}$ influence the instability curve, however here we are unable to consider the effect of ξ . It is not possible to

carry out the following non-linear analysis with the conditions on the lower boundary in their current form. We therefore consider the situation where the reaction is well catalysed and the temperature on the upper boundary is high so that E is small, T_U is large and consequently ξ is small. As we let $\xi \rightarrow 0$ the non-dimensional perturbation boundary conditions become

$$\begin{aligned} u_i n_i &= 0, & \theta &= 0, & \gamma &= 0 & \text{on } z = 1, \\ u_i n_i &= 0, & D\theta &= -A\gamma, & D\gamma &= B\gamma & \text{on } z = 0. \end{aligned} \quad (3.2)$$

3.2 The energy method

Our aim now is to derive an energy of the system and show that it decays with time given certain restraints on R . This will demonstrate that the system is stable for $R < R_s$, where we can calculate R_s .

We begin by rescaling θ and γ to define new variables $\hat{\theta}$ and $\hat{\gamma}$ by $\hat{\theta} = \sqrt{R}\theta$ and $\hat{\gamma} = \sqrt{R}\gamma$. After using these new variables and dropping the $\hat{}$ symbols equations (3.1) become

$$\begin{aligned} \pi_{,i} &= -u_i + R_a \theta k_i, \\ u_{i,i} &= 0, \\ \theta_{,t} &= -\beta_1 R_a w - u_i \theta_{,i} + \Delta \theta, \\ M\phi\gamma_{,t} &= -\beta_3 R_a w - u_i \gamma_{,i} + \frac{1}{Le} \Delta \gamma, \end{aligned} \quad (3.3)$$

where $R_a = \sqrt{R}$, whilst the boundary conditions (3.2) remain unchanged.

Next we multiply equations (3.3)₁, (3.3)₃ (3.3)₄ by u_i , $\lambda\theta$ and $\hat{\mu}\gamma/M\phi$, respectively, where λ and $\hat{\mu}$ are positive constants. The results are integrated over a general periodic cell V and, after integrating once using the boundary conditions, we find

$$\begin{aligned} 0 &= -\|\mathbf{u}\|^2 + R_a(\theta, w), \\ \frac{\lambda}{2} \frac{d}{dt} \|\theta\|^2 &= -\beta_1 \lambda R_a(w, \theta) - \lambda \|\nabla \theta\|^2 + \lambda A \int_{z=0} \theta \gamma dA, \\ \frac{\hat{\mu}}{2} \frac{d}{dt} \|\gamma\|^2 &= -\beta_3 \frac{\hat{\mu}}{M\phi} R_a(w, \gamma) - \frac{\hat{\mu}}{LeM\phi} \|\nabla \gamma\|^2 - \frac{\hat{\mu}B}{LeM\phi} \int_{z=0} \gamma^2 dA. \end{aligned} \quad (3.4)$$

We define an energy as

$$E = \frac{1}{2} (\lambda \|\theta\|^2 + \hat{\mu} \|\gamma\|^2)$$

and add the equations (3.4) to obtain

$$\begin{aligned} \frac{dE}{dt} = & -\|\mathbf{u}\|^2 - \lambda\|\nabla\theta\|^2 - \frac{\hat{\mu}}{LeM\phi}\|\nabla\gamma\|^2 + R_a(1 - \lambda\beta_1)(\theta, w) \\ & - \frac{\hat{\mu}}{M\phi}\beta_3R_a(w, \gamma) + \lambda A \oint_{z=0} \theta\gamma dA - \frac{\hat{\mu}B}{LeM\phi} \oint_{z=0} \gamma^2 dA. \end{aligned} \quad (3.5)$$

We now collect together the terms on the right hand side of (3.5) that we know to be positive and define a function

$$\mathcal{D} = \|\mathbf{u}\|^2 + \lambda\|\nabla\theta\|^2 + \frac{\hat{\mu}}{LeM\phi}\|\nabla\gamma\|^2 + \frac{\hat{\mu}B}{LeM\phi} \oint_{z=0} \gamma^2 dA.$$

The other terms are collected to define a second function as

$$\mathcal{I} = R_a(1 - \lambda\beta_1)(\theta, w) - \frac{\hat{\mu}}{M\phi}\beta_3R_a(w, \gamma) + \lambda A \oint_{z=0} \theta\gamma dA.$$

Equation (3.5) may then be written as

$$\frac{dE}{dt} = \mathcal{I} - \mathcal{D}.$$

The function \mathcal{D} is known to be positive and so may be factorised to find the inequality

$$\frac{dE}{dt} \leq -\mathcal{D} \left(1 - \max_{\mathcal{H}} \frac{\mathcal{I}}{\mathcal{D}} \right),$$

where \mathcal{H} is the set of admissible functions defining \mathcal{I} and \mathcal{D} . This set is restricted to divergence free functions due to equation (3.3)₂. To impose this restriction we use a Lagrange multiplier and add the term $-\int_{\Omega} \pi(\mathbf{x})u_{i,i} = 0$ to \mathcal{I} so that now

$$\mathcal{I} = R_a(1 - \lambda\beta_1)(\theta, w) - \frac{\hat{\mu}}{M\phi}\beta_3R_a(w, \gamma) + \lambda A \oint_{z=0} \theta\gamma dA - (\pi(\mathbf{x}), u_{i,i}).$$

As each term in \mathcal{D} is positive we see that

$$\begin{aligned} \mathcal{D} & \geq \lambda\|\nabla\theta\|^2 + \frac{\hat{\mu}}{LeM\phi}\|\nabla\gamma\|^2 \\ & \geq \pi^2 \left(\lambda\|\theta\|^2 + \frac{\hat{\mu}}{LeM\phi}\|\gamma\|^2 \right) \\ & \geq \zeta^2 E, \end{aligned}$$

where in the second step we have used Poincaré's inequality (see e.g. Straughan [105] page 387), and $\zeta^2 = \pi^2 \min(1, 1/LeM\phi) > 0$. Hence if $R_E \geq 1$ then

$$\frac{dE}{dt} \leq -\zeta^2 E \left(1 - \frac{1}{R_E} \right),$$

where, following the method in Chapters 2 and 4 of Straughan [105], we define

$$\frac{1}{R_E} = \max_{\mathcal{H}} \frac{\mathcal{I}}{\mathcal{D}}.$$

From here we see that if $R_E > 1$ the energy decays exponentially and hence $R_E = 1$ gives a stability boundary. The problem now becomes to find the values of R_a for which $\max_{\mathcal{H}} (\mathcal{I}/\mathcal{D}) = 1$. The maximum is the point at which $\delta(\mathcal{I}/\mathcal{D}) = 0$ and we find a condition for this by first expanding as

$$\begin{aligned} \delta \left(\frac{\mathcal{I}}{\mathcal{D}} \right) &= \frac{\delta \mathcal{I}}{\mathcal{D}} - \frac{\mathcal{I}}{\mathcal{D}^2} \delta \mathcal{D} \\ &= \frac{1}{\mathcal{D}} \left(\delta \mathcal{I} - \frac{1}{R_E} \delta \mathcal{D} \right). \end{aligned}$$

Hence at the maximum, and with $R_E = 1$, we find the condition that

$$\delta \mathcal{D} - \delta \mathcal{I} = 0. \quad (3.6)$$

We notice that in (3.6) the parameter $\hat{\mu}$ always occurs as $\hat{\mu}/M\phi$ and so we now define a new parameter

$$\mu = \hat{\mu}/M\phi > 0. \quad (3.7)$$

3.3 Euler-Lagrange equations

The equations which satisfy the condition (3.6) are the Euler-Lagrange equations and in order to find these we must first derive $\delta \mathcal{D}$ and $\delta \mathcal{I}$. To do this we vary the perturbation variables \mathbf{u} , θ , γ by arbitrary functions \mathbf{h} , η_1 , η_2 , respectively. This method is described in detail in Section IV of Courant & Hilbert [18]. We now find that $\delta \mathcal{I}$ and $\delta \mathcal{D}$ are defined as

$$\begin{aligned} \delta \mathcal{I} &= \left[\frac{d}{d\epsilon} (R_a(1 - \lambda\beta_1)(\theta + \epsilon\eta_1, w + \epsilon h_3) - \mu\beta_3 R_a(w + \epsilon h_3, \gamma + \epsilon\eta_2)) \right]_{\epsilon=0} \\ &\quad + \left[\frac{d}{d\epsilon} \left(\lambda A \oint_{z=0} (\theta + \epsilon\eta_1)(\gamma + \epsilon\eta_2) dA - (\pi(\mathbf{x}), (u_i + h_i), i) \right) \right]_{\epsilon=0} \end{aligned} \quad (3.8)$$

and

$$\begin{aligned} \delta \mathcal{D} &= \left[\frac{d}{d\epsilon} \left(\|\mathbf{u} + \epsilon\mathbf{h}\|^2 + \lambda \|\nabla(\theta + \epsilon\eta_1)\|^2 + \frac{\mu}{Le} \|\nabla(\gamma + \epsilon\eta_2)\|^2 \right) \right]_{\epsilon=0} \\ &\quad + \left[\frac{d}{d\epsilon} \left(\frac{\mu B}{Le} \oint_{z=0} (\gamma + \epsilon\eta_2)^2 dA \right) \right]_{\epsilon=0}, \end{aligned} \quad (3.9)$$

where ϵ is a small, positive constant. After performing the differentiation and evaluating at $\epsilon = 0$ equations (3.8) and (3.9) reduce to

$$\begin{aligned} \delta I = & R_a(1 - \lambda\beta_1)[(w, \eta_1) + (h_3, \theta)] - \mu\beta_3 R_a[(w, \eta_2) + (h_3, \gamma)] \\ & + \lambda A \oint_{z=0} (\theta\eta_2 + \gamma\eta_1) dA + (\pi_{,i}, h_i), \end{aligned} \quad (3.10)$$

where in the final term we have used the fact that $-(\pi, h_{i,i}) = (\pi_{,i}, h_i)$, and

$$\delta D = 2(u_i, h_i) + 2\lambda(\nabla\theta, \nabla\eta_1) + 2\frac{\mu}{Le}(\nabla\gamma, \nabla\eta_2) + 2\frac{\mu B}{Le} \oint_{z=0} \eta_2\gamma dA. \quad (3.11)$$

We integrate the second and third terms of (3.11), using the boundary conditions, to remove the $\nabla\eta_1$ and $\nabla\eta_2$ terms and obtain

$$\begin{aligned} \delta D = & 2(u_i, h_i) - 2\lambda(\Delta\theta, \eta_1) - 2\frac{\mu}{Le}(\Delta\gamma, \eta_2) \\ & + 2\frac{\mu B}{Le} \oint_{z=0} \eta_2\gamma dA + 2\lambda \oint_{z=0} \frac{\partial\theta}{\partial n} \eta_1 dA + 2\frac{\mu}{Le} \oint_{z=0} \frac{\partial\gamma}{\partial n} \eta_2 dA. \end{aligned} \quad (3.12)$$

The condition (3.6) must hold for any arbitrary \mathbf{h} , η_1 or η_2 and so considering each in turn from (3.10) and (3.12) we find three conditions, the Euler-Lagrange equations, to be

$$\begin{aligned} R_a(1 - \lambda\beta_1)\theta k_i - \mu\beta_3 R_a\gamma k_i + \pi_{,i} - 2u_i &= 0, \\ R_a(1 - \lambda\beta_1)w + 2\lambda\Delta\theta &= 0, \\ -\mu\beta_3 R_a w + 2\frac{\mu}{Le}\Delta\gamma &= 0. \end{aligned} \quad (3.13)$$

The natural boundary conditions, c.f. Courant & Hilbert [18], pages 208-211, that arise from the surface boundary integrals are

$$\begin{aligned} w &= 0, \\ \lambda A\gamma - 2\lambda \frac{\partial\theta}{\partial n} &= 0, \\ \lambda A L e \theta - 2\mu B \gamma - 2\mu \frac{\partial\gamma}{\partial n} &= 0 \quad \text{on } z = 0 \end{aligned}$$

and

$$w = \theta = \gamma = 0 \quad \text{on } z = 1.$$

We now have a system of linear equations and boundary conditions and can use the same method as in Chapter 2 to solve them numerically. First, to (3.13)₁ we

take the *curl* twice and then employ the Fourier transformations (2.15). After this we find

$$\begin{aligned} k^2 R_a (1 - \lambda \beta_1) \Theta - k^2 R_a \mu \beta_3 \Phi + 2(D^2 - k^2)W &= 0, \\ R_a (1 - \lambda \beta_1)W + 2\lambda(D^2 - k^2)\Theta &= 0, \\ -R_a \mu \beta_3 W + 2\frac{\mu}{Le}(D^2 - k^2)\Phi &= 0, \end{aligned} \quad (3.14)$$

where k is a wave number, with the boundary conditions

$$\begin{aligned} W &= 0, \\ \lambda A \Phi + 2\lambda D \Theta &= 0, \\ \lambda A L e \Theta - 2\mu B \Phi + 2\mu D \Phi &= 0 \quad \text{on } z = 0 \end{aligned} \quad (3.15)$$

and

$$W = \Theta = \Phi = 0 \quad \text{on } z = 1. \quad (3.16)$$

We may now solve (3.14) with the boundary conditions (3.15) and (3.16) and chosen values of λ and μ to find a value for $R_a = \sqrt{R}$, which defines a stability boundary.

3.4 Numerical method and results

For any values of λ and μ we may use the method described above to find an energy which decays for Rayleigh numbers less than a numerically computable value, R_a . This value may vary for different values of λ and μ and so we use an optimisation process to find the maximum value of R_a .

We first notice that if we consider R_a to be the eigenvalue of the (3.14) then the problem is symmetric. This should be expected as the Rayleigh number must be real. We now form natural variables χ_1, χ_2, χ_3 from the boundary conditions by

$$\begin{aligned} \chi_1 &= DW, \\ \chi_2 &= D\Theta + \frac{A}{2}\Phi, \\ \chi_3 &= D\Phi - B\Phi + \frac{\lambda A L e}{2\mu}\Theta. \end{aligned}$$

Using these new variables (3.14) become

$$\begin{aligned}
DW - \chi_1 &= 0, \\
-2k^2W + 2D\chi_1 + R_a k^2(1 - \lambda\beta_1)\Theta - R_a k^2\beta_3\mu\Phi &= 0, \\
D\Theta - \chi_2 + \frac{A}{2}\Phi &= 0, \\
R_a(1 - \lambda\beta_1)W + \left(\frac{A^2\lambda^2 Le}{2\mu} - 2\lambda k^2\right)\Theta + 2\lambda D\chi_2 - AB\lambda\Phi - A\lambda\chi_3 &= 0, \\
\frac{\lambda A Le}{2\mu}\Theta + D\Phi - B\Phi - \chi_3 &= 0, \\
-R_a\mu\beta_3W - \lambda AB\Theta - \lambda A\chi_2 + \left(\frac{2\mu B^2}{Le} + \frac{\lambda A^2}{2} - \frac{2\mu k^2}{Le}\right)\Phi + \frac{2\mu}{Le}(B\chi_3 + D\chi_3) &= 0
\end{aligned}$$

with the much simpler boundary conditions

$$\begin{aligned}
W = \Theta = \Phi = 0 \quad \text{on } z = 1, \\
W = \chi_2 = \chi_3 = 0 \quad \text{on } z = 0.
\end{aligned}$$

Next we use the Natural D Chebyshev-tau method, c.f. Dongarra *et al* [20], Payne & Straughan [79], to transform the problem into a generalised matrix eigenvalue problem, where R_a is the eigenvalue.

We transform the domain from $z \in [0, 1]$ to $\hat{z} \in [-1, 1]$ and expand the variables $W, \chi_1, \Theta, \chi_2, \Phi, \chi_3$ as Chebyshev polynomials series, for example

$$W(\hat{z}) = \sum_{n=0}^{\infty} W_n T_n.$$

These expansions are then truncated at the $n = N^{\text{th}}$ term and the D method described in Appendix A is used to construct

$$\mathbf{A}\mathbf{p} = R_a\mathbf{B}\mathbf{p},$$

where \mathbf{A} and \mathbf{B} are $(6N + 6) \times (6N + 6)$ matrices and \mathbf{p} is a $(6N + 6)$ vector constructed from the Chebyshev expansions of the variables $W, \chi_1, \Theta, \chi_2, \Phi, \chi_3$.

We begin by fixing the value of Le , setting λ and μ to almost zero and use the QZ algorithm to solve the eigenvalue problem, minimising over the wave number, k . We then increase λ and μ in small increments to maximise R_a , therefore finding the optimum stability boundary. We define the boundary of stability by $R_s = \max_{\lambda, \mu} R_a^2$.

We define λ_s and μ_s to be the values of λ and μ for which the maximum of R_a occurs and k_s to be the corresponding wave number. In Table 3.1 we give the values

of $R_s = R_a^2$ obtained for values of Le between 0 and 20. The corresponding values of R_c found in Chapter 2 that are on the instability boundary are also given for comparison. These results are displayed graphically in Figures 3.1-3.3.

Table 3.1: For $A = 0.5$, $B = 0.5$, values of μ , λ , k for which the non-linear stability curve is optimised and the corresponding values of R_s . The linear instability boundary R_c is given for comparison.

Le	μ_s	λ_s	k_s	R_a	R_s	R_c
0.1	0.37	2.99	2.325	9.0055	81.100	81.847
1.0	0.38	2.93	2.315	8.9097	79.382	86.836
2.0	0.39	2.86	2.295	8.8046	77.520	92.292
3.0	0.40	2.78	2.270	8.7011	75.709	97.550
4.0	0.44	2.64	2.300	8.5924	73.829	97.804
5.0	0.50	2.40	2.395	8.4364	71.174	93.145
6.0	0.53	2.12	2.450	8.2482	68.032	89.935
7.0	0.56	1.92	2.490	8.0455	64.730	87.577
8.0	0.58	1.74	2.520	7.8395	61.457	85.765
9.0	0.60	1.60	2.545	7.6367	58.319	84.329
10.0	0.61	1.46	2.560	7.4380	55.323	83.160
12.5	0.64	1.22	2.595	6.9811	48.736	81.016
15.0	0.65	1.04	2.615	6.5963	43.511	79.559
20.0	0.65	0.78	2.630	5.9595	35.516	77.716

To the left of the peak in the instability curve stationary convection occurs and the two boundaries are reasonably close together. However, to the right of the peak, when oscillatory convection, occurs the stability boundary drops away from the instability boundary.

The linear instability results obtained in Chapter 2 are useful as they provide a boundary above which we know that the system (3.1) with boundary conditions (3.2) is unstable, however they provide no information about stability or instability below this curve. For the greater value of B we see that for small Le there is increased stability, however the stability curve falls away from the instability curve

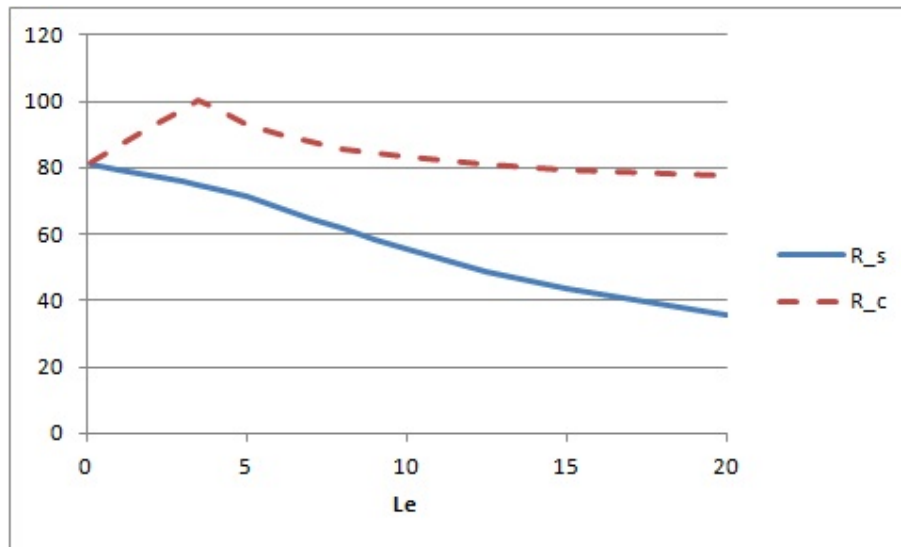


Figure 3.1: Linear instability (R_c) and non-linear energy stability (R_s) curves, for $A = 0.5$, $B = 0.5$.

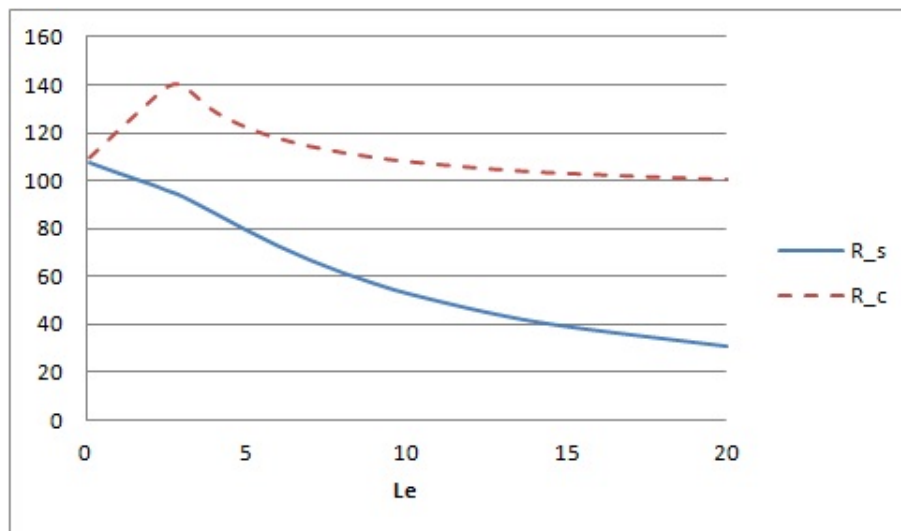


Figure 3.2: Linear instability (R_c) and non-linear energy stability (R_s) curves, for $A = 0.5$, $B = 1$.

more rapidly and hence for larger Le increasing B decreases the non-linear stability boundary, R_s . In Chapter 2 we found that when $\xi = 0$ doubling A doubled R_c , and Figures 3.2 and 3.3 show that doubling A also doubles R_s . For $0 < Le < 10$ the stability curve remains relatively close to the instability curve, irrespective of which value of A or B we choose, and the non-linear energy analysis used here is therefore of use.

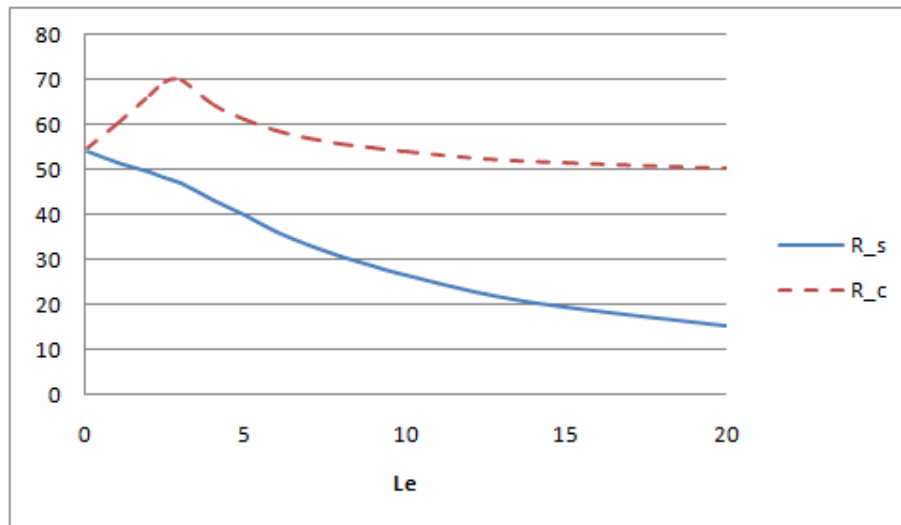


Figure 3.3: Linear instability (R_c) and non-linear energy stability (R_s) curves, for $A = 1$, $B = 1$.

From definition (3.7) we see that the value of $M\hat{\phi}$ does not influence the non-linear stability boundary, however it will affect the value of μ_s for which this boundary occurs.

Between the stability and instability boundaries we have no information about the stability and sub-critical instabilities may occur, however three dimensional computations would be needed to verify this.

Chapter 4

Continuous dependence of the Darcy model on the reaction parameters

An important concept in continuum mechanics problems is that of continuous dependence, or structural stability, of the model. Continuous dependence on a particular parameter means that if its value is altered by a small amount then the resulting change in the solution will remain relatively close. This is discussed in terms of differential equations by Hirsch & Smale [36] and in the area of porous media there have been many studies including those of Aulisa *et al.* [4], Celebi *et al.* [13], Franchi & Straughan [27], Hoang & Ibragimov [37], Lin & Payne [51–53], Liu [54], Liu *et al.* [55, 56], Ouyang & Yang [71], Payne *et al.* [74], Payne & Straughan [75, 76, 78], Rionero & Vergori [92], Straughan & Hutter [110], Straughan [109], Ugurlu [114], Wang & Lin [120], more references may be found in Chapter 2 of Straughan [107]. Of particular relevance to this chapter is Payne & Straughan [77], which shows that a Darcy porous medium of Newton cooling type depends continuously on both the cooling coefficient and a change in the equation of state in the body force.

In Chapters 2 and 3 we established instability and stability boundaries for a horizontal layer of a Darcy porous medium with a surface reaction. Due to the fact that the reaction terms are on the surface it is not obvious that the solution depends continuously on the reaction parameters and it is this that we aim to prove in this

chapter. We allow the density of the medium to have a linear dependence on the reactant concentration as well as the temperature, but as in Chapter 3 simplify the boundary conditions by assuming that the activation energy of the reaction is low.

Later in this thesis we discuss continuous dependence of a similar model employing the Brinkman model. The current problem is more complicated than in the later case as it is of lower order in the velocity. This means that a number of bounds that it is possible to derive there do not apply here. Due to the presence of the Laplacian velocity term in the Brinkman problem we may specify all of the velocity components on the boundary and employ the Sobolev inequality. We are not able to do this here and this is where the main issue arises. Instead we first derive a bound for the velocity gradient by splitting the velocity into symmetric and skew parts. It is then possible to use a result in Lin & Payne [53] to bound the L^4 velocity norm and proceed to establish continuous dependence.

4.1 The boundary-initial value problem

We assume that the porous medium occupies a general bounded region Ω in \mathbb{R}^3 and that the boundary of this region, Γ , is sufficiently smooth that the divergence theorem may be employed. The variables v_i , T , C and p again represent velocity, temperature, concentration and pressure respectively. Allowing the density to depend linearly on the concentration the analogue of the problem considered in Chapters 2 and 3 may then be written, without loss of generality, as

$$\begin{aligned} v_i &= -p_{,i} + g_i T + h_i C, \\ v_{i,i} &= 0, \\ T_{,t} + v_i T_{,i} &= \Delta T, \\ C_{,t} + v_i C_{,i} &= \Delta C, \end{aligned} \tag{4.1}$$

on $\Omega \times (0, \mathcal{T})$, for some $\mathcal{T} < \infty$, where Δ is the Laplace operator, g_i , h_i are gravity terms with $|\mathbf{g}| \leq 1$ and $|\mathbf{h}| \leq 1$.

We assume that the reaction is well catalysed so that the activation energy is low and that the temperature throughout the system is not small. The reaction

boundary conditions are then

$$v_i n_i = 0, \quad \frac{\partial T}{\partial n} = AC, \quad \frac{\partial C}{\partial n} = -BC, \quad (4.2)$$

on $\Gamma \times [0, \mathcal{T})$, where $\partial/\partial n$ denotes the unit normal derivative pointing out of Γ and A and B are positive constants.

We must also provide initial conditions that need to be satisfied and write these as

$$T(\mathbf{x}, 0) = T_0(\mathbf{x}), \quad C(\mathbf{x}, 0) = C_0(\mathbf{x}), \quad (4.3)$$

for general prescribed functions T_0 and C_0 .

The boundary-initial value problem is now comprised of (4.1) - (4.3) and we denote it by \mathcal{P} . In the following section we establish some auxilliary results and *a priori* estimates for T and C before going on to demonstrate continuous dependence on A and B .

4.2 *A priori estimates*

Before obtaining bounds for C and $\|T\|_4$ we first derive a bound for $\oint_{\Gamma} \psi^2 dA$, where ψ is a function defined on the closure of the domain, $\bar{\Omega}$, using a Rellich-like identity cf. Payne & Weinberger [73].

We commence by letting f_i , defined on Γ , be some function such that

$$f_i n_i \geq f_0 > 0 \quad \text{on } \Gamma,$$

where f_0 is a constant and n_i is the unit outward normal. Using the above estimate and employing the divergence theorem allows us to write

$$\begin{aligned} f_0 \oint_{\Gamma} \psi^2 dA &\leq \oint_{\Gamma} f_i n_i \psi^2 dA \\ &= \int_{\Omega} (f_i \psi^2)_{,i} dx \\ &= \int_{\Omega} f_{i,i} \psi^2 dx + 2 \int_{\Omega} f_i \psi \psi_{,i} dx. \end{aligned} \quad (4.4)$$

Assuming now that $|f_i| \leq m_2$ in Ω , where m_2 is dependent on the shape of Ω , and $f_{i,i} \leq m_1$ with m_1 and m_2 are both positive constants, the second term on the right

of (4.4) may be bounded as

$$\int_{\Omega} f_i \psi \psi_{,i} dx \leq \frac{m_2}{2\alpha} \int_{\Omega} \psi^2 dx + \frac{\alpha m_2}{2} \int_{\Omega} \psi_{,i} \psi_{,i} dx, \quad (4.5)$$

where we have used the arithmetic-geometric inequality with weight $\alpha > 0$ at our disposal. Finally, inserting inequality (4.5) into (4.4) we find the bound

$$f_0 \oint_{\Gamma} \psi^2 dA \leq \left(m_1 + \frac{m_2}{\alpha}\right) \int_{\Omega} \psi^2 dx + \alpha m_2 \int_{\Omega} \psi_{,i} \psi_{,i} dx. \quad (4.6)$$

4.2.1 C bound

We now derive a bound for C by considering

$$\frac{d}{dt} \int_{\Omega} C^{2p} dx = 2p \int_{\Omega} C^{2p-1} C_{,t} dx, \quad (4.7)$$

for $p \in \mathbb{N}$. Inserting (4.1)₄ into (4.7) and integrating by parts using the boundary conditions we find that

$$\begin{aligned} \frac{d}{dt} \int_{\Omega} C^{2p} dx &= 2p \int_{\Omega} C^{2p-1} (\Delta C - v_i C_{,i}) dx \\ &= -2p(2p-1) \int_{\Omega} C^{2p-2} |\nabla C|^2 dx - 2pB \oint_{\Gamma} C^{2p} dA \\ &\leq 0 \end{aligned}$$

and hence $\int_{\Omega} C^{2p} dx$ is decreasing in time. After integration we find that

$$\left(\int_{\Omega} C^{2p} dx \right)^{1/2p} \leq \left(\int_{\Omega} C_0^{2p} dx \right)^{1/2p},$$

where $C_0 = C(\mathbf{x}, 0)$. Finally, allowing $p \rightarrow \infty$ and using the definition of the supremum norm, $\|f\|_{\infty} = \sup\{\|f(\mathbf{x}, t)\| : \mathbf{x} \in \Omega, t \in [0, \mathcal{T}]\}$, we obtain

$$\sup_{\Omega \times [0, \mathcal{T}]} |C| \leq \max_{\Omega} |C_0| \equiv C_m. \quad (4.8)$$

4.2.2 $\|T\|_4$ bound

Next, we derive a bound for $\|T\|_4$, where $\|\cdot\|_4$ denotes the $L^4(\Omega)$ norm. Standard notation is used where $\|\cdot\|$ and (\cdot, \cdot) represent the $L^2(\Omega)$ norm and inner product.

To derive the desired bound we begin by writing

$$\frac{d}{dt} \frac{1}{4} \int_{\Omega} T^4 dx = \int_{\Omega} T^3 T_{,t} dx$$

and then, similarly to the derivation of the C bound, insert (4.1)₃. After integrating this by parts we may then find

$$\begin{aligned}
\frac{d}{dt} \frac{1}{4} \int_{\Omega} T^4 &= \int_{\Omega} T^3 (\Delta T - v_i T_{,i}) dx \\
&= -3 \int_{\Omega} T^2 T_{,i} T_{,i} dx + \oint_{\Gamma} T^3 \frac{\partial T}{\partial n} dA \\
&= -\frac{3}{4} \int_{\Omega} (T^2)_{,i} (T^2)_{,i} dx + A \oint_{\Gamma} T^3 C dA \\
&\leq -\frac{3}{4} \int_{\Omega} (T^2)_{,i} (T^2)_{,i} dx + \frac{3A}{4} \oint_{\Gamma} T^4 dA + \frac{A}{4} \oint_{\Gamma} C^4 dA, \quad (4.9)
\end{aligned}$$

where in the first step we have used the boundary conditions and in the final step we have used Young's inequality, $ab \leq a^p/p + b^q/q$ for $p, q > 0$ such that $1/p + 1/q = 1$. Estimate (4.6) is used on the second term in (4.9), where here the function ψ is T^2 , and we obtain

$$\begin{aligned}
\frac{d}{dt} \frac{1}{4} \int_{\Omega} T^4 dx &\leq -\frac{3}{4} \int_{\Omega} |\nabla T^2|^2 dx + \frac{A}{4} \oint_{\Gamma} C^4 dA \\
&\quad + \frac{3A}{4} \left(\frac{m_1}{f_0} + \frac{m_2}{f_0 \alpha} \right) \int_{\Omega} T^4 dx + \frac{3A \alpha m_2}{4 f_0} \int_{\Omega} |\nabla T^2|^2 dx.
\end{aligned}$$

We choose $\alpha = f_0/(m_2 A)$ in order to cancel the first and fourth terms. Now defining D_1 and λ to be

$$D_1 = AC_m^4 |\Gamma|, \quad \lambda = \frac{3m_1 A}{f_0} + \frac{3m_2^2 A^2}{f_0^2},$$

where in the definition of D_1 we have used estimate (4.8) and $|\Gamma|$ is the measure of Γ we find

$$\frac{d}{dt} \int_{\Omega} T^4 dx \leq D_1 + \lambda \int_{\Omega} T^4 dx. \quad (4.10)$$

Setting $F(t) = \int_{\Omega} T^4 dx$ inequality (4.10) becomes

$$\frac{dF}{dt} \leq D_1 + \lambda F$$

and, after integrating, we find

$$F(t) \leq F(0)e^{\lambda t} + \frac{D_1}{\lambda} e^{\lambda t}. \quad (4.11)$$

From (4.11) we now find a bound for $\|T\|_4$ in terms of given data by observing that

$$\|T(t)\|_4 \leq D_2, \quad (4.12)$$

where

$$D_2^4 = (F(0) + D_1 \lambda^{-1}) \exp[\lambda T].$$

4.2.3 $\|\mathbf{v}\|^2$ bound

We now derive a bound for $\|\mathbf{v}\|^2$, beginning by multiplying equation (4.1)₁ by v_i and integrating over Ω to form

$$\int_{\Omega} |\mathbf{v}|^2 dx = \int_{\Omega} v_i (-p_{,i} + g_i T + h_i C) dx. \quad (4.13)$$

After integrating the first term by parts, using the boundary conditions and the incompressibility condition, (4.1)₂, we find that

$$\int_{\Omega} v_i p_{,i} dx = 0.$$

We next use the arithmetic-geometric inequality on the second and third terms on the right hand side of (4.13) with weights $\alpha_1, \alpha_2 > 0$, respectively, to find

$$\int_{\Omega} |\mathbf{v}|^2 dx \leq \frac{\alpha_1}{2} \int_{\Omega} |g|^2 T^2 dx + \frac{1}{2\alpha_1} \int_{\Omega} |\mathbf{v}|^2 dx + \frac{\alpha_2}{2} \int_{\Omega} |h|^2 C^2 dx + \frac{1}{2\alpha_2} \int_{\Omega} |\mathbf{v}|^2 dx.$$

Setting $\alpha_1 = \alpha_2 = 2$ and remembering that $|g|^2 \leq 1$ and $|h|^2 \leq 1$ we obtain the bound

$$\|\mathbf{v}\|^2 = \int_{\Omega} |\mathbf{v}|^2 dx \leq 2 \int_{\Omega} T^2 dx + 2 \int_{\Omega} C^2 dx. \quad (4.14)$$

4.2.4 $\|\nabla \mathbf{v}\|^2$ bound

The final *a priori* bound that we must derive is for $\|\nabla \mathbf{v}\|^2$. We commence this following the technique used in Lin & Payne [53] and split the velocity gradient into symmetric and skew parts. It may then be written as

$$\int_{\Omega} |\nabla \mathbf{v}|^2 dx = \int_{\Omega} (v_{i,j} - v_{j,i}) v_{i,j} dx + \int_{\Omega} v_{i,j} v_{j,i} dx, \quad (4.15)$$

and we continue by separately bounding the two terms on the right hand side.

To handle the first term we differentiate (4.1)₁ and form

$$\begin{aligned} \int_{\Omega} (v_{i,j} - v_{j,i}) v_{i,j} dx &= \int_{\Omega} (g_i T_{,j} + h_i C_{,j} - g_j T_{,i} - h_j C_{,i}) v_{i,j} dx \\ &= \int_{\Omega} (g_i T_{,j} - g_j T_{,i}) v_{i,j} dx + \int_{\Omega} (h_i C_{,j} - h_j C_{,i}) v_{i,j} dx \end{aligned}$$

where we have used the fact that as g_i and h_i are gravity terms $g_{i,j} = 0$ and $h_{i,j} = 0$.

We now employ the arithmetic-geometric inequality on each of the two terms, with

weights $\mu_1 > 0$ and $\mu_2 > 0$ at our disposal to obtain the inequality

$$\begin{aligned} \int_{\Omega} (v_{i,j} - v_{j,i}) v_{i,j} dx &\leq \frac{\mu_1}{2} \int_{\Omega} (g_i T_{,j} - g_j T_{,i}) (g_i T_{,j} - g_j T_{,i}) dx \\ &\quad + \frac{\mu_2}{2} \int_{\Omega} (h_i C_{,j} - h_j C_{,i}) (h_i C_{,j} - h_j C_{,i}) dx \\ &\quad + \frac{1}{2\mu_1} \int_{\Omega} |\nabla \mathbf{v}|^2 dx + \frac{1}{2\mu_2} \int_{\Omega} |\nabla \mathbf{v}|^2 dx. \end{aligned}$$

We now choose $\mu_1 = \mu_2 = 2$ to obtain

$$\begin{aligned} \int_{\Omega} (v_{i,j} - v_{j,i}) v_{i,j} dx &\leq 2 \int_{\Omega} (|\nabla T|^2 - g_i T_{,i} g_j T_{,j}) dx \\ &\quad + 2 \int_{\Omega} (|\nabla C|^2 - h_i C_{,i} h_j C_{,j}) dx + \frac{1}{2} \int_{\Omega} |\nabla \mathbf{v}|^2 dx, \end{aligned}$$

where we have used the fact that $|\mathbf{g}|^2 \leq 1$ and $|\mathbf{h}|^2 \leq 1$. Further use of the arithmetic-geometric inequality on the temperature and concentration cross terms with weights $\mu_3 > 0$, $\mu_4 > 0$ yields

$$\begin{aligned} \int_{\Omega} (v_{i,j} - v_{j,i}) v_{i,j} dx &\leq 2 \int_{\Omega} \left(|\nabla T|^2 + \frac{1}{2\mu_3} |\nabla T|^2 + \frac{\mu_3}{2} |\nabla T|^2 \right) dx \\ &\quad + 2 \int_{\Omega} \left(|\nabla C|^2 + \frac{1}{2\mu_4} |\nabla C|^2 + \frac{\mu_4}{2} |\nabla C|^2 \right) dx \\ &\quad + \frac{1}{2} \int_{\Omega} |\nabla \mathbf{v}|^2 dx. \end{aligned} \quad (4.16)$$

We choose the optimum values of $\mu_3 = \mu_4 = 1$, and then inequality (4.16) simplifies to

$$\int_{\Omega} (v_{i,j} - v_{j,i}) v_{i,j} dx \leq 4 \int_{\Omega} |\nabla T|^2 dx + 4 \int_{\Omega} |\nabla C|^2 dx + \frac{1}{2} \int_{\Omega} |\nabla \mathbf{v}|^2 dx. \quad (4.17)$$

To handle the second term on the right hand side of (4.15) we use the divergence theorem and integrate by parts, obtaining

$$\int_{\Omega} v_{i,j} v_{j,i} = \oint_{\partial\Omega} (v_i n_i)_{,j} v_j dS - \oint_{\partial\Omega} n_{i,j} v_i v_j dS = - \oint_{\partial\Omega} n_{i,j} v_i v_j dS, \quad (4.18)$$

where we have used the fact that the product of a tangential vector and a normal vector is zero. Lin & Payne [53] state that

$$\int_{\Omega} v_{i,j} v_{j,i} dx \leq 0$$

for convex Ω and

$$\int_{\Omega} v_{i,j} v_{j,i} dx \leq k_0 \oint_{\partial\Omega} |\mathbf{v}|^2 dS,$$

for non-convex Ω with bounded curvature, where k_0 depends on the Gaussian curvature of Ω . We do not believe this to be immediately obvious and therefore use differential geometry to prove the results.

We begin by letting $x^i = x^i(u^\alpha)$ be functions that represent a surface, where Latin indices run from 1 to 3 and represent the spacial coordinates and Greek indices take the values 1 or 2 and represent the surface coordinates. We also use the results

$$\begin{aligned}
v_i &= g_{ik}v^k, & \text{where } g_{ik} \text{ is the spacial metric,} \\
v_\beta &= a_{\alpha\beta}v^\alpha, & \text{where } a_{\alpha\beta} \text{ is the surface metric,} \\
A^i &= x^i_{,\alpha}A^\alpha, & \text{where } x^i_{,\alpha} \equiv \partial x^i / \partial u^\alpha, \\
g_{ij}g^{jk} &= \delta_i^k, \\
g_{ij}x^i_{,\alpha}x^j_{,\beta}A^\alpha B^\beta &= a_{\alpha\beta}A^\alpha B^\beta,
\end{aligned} \tag{4.19}$$

c.f. Spain [104].

The indices of the velocity vectors in (4.18) are raised using (4.19)₁ and we then use (4.19)₃ to find

$$\begin{aligned}
\int_{\Omega} v_{i,j}v_{j,i}dx &= - \oint_{\partial\Omega} n_{i,j}v_i v_j dS \\
&= - \oint_{\partial\Omega} n_{i,j}g_{ik}x^k_{,\alpha}v^\alpha g_{jm}x^m_{,\beta}v^\beta dS.
\end{aligned}$$

In order to employ (4.19)₅ we require g_{km} to be present and so first multiply by $g_{km}g^{km} = 1$. Then, also using (4.19)₄ and (4.19)₂, we obtain

$$\begin{aligned}
\int_{\Omega} v_{i,j}v_{j,i}dx &= - \oint_{\partial\Omega} n_{i,j}g_{ik}x^k_{,\alpha}v^\alpha g_{jm}x^m_{,\beta}v^\beta g_{km}g^{km}dS \\
&= - \oint_{\partial\Omega} n_{i,j}g_{ik}v^\alpha g_{jm}v^\beta a_{\alpha\beta}g^{km}dS \\
&= - \oint_{\partial\Omega} n_{i,j}g_{ij}v^\alpha v_\alpha dS \\
&= - \oint_{\partial\Omega} n_{i,j}g_{ij}|\mathbf{v}|^2 dS.
\end{aligned}$$

The term $n_{i,j}g_{ij}$ may be positive or negative depending on the shape of the surface; if the curvature of the surface is bounded then $n_{i,j}g_{ij}$ is finite and if Ω is convex then $n_{i,j}g_{ij} > 0$. We may therefore derive

$$\int_{\Omega} v_{i,j}v_{j,i}dx \leq k_0 \oint_{\partial\Omega} |\mathbf{v}|^2 dS$$

for some $k_0 > 0$ for Ω which is either convex or non-convex with bounded curvature.

To bound $\oint_{\partial\Omega} |\mathbf{v}|^2 dS$ we introduce a vector field $q_i(x)$ satisfying

$$\begin{aligned} |q_i| &\leq M, & |q_{i,i}| &\leq M \quad \text{in } \Omega, \\ q_i n_i &\geq q_0 > 0 & & \text{on } \partial\Omega, \end{aligned}$$

as in Lin & Payne [53]. We use these bounds, the divergence theorem and the arithmetic-geometric inequality, with weight $\mu_5 > 0$ at our disposal, to finally bound $\int_{\Omega} v_{i,j} v_{j,i} dx$ in terms of $\int_{\Omega} |\mathbf{v}|^2 dx$ and $\int_{\Omega} |\nabla \mathbf{v}|^2 dx$;

$$\begin{aligned} q_0 \int_{\Omega} v_{i,j} v_{j,i} dx &\leq k_0 \oint_{\partial\Omega} q_i n_i |\mathbf{v}|^2 dS \\ &= k_0 \int_{\Omega} q_{i,i} |\mathbf{v}|^2 dx + 2k_0 \int_{\Omega} q_i v_j v_{j,i} dx \\ &= k_0 M \int_{\Omega} |\mathbf{v}|^2 dx + 2k_0 M \int_{\Omega} v_j v_{j,i} dx \\ &\leq k_0 \left(M + \frac{M}{\mu_5} \right) \int_{\Omega} |\mathbf{v}|^2 dx + k_0 M \mu_5 \int_{\Omega} |\nabla \mathbf{v}|^2 dx. \end{aligned} \quad (4.20)$$

Inserting inequalities (4.17) and (4.20) into (4.15) and using (4.14) we finally find

$$\begin{aligned} \left(\frac{1}{2} - \frac{k_0}{q_0} M \mu_5 \right) \int_{\Omega} |\nabla \mathbf{v}|^2 dx &\leq 4 \int_{\Omega} (|\nabla T|^2 + |\nabla C|^2) dx \\ &\quad + \frac{2k_0 M}{q_0} \left(1 + \frac{1}{\mu_5} \right) \int_{\Omega} (T^2 + C^2) dx, \end{aligned}$$

with the condition that μ_5 is chosen sufficiently small that $1 - 2k_0 M \mu_5 / q_0 > 0$. This may be written as

$$\|\nabla \mathbf{v}\|^2 = \int_{\Omega} |\nabla \mathbf{v}|^2 dx \leq \hat{M} \int_{\Omega} (|\nabla T|^2 + |\nabla C|^2 + T^2 + C^2) dx, \quad (4.21)$$

where

$$\hat{M} = \frac{2q_0}{(q_0 - 2k_0 M \mu_5)} \max \left[4, \frac{2k_0 M}{q_0} \left(1 + \frac{1}{\mu_5} \right) \right].$$

4.3 Continuous dependence on the boundary reaction terms

We now consider two solutions to our initial value problem \mathcal{P} , namely (v_i, T, C, p) and (v_i^*, T^*, C^*, p^*) , for different boundary parameters (A, B) and (A^*, B^*) in (4.2),

respectively, but with the same initial conditions. We define difference variables u_i , π , θ , ϕ , a and b by

$$\begin{aligned} u_i &= v_i - v_i^*, & \pi &= p - p^*, & \theta &= T - T^*, \\ \phi &= C - C^*, & a &= A - A^*, & b &= B - B^*. \end{aligned}$$

We find that these satisfy the boundary-initial value problem

$$\begin{aligned} u_i + \pi_{,i} - g_i \theta - h_i \phi &= 0, \\ u_{i,i} &= 0, \\ \theta_{,t} + v_i \theta_{,i} + u_i T_{,i}^* &= \Delta \theta, \\ \phi_{,t} + v_i \phi_{,i} + u_i C_{,i}^* &= \Delta \phi, \end{aligned} \tag{4.22}$$

in $\Omega \times (0, \mathcal{T})$ with the boundary conditions

$$u_i n_i = 0, \quad \frac{\partial \theta}{\partial n} = aC + A^* \phi, \quad \frac{\partial \phi}{\partial n} = -(bC + B^* \phi),$$

on $\Gamma \times [0, \mathcal{T}]$, and the initial data

$$\theta(\mathbf{x}, 0) = 0, \quad \phi(\mathbf{x}, 0) = 0, \quad \mathbf{x} \in \Omega.$$

We are now in a position to prove that the solution is continuously dependent on the boundary condition parameters, i.e. that it may be shown to satisfy

$$\|\theta(t)\|^2 + \|\phi(t)\|^2 \leq c_1(a^2 + b^2)$$

and

$$\|\mathbf{u}(t)\|^2 \leq c_2(a^2 + b^2)$$

for $t \in (0, \mathcal{T})$, computable for specific *a priori* time dependent coefficients c_1 and c_2 .

We begin the proof of this by multiplying (4.22)₁ by u_i , and integrating over Ω . The arithmetic-geometric mean inequality is then used twice to obtain

$$\begin{aligned} \|\mathbf{u}\|^2 &= (g_i \theta, u_i) + (h_i \phi, u_i) \\ &\leq \|\theta\|^2 + \frac{1}{4} \|\mathbf{u}\|^2 + \|\phi\|^2 + \frac{1}{4} \|\mathbf{u}\|^2. \end{aligned}$$

This then yields a bound for $\|\mathbf{u}\|^2$ in terms of $\|\theta\|^2$ and $\|\phi\|^2$ given by;

$$\frac{1}{2} \|\mathbf{u}\|^2 \leq \|\theta\|^2 + \|\phi\|^2. \tag{4.23}$$

Equations (4.22)₃ and (4.22)₄ are now multiplied by θ and ϕ , respectively, and we find that after integration by parts and use of the boundary conditions

$$\frac{d}{dt} \frac{1}{2} \|\theta\|^2 = (u_i T^*, \theta_{,i}) - \|\nabla \theta\|^2 + a \oint_{\Gamma} C \theta dA + A^* \oint_{\Gamma} \theta \phi dA, \quad (4.24)$$

and

$$\frac{d}{dt} \frac{1}{2} \|\phi\|^2 = (u_i C^*, \phi_{,i}) - \|\nabla \phi\|^2 - b \oint_{\Gamma} C \phi dA - B^* \oint_{\Gamma} \phi^2 dA. \quad (4.25)$$

On the third and fourth terms of the right hand side of (4.24) and the third term on the right hand side of (4.25) we use the arithmetic-geometric inequality with weights $\lambda_1, \lambda_2, \lambda_3 > 0$, respectively, and add the results to obtain

$$\begin{aligned} \frac{1}{2} \frac{d}{dt} (\|\theta\|^2 + \|\phi\|^2) &\leq (u_i T^*, \theta_{,i}) + (u_i C^*, \phi_{,i}) - \|\nabla \theta\|^2 - \|\nabla \phi\|^2 \\ &\quad + \left(\frac{a^2}{2\lambda_1} + \frac{b^2}{2\lambda_3} \right) \oint_{\Gamma} C^2 dA + \left(\frac{\lambda_1}{2} + \frac{A^*}{2\lambda_2} \right) \oint_{\Gamma} \theta^2 dA \\ &\quad + \left(\frac{A^* \lambda_2}{2} - B^* + \frac{\lambda_3}{2} \right) \oint_{\Gamma} \phi^2 dA. \end{aligned} \quad (4.26)$$

On the concentration cubic term we use estimate (4.8) and the Cauchy-Schwarz inequality, followed by the arithmetic-geometric inequality with weight $\lambda_4 > 0$ to find

$$(u_i C^*, \phi_{,i}) \leq C_m \|\mathbf{u}\| \|\nabla \phi\| \leq \frac{C_m^2}{2\lambda_4} \|\mathbf{u}\|^2 + \frac{\lambda_4}{2} \|\nabla \phi\|^2. \quad (4.27)$$

On the temperature cubic term we use the Cauchy-Schwarz inequality twice, employ estimate (4.12) and then use the arithmetic-geometric inequality with weight $\lambda_5 > 0$. From this we obtain

$$\begin{aligned} (u_i T^*, \theta_{,i}) &\leq \|\nabla \theta\| \left(\int_{\Omega} u_i u_i T^* T^* dx \right)^{\frac{1}{2}} \\ &\leq \|\nabla \theta\| \|\mathbf{u}\|_4 \|T^*\|_4 \\ &\leq D_2 \|\nabla \theta\| \|\mathbf{u}\|_4 \\ &\leq \frac{D_2^2}{2\lambda_5} \|\nabla \theta\|^2 + \frac{\lambda_5}{2} \|\mathbf{u}\|_4. \end{aligned} \quad (4.28)$$

Inserting inequalities (4.27) and (4.28) into (4.26) yields

$$\begin{aligned} \frac{1}{2} \frac{d}{dt} (\|\theta\|^2 + \|\phi\|^2) &\leq \frac{\lambda_5}{2} \|\mathbf{u}\|_4^2 + \frac{C_m^2}{2\lambda_4} \|\mathbf{u}\|^2 + \left(\frac{\lambda_4}{2} - 1\right) \|\nabla\phi\|^2 \\ &\quad + \left(\frac{D_2^2}{2\lambda_5} - 1\right) \|\nabla\theta\|^2 + \left(\frac{a^2}{2\lambda_1} + \frac{b^2}{2\lambda_3}\right) C_m^2 |\Gamma| \\ &\quad + \left(\frac{\lambda_1}{2} + \frac{A^*}{2\lambda_2}\right) \oint_{\Gamma} \theta^2 dA \\ &\quad + \left(\frac{A^*\lambda_2}{2} - B^* + \frac{\lambda_3}{2}\right) \oint_{\Gamma} \phi^2 dA. \end{aligned}$$

We now let the function ψ in (4.6) be θ to obtain the Rellich identity

$$\oint_{\Gamma} \theta^2 dA \leq \left(\frac{m_1}{f_0} + \frac{m_2}{\hat{\alpha}f_0}\right) \|\theta\|^2 + \frac{\hat{\alpha}m_2}{f_0} \|\nabla\theta\|^2.$$

Using this identity and the estimate (4.23) for $\|\mathbf{u}\|^2$ we find

$$\begin{aligned} \frac{1}{2} \frac{d}{dt} (\|\theta\|^2 + \|\phi\|^2) &\leq \frac{\lambda_5}{2} \|\mathbf{u}\|_4^2 + \kappa_1 (\|\theta\|^2 + \|\phi\|^2) + \left(\frac{\lambda_4}{2} - 1\right) \|\nabla\phi\|^2 \\ &\quad + \left(\frac{D_2^2}{2\lambda_5} - 1 + \left(\frac{\lambda_1}{2} + \frac{A^*}{2\lambda_2}\right) \frac{\hat{\alpha}m_2}{f_0}\right) \|\nabla\theta\|^2 \\ &\quad + \left(\frac{a^2}{2\lambda_1} + \frac{b^2}{2\lambda_3}\right) C_m^2 |\Gamma| \\ &\quad + \left(\frac{A^*\lambda_2}{2} - B^* + \frac{\lambda_3}{2}\right) \oint_{\Gamma} \phi^2 dA, \end{aligned} \tag{4.29}$$

where

$$\kappa_1 = \frac{C_m^2}{\lambda_4} + \left(\frac{\lambda_1}{2} + \frac{A^*}{2\lambda_2}\right) \left(\frac{m_1}{f_0} + \frac{m_2}{\hat{\alpha}f_0}\right).$$

We find that the result given in Appendix B of Lin & Payne [53] for $\|\mathbf{u}\|_4^2$:

$$\begin{aligned} \left(\int_{\Omega} |\mathbf{u}|^4 dx\right)^{1/2} &\leq \frac{1}{2\sqrt{2}} \left(\int_{\Omega} |\mathbf{u}|^2 dx\right)^{1/4} \\ &\quad \cdot \left[\frac{3}{p_0} \left(\int_{\Omega} |\mathbf{u}|^2 dx\right)^{1/2} + \frac{2(R+p_0)}{p_0} \left(\int_{\Omega} |\nabla\mathbf{u}|^2 dx\right)^{1/2} \right]^{1/2} \\ &\quad \cdot \left[\frac{3}{p_0} \left(\int_{\Omega} |\mathbf{u}|^2 dx\right)^{1/2} + \frac{3(R+p_0)}{p_0} \left(\int_{\Omega} |\nabla\mathbf{u}|^2 dx\right)^{1/2} \right], \end{aligned}$$

holds here, where $p_0 = \min_{\bar{\Omega}} x_i n_i$ and $R^2 = \max_{\bar{\Omega}} |x|^2$. To simplify this result we rewrite it as

$$\left(\int_{\Omega} |\mathbf{u}|^4 dx\right)^{1/2} \leq \hat{\kappa}_2 \left(\int_{\Omega} |\mathbf{u}|^2 dx\right)^{1/4} \left[\left(\int_{\Omega} |\mathbf{u}|^2 dx\right)^{1/2} + \left(\int_{\Omega} |\nabla\mathbf{u}|^2 dx\right)^{1/2} \right]^{3/2}$$

where

$$\hat{\kappa}_2 = \frac{1}{2\sqrt{2}} \max \left[\sqrt{\frac{3}{p_0}}, \sqrt{\frac{2(R+p_0)}{p_0}} \right] \cdot \max \left[\frac{3}{p_0}, \frac{3(R+p_0)}{p_0} \right].$$

Using the inequality

$$(a^{1/2} + b^{1/2})^{3/2} \leq \sqrt{2}(a^{3/4} + b^{3/4})$$

it can then be shown that

$$\begin{aligned} \left(\int_{\Omega} |\mathbf{u}|^4 dx \right)^{1/2} &\leq \hat{\kappa}_2 \left(\int_{\Omega} |\mathbf{u}|^2 dx \right)^{1/4} \cdot \sqrt{2} \left[\left(\int_{\Omega} |\mathbf{u}|^2 dx \right)^{3/4} + \left(\int_{\Omega} |\nabla \mathbf{u}|^2 dx \right)^{3/4} \right] \\ &= \kappa_2 \left(\int_{\Omega} |\mathbf{u}|^2 dx \right) + \kappa_2 \left(\int_{\Omega} |\mathbf{u}|^2 dx \right)^{1/4} \left(\int_{\Omega} |\nabla \mathbf{u}|^2 dx \right)^{3/4}, \end{aligned}$$

where $\kappa_2 = \sqrt{2}\hat{\kappa}_2$.

Next we use Young's inequality on the second term,

$$\left(\int_{\Omega} |\mathbf{u}|^2 dx \right)^{1/4} \left(\int_{\Omega} |\nabla \mathbf{u}|^2 dx \right)^{3/4} \leq \frac{1}{4} \left(\int_{\Omega} |\mathbf{u}|^2 dx \right) + \frac{3}{4} \left(\int_{\Omega} |\nabla \mathbf{u}|^2 dx \right),$$

and then estimate (4.21) to derive

$$\|\mathbf{u}\|_4^2 \leq \frac{5\kappa_2}{4} \|\mathbf{u}\|^2 + \frac{3\kappa_2}{4} \hat{M} [\|\nabla \theta\|^2 + \|\nabla \phi\|^2 + \|\theta\|^2 + \|\phi\|^2]. \quad (4.30)$$

Inserting (4.30) into (4.29) and again using the estimate (4.23) we see that

$$\begin{aligned} \frac{1}{2} \frac{d}{dt} (\|\theta\|^2 + \|\phi\|^2) &\leq \kappa_3 (\|\theta\|^2 + \|\phi\|^2) + \left(\frac{\lambda_4}{2} - 1 + \frac{3\kappa_2\lambda_5}{8} \hat{M} \right) \|\nabla \phi\|^2 \\ &\quad + \left(\frac{D_2^2}{2\lambda_5} - 1 + \left(\frac{\lambda_1}{2} + \frac{A^*}{2\lambda_2} \right) \frac{\hat{a}m_2}{f_0} + \frac{3\kappa_2\lambda_5}{8} \hat{M} \right) \|\nabla \theta\|^2 \\ &\quad + \left(\frac{a^2}{2\lambda_1} + \frac{b^2}{2\lambda_3} \right) C_m^2 |\Gamma| \\ &\quad + \left(\frac{A^*\lambda_2}{2} - B^* + \frac{\lambda_3}{2} \right) \oint_{\Gamma} \phi^2 dA, \end{aligned} \quad (4.31)$$

where

$$\kappa_3 = \kappa_1 + \frac{\kappa_2\lambda_5}{4} (3\hat{M} + 5).$$

We require that the coefficients of the $\|\nabla \phi\|^2$, $\|\nabla \theta\|^2$ and $\oint_{\Gamma} \phi^2 dA$ terms are ≤ 0

and make the choices

$$\begin{aligned}\lambda_1 &= \frac{f_0}{\hat{\alpha}m_2} \left(1 - \frac{3}{4}D_2^2\kappa_2\hat{M} \right) - \frac{A^*A^*}{B^*}, \\ \lambda_2 &= \frac{B^*}{A^*}, \\ \lambda_3 &= B^*, \\ \lambda_4 &= 1, \\ \lambda_5 &= \frac{4}{3\kappa_2\hat{M}}\end{aligned}$$

in order that equality holds and we may cancel the terms. This gives the restriction

$$\frac{4}{3\kappa_2\hat{M}} \geq D_2^2$$

on the data and we must choose $\hat{\alpha}$ to be sufficiently small that $\lambda_1 > 0$. Inequality (4.31) then simplifies to leave

$$\frac{d}{dt} (\|\theta\|^2 + \|\phi\|^2) \leq 2\kappa_3 (\|\theta\|^2 + \|\phi\|^2) + \kappa_4 (a^2 + b^2), \quad (4.32)$$

where

$$\kappa_4 = C_m^2 |\Gamma| \max \left[\frac{1}{\lambda_1}, \frac{1}{\lambda_3} \right].$$

We now define an energy $G(t)$ by

$$G(t) = \|\theta\|^2 + \|\phi\|^2$$

and write (4.32) in the form

$$\frac{d}{dt} G \leq 2\kappa_3 G + \kappa_4 (a^2 + b^2).$$

This function is easily integrated to find

$$G(t) \leq \frac{\kappa_4}{2\kappa_3} e^{2\kappa_3 t} (a^2 + b^2),$$

which demonstrates continuous dependence on the boundary parameters A and B in the measures $\|\theta\|$ and $\|\phi\|$. Finally, from inequality (4.23) we deduce that there is also continuous dependence on A and B in the measure $\|\mathbf{u}\|$.

Chapter 5

Influence of the Soret effect on instability boundaries for the Darcy model

It is well known in the literature regarding convection in fluids and porous media that a thermal gradient may induce a small matter flow called the Soret effect, this is discussed in, for example, Piazza & Guarino [80] and Soret [103]. This cross-diffusion effect may cause the denser component of a multi-component system to diffuse to a cooler region, considered the positive direction, or to a warmer region, which is the negative direction. When studying many natural processes, such as chemical reactions in sediments, c.f. Domenico [19], the Soret effect may be significant and cannot be neglected. The reciprocal effect in which a solutal gradient causes a thermal flux is called the Dufour effect. In recent years a large number of articles on these cross-diffusion effects have been published and references to these may be found in Section 9.1.4 of Nield & Bejan [70].

Continuous dependence on the Soret coefficient has been established for fixed boundary conditions using both the Brinkman model, Straughan & Hutter [110], and the Darcy model, Lin & Payne [53]. The influence of both the Soret and Dufour effects has been studied in many different models, vertical studies include those of Tai & Char [113] who considered non-Newtonian fluids and Postelnicu [83] who modelled a chemical reaction in a porous medium, a visco elastic fluid flow over

a stretching sheet is investigated by Salem [93], Alam *et al* [2] examine magneto-hydrodynamic mixed convection on an inclined plate and include a chemical reaction and heat generation, Malashetty and & Biradar [58] study a Maxwell fluid and Lakshmi Narayana & Murthy [47] analyse free convection in a horizontal plate of a Darcy porous medium.

In this chapter we will investigate how the Soret effect influences the stability of our previous problem in Chapter 2, namely that of a horizontal layer of a Darcy porous medium saturated by an incompressible fluid and with an exothermic surface reaction on the lower boundary. We again assume that the density is independent of concentration and depends linearly on temperature. With this assumption the momentum equation, incompressibility condition and temperature conservation equation are

$$\begin{aligned} p_{,i} &= \frac{\mu}{K}v_i - g\rho_0(1 - \alpha(T - T_0))k_i, \\ v_{i,i} &= 0, \\ \frac{1}{M}T_{,t} + v_iT_{,i} &= \kappa\Delta T, \end{aligned} \tag{5.1}$$

where the variables \mathbf{v} , T and p are the fluid velocity, temperature and pressure, respectively, and the parameters μ , K , g , ρ_0 , α , T_0 , M and κ are as defined in Chapter 2. The Soret effect is included in the reactant concentration conservation equation, which becomes

$$\phi C_{,t} + v_i C_{,i} = \phi k_c \Delta C + \phi k_s \Delta T, \tag{5.2}$$

where C is the reactant concentration, ϕ is the porosity of the medium, k_c is the diffusivity of the reactant and k_s is a Soret coefficient.

On the upper boundary wall the temperature and reactant concentration are held constant and there is no mass flux across the boundary so we find the conditions

$$n_i v_i = 0, \quad T = T_U, \quad C = C_U \quad \text{on } z = h,$$

where $\mathbf{n} = (0, 0, 1)$ is the unit outward normal.

We assume that the exothermic reaction on the lower boundary wall occurs at a rate r , where

$$r = k_0 C \exp\left(\frac{-E}{R^*T}\right).$$

As in Chapter 2, k_0 is a rate constant, R^* is the universal gas constant, E is the reaction's activation energy and the product of the reaction is assumed to be inert. The boundary conditions are now obtained by consideration of the mass, temperature and reactant concentration fluxes. As the boundary is solid there is no mass flux across it. The heat flux $\mathbf{q} = -k_m \nabla T$ is the rate at which heat crosses the boundary and is proportional to the heat of the reaction, Q , and the rate at which it occurs. Due to the presence of the Soret term the concentration flux is also influenced by the temperature gradient. We rewrite the right-hand side of (5.2) as $-\phi \nabla \mathbf{J}$, where $\mathbf{J} = -k_c \nabla C - k_s \nabla T$. This flux \mathbf{J} is proportional to the rate at which the reaction occurs and inversely proportional to the porosity. We then obtain the boundary conditions

$$\begin{aligned} v_i n_i &= 0, \\ k_m \frac{dT}{dz} &= -Q k_0 C \exp\left(\frac{-E}{R^* T}\right), \\ \phi k_c \frac{dC}{dz} + \phi k_s \frac{dT}{dz} &= k_0 C \exp\left(\frac{-E}{R^* T}\right) \quad \text{on } z = 0. \end{aligned}$$

5.1 Non-dimensional linear perturbation equations

We begin by following the standard linear analysis that was used in Chapter 2 and non-dimensionalise equations (5.1) and (5.2) using the variables

$$\begin{aligned} x_i &= h x_i^*, & t &= \frac{h^2}{\kappa M} t^*, & v_i &= \frac{\kappa}{h} v_i^*, \\ C &= C_U C^*, & T &= T_U T^*, & p &= \frac{\kappa \mu}{K} p^*. \end{aligned}$$

After dropping the $\hat{}$ symbols we find

$$\begin{aligned} p_{,i} &= v_i - \frac{Kh}{\kappa \mu} g \rho_0 (1 - \alpha T_U (T - T_0)) k_i, \\ v_{i,i} &= 0, \\ T_{,t} + v_i T_{,i} &= \Delta T, \\ M \phi C_{,t} + v_i C_{,i} &= \frac{1}{Le} \Delta C + S \Delta T, \end{aligned} \tag{5.3}$$

where $Le = \kappa / (\phi k_c)$ and

$$S = \frac{T_U \phi k_s}{C_U \kappa}$$

is the Soret parameter with the boundary conditions

$$n_i v_i = 0, \quad T = 1, \quad C = 1 \quad \text{on } z = 1, \quad (5.4)$$

and

$$\begin{aligned} v_i n_i &= 0, \\ \frac{dT}{dz} &= -AC \exp\left(\frac{-\xi}{T}\right), \\ \frac{dC}{dz} + H \frac{dT}{dz} &= BC \exp\left(\frac{-\xi}{T}\right) \quad \text{on } z = 0, \end{aligned} \quad (5.5)$$

where

$$A = \frac{Qk_0 C_U h}{k_m T_U}, \quad B = \frac{k_0 h}{\phi k_c}, \quad H = \frac{k_s T_U}{k_c C_U}, \quad \xi = \frac{E}{R^* T_U}.$$

We consider a steady state $(\bar{\mathbf{v}}, \bar{T}, \bar{C}, \bar{p})$ to exist, such that $v_i = 0$, $T_{,t} = 0$ and $C_{,t} = 0$. After again employing the assumption that T and C are functions of z only we find from (5.3) that

$$\bar{T} = \beta_1 z + \beta_2,$$

$$\bar{C} = \beta_3 z + \beta_4,$$

where the β_i will be obtained by evaluating the steady state on the lower boundary and take different values to those in Chapter 2. We now introduce small perturbations u_i, π, θ, γ , from the steady state to (5.3) where

$$v_i = \bar{v}_i + u_i, \quad p = \bar{p} + \pi,$$

$$T = \bar{T} + \theta, \quad C = \bar{C} + \gamma,$$

then subtract the steady state and neglect terms which are the product of two perturbations to find the linearised, non-dimensional perturbation equations

$$0 = \Delta w - R \Delta^* \theta,$$

$$\theta_{,t} + \beta_1 w = \Delta \theta,$$

$$M \phi \gamma_{,t} + \beta_3 w = \frac{1}{Le} \Delta \gamma + S \Delta \theta,$$

where $w = u_3$ and the Rayleigh number is

$$R = \frac{\rho_0 g \alpha h K T_U}{\mu \kappa}.$$

The Fourier mode analysis is now used where we transform our variables using (2.15) and consider a general eigenvalue, σ , which now satisfies

$$\begin{aligned} 0 &= (D^2 - k^2)W + Rk^2\Theta, \\ \sigma\Theta &= -\beta_1W + (D^2 - k^2)\Theta, \\ M\phi\sigma\Phi &= -\beta_3W + \frac{1}{Le}(D^2 - k^2)\Phi + S(D^2 - k^2)\Theta, \end{aligned} \quad (5.6)$$

where k is a wave number.

As Φ only appears in (5.6)₃ it may initially seem possible to de-couple this equation, however the reaction boundary conditions mean that this is not possible.

By evaluating the steady state on the boundaries using (5.4) and (5.5) we find that the β_i satisfy

$$\begin{aligned} 1 &= \beta_1 + \beta_2, \\ 1 &= \beta_3 + \beta_4, \\ \beta_1 &= -A\beta_4 \exp(-\xi/\beta_2), \\ \beta_3 + H\beta_1 &= B\beta_4 \exp(-\xi/\beta_2), \end{aligned} \quad (5.7)$$

These may be solved for given values of A , B , H and ξ to obtain the required values of β_1 and β_3 . As in Chapter 2 we observe that the thermal gradient β_1 is negative, whereas the solutal gradient β_3 is positive. Both the thermal and solutal gradients are therefore destabilising and increasing either $|\beta_1|$ or β_3 will have a destabilising effect.

After introducing the perturbations to the steady state on the boundaries and then subtracting the steady state we find that the linearised non-dimensional boundary conditions are

$$W = 0, \quad \Theta = 0, \quad \Phi = 0, \quad \text{on } z = 1 \quad (5.8)$$

and

$$\begin{aligned} W &= 0, \\ D\Theta &= -A\frac{\beta_4\xi}{\beta_2^2} \exp\left(\frac{-\xi}{\beta_2}\right) \Theta - A \exp\left(\frac{-\xi}{\beta_2}\right) \Phi, \\ D\Phi + HD\Theta &= B\frac{\beta_4\xi}{\beta_2^2} \exp\left(\frac{-\xi}{\beta_2}\right) \Theta + B \exp\left(\frac{-\xi}{\beta_2}\right) \Phi \quad \text{on } z = 0. \end{aligned} \quad (5.9)$$

5.2 Numerical results and conclusions

The aim of this chapter was to examine how inclusion of the Soret effect alters the onset of convection. We therefore chose values of A , B and ξ to coincide with those in Chapter 2. Using these values we solved equations (5.7) to find values for β_1 and β_3 . Some of the values obtained are given in Table 5.1.

Table 5.1: Values of β_1 and β_3 for given reaction parameters A , B , and ξ and a Soret boundary parameter H .

A	B	H	ξ	β_1	β_3
1	1	0.5	0.5	-0.338659	0.507989
1	1	1	0.5	-0.287819	0.575638
1	1	5	0.5	-0.132360	0.794163
1	0.5	5	0.5	-0.199312	0.997413
1	1	5	0.5	-0.132360	0.794163
1	5	5	0.5	-0.036205	0.799571
0.5	1	1	0.5	-0.164680	0.494041
1	1	1	0.5	-0.287819	0.575638
5	1	1	0.5	-0.680596	0.816715

In Chapter 2 we found that for the chosen values of A , B and ξ a switch from stationary to oscillatory convection occurs in the range $0 \leq Le \leq 5$. We therefore chose to concentrate on this range for the current work. We also chose to consider the case where $M\phi = 1$. We fixed Le and solved the system of equations (5.6) with the boundary conditions (5.8) and (5.9) using the D^2 Chebyshev-tau method described in Section 2.3 and Appendix A, and the QZ algorithm to find the critical Rayleigh number, R_c . Values of R_c , the critical wave number, k_c , and the imaginary part of the dominant eigenvalue, $\text{Im}(\sigma_1)$ for a range of values of Le and S are given in Tables 5.2 and 5.3.

Figure 5.1 shows that the current Darcy-Soret model exhibits instability curves with a similar shape to those in the $S = 0$ case considered in Chapter 2. For a fixed Soret coefficient increasing the Lewis number from 0 increases the critical Rayleigh number, R_c . Here we find that the dominant eigenvalue is real and therefore the convection is stationary. At a critical Lewis number R_c reaches a peak and if Le is

Table 5.2: Values of R_c , k_c and $\text{Im}(\sigma_1)$ for various values of Le and S , for $A = 1$, $B = 1$, $H = 1$, $\xi = 0.5$, $M\phi = 1$.

Le	0.01	0.25	0.5	0.75	1	1.25	1.5	2	2.5	3	3.5	4	4.5	5
S=1														
R_c	91.306	96.523	102.036	107.520	112.884	118.063	123.021	125.875	113.962	105.707	99.594	94.853	91.047	87.909
k_c	2.263	2.381	2.516	2.658	2.800	2.939	3.071	2.164	2.102	2.051	2.007	1.969	1.936	1.906
$\text{Im}(\sigma_1)$	0.000	0.000	0.000	0.000	0.000	0.000	0.000	-3.044	-3.591	3.740	3.758	3.725	3.670	3.606
S=2														
R_c	91.377	98.357	105.702	112.884	119.741	126.196	132.226	112.861	99.642	90.179	82.917	77.061	72.161	67.940
k_c	2.265	2.425	2.610	2.800	2.984	3.154	3.310	1.924	1.818	1.725	1.640	1.563	1.491	1.423
$\text{Im}(\sigma_1)$	0.000	0.000	0.000	0.000	0.000	0.000	0.000	4.210	4.256	-4.130	-3.953	3.768	-3.585	3.408
S=3														
R_c	91.449	100.196	109.325	118.063	126.196	133.669	119.205	95.356	78.225	63.331				
k_c	2.266	2.470	2.705	2.939	3.154	3.346	1.795	1.566	1.323	1.014				
$\text{Im}(\sigma_1)$	0.000	0.000	0.000	0.000	0.000	0.000	4.605	4.530	4.019	-3.286				
S=4														
R_c	91.520	102.036	112.884	123.021	132.226	119.830	98.503							
k_c	2.268	2.516	2.800	3.071	3.310	1.618	1.377							
$\text{Im}(\sigma_1)$	0.000	0.000	0.000	0.000	0.000	4.997	-4.763							

Table 5.3: Values of R_c , k_c and $\text{Im}(\sigma_1)$ for various values of Le and S , for $A = 1$, $B = 1$, $\xi = 0.5$, $M\phi = 1$.

S	0.01	0.25	0.5	0.75	1	1.5	2	2.5	3	3.5	4	4.5	5
Le=1, H=1													
R_c	105.775	107.520	109.325	111.114	112.884	116.360	119.741	123.021	126.196	129.264	132.226	135.085	128.997
k_c	2.612	2.658	2.705	2.753	2.800	2.893	2.984	3.071	3.154	3.234	3.310	3.382	1.517
$\text{Im}(\sigma_1)$	0.000	0.000	0.000	0.000	0.000	0.000	0.000	0.000	0.000	0.000	0.000	0.000	-5.277
Le=2, H=1													
R_c	119.874	123.021	126.196	128.786	125.875	119.705	112.861	104.973	95.356	82.156			
k_c	2.987	3.071	3.154	2.215	2.164	2.053	1.924	1.769	1.566	1.250			
$\text{Im}(\sigma_1)$	0.000	0.000	0.000	-2.557	3.044	3.745	4.210	-4.482	-4.530	-4.197			
Le=1, H=0.5													
R_c	87.195	88.875	90.610	92.328	94.026	97.348	100.564	103.667	106.653	109.524	112.281	102.216	82.640
k_c	2.539	2.592	2.646	2.701	2.755	2.862	2.964	3.062	3.156	3.244	3.327	1.358	0.792
$\text{Im}(\sigma_1)$	0.000	0.000	0.000	0.000	0.000	0.000	0.000	0.000	0.000	0.000	0.000	-4.903	4.136
Le=2, H=0.5													
R_c	97.479	100.564	103.667	106.653	104.083	97.775	90.544	81.696	69.223				
k_c	2.866	2.964	3.062	3.156	2.099	1.963	1.796	1.576	1.217				
$\text{Im}(\sigma_1)$	0.000	0.000	0.000	0.000	-2.888	3.617	4.039	4.176	3.849				

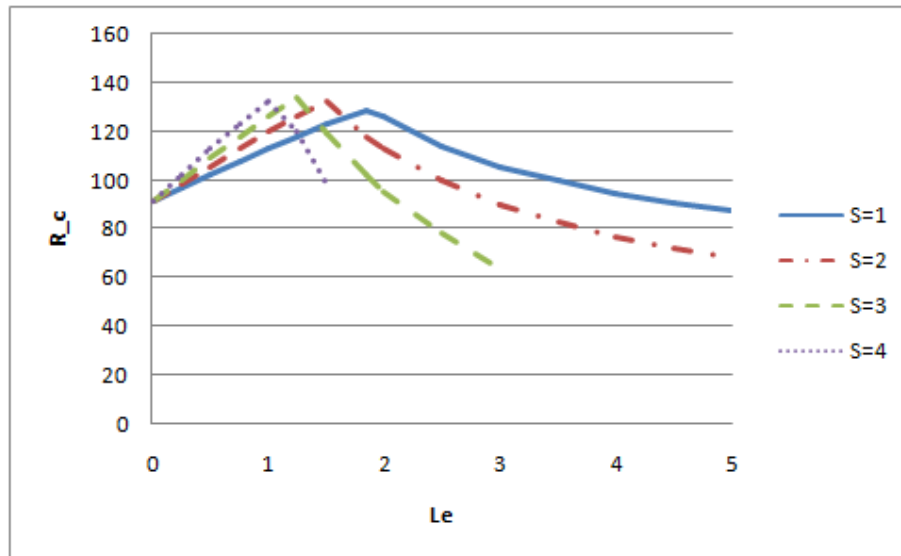


Figure 5.1: Variation of the critical Rayleigh number with the Lewis number for $A = 1$, $B = 1$, $H = 1$, $\xi = 0.5$, $M\phi = 1$.

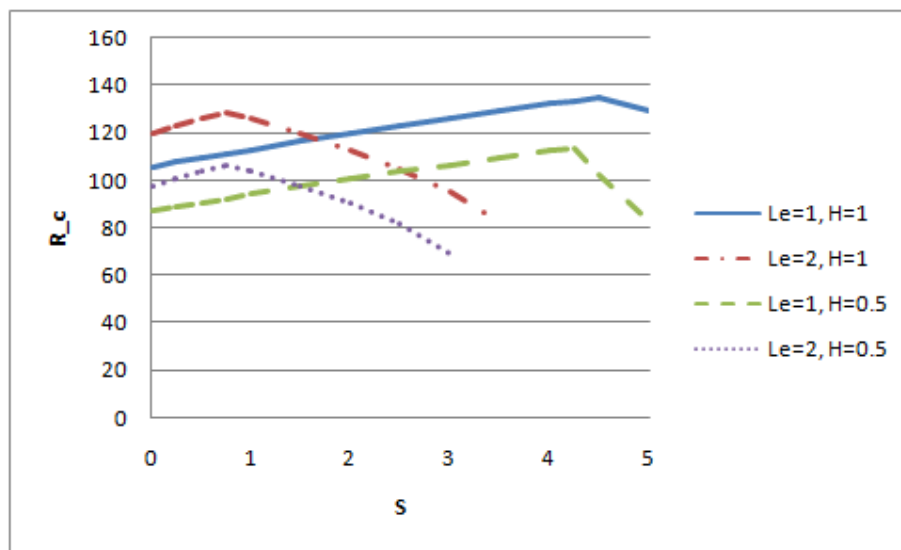


Figure 5.2: Variation of the critical Rayleigh number with the Soret coefficient for $A = 1$, $B = 1$, $\xi = 0.5$, $M\phi = 1$.

further increased then oscillatory convection becomes dominant and R_c decreases. The critical Lewis number is dependent on the Soret coefficient, S , and is lower for greater S , see Figure 5.1. Where stationary convection is observed R_c increases at a higher rate for larger S and where oscillatory convection is observed R_c decreases at a higher rate for larger S . It is shown in Figure 5.1 that stationary convection is only possible for small values of Le . For $S = 3$ and $S = 4$ the numerical method

used breaks down as we increase Le , this is due to R_c decreasing at a high rate.

At the onset of stationary convection the dominant eigenvalue is real and so we may set $\sigma = 0$ to write the system of equations (5.6) as

$$\begin{aligned} 0 &= (D^2 - k^2)W + Rk^2\Theta, \\ 0 &= -\beta_1 W + (D^2 - k^2)\Theta, \\ 0 &= -\beta_3 W + \frac{1}{Le}(D^2 - k^2)\Phi + S(D^2 - k^2)\Theta \end{aligned} \quad (5.10)$$

and further use of (5.10)₂ shows (5.10) may be rewritten as

$$\begin{aligned} 0 &= (D^2 - k^2)W + Rk^2\Theta, \\ 0 &= -\beta_1 W + (D^2 - k^2)\Theta, \\ 0 &= -(\beta_3 - S\beta_1)W + \frac{1}{Le}(D^2 - k^2)\Phi. \end{aligned} \quad (5.11)$$

This may now be compared to the model studied in Chapter 2, where $S = 0$. The system of equations (2.16) with boundary conditions (2.20) and (2.21) derived there is recovered by setting $S = 0$ in (5.10) and $H = 0$ in (5.9). The parameter β_3 is the solutal gradient and it was found that increasing this had a linearly stabilising effect and thus increased R_c . It may be seen that, as $\beta_1 < 0$, increasing S whilst keeping β_1 and β_3 constant makes $(\beta_3 - S\beta_1)$ more positive and has an equivalent effect to increasing β_3 in the $S = 0$ case. We observe that increasing S has a larger effect for larger Le as (5.11)₃ may be written as

$$0 = -Le(\beta_3 - S\beta_1)W + (D^2 - k^2)\Phi. \quad (5.12)$$

We conclude from this that, where the convection is stationary, increasing S increases R_c , and this increase is greater for greater Le . This is demonstrated by Figure 5.1, where we have chosen $A = B = H = M\phi = 1$ and $\xi = 0.5$.

By inserting (5.9)₂ into (5.9)₃ the boundary conditions on the lower wall may be rewritten as

$$\begin{aligned} W &= 0, \\ D\Theta &= -A\frac{\beta_4\xi}{\beta_2^2}\exp\left(\frac{-\xi}{\beta_2}\right)\Theta - A\exp\left(\frac{-\xi}{\beta_2}\right)\Phi, \\ D\Phi &= (B + AH)\frac{\beta_4\xi}{\beta_2^2}\exp\left(\frac{-\xi}{\beta_2}\right)\Theta + (B + AH)\exp\left(\frac{-\xi}{\beta_2}\right)\Phi \quad \text{on } z = 0. \end{aligned} \quad (5.13)$$

These boundary conditions may be compared to those obtained in Chapter 2, which are recovered by setting $H = 0$. It was discussed there that increasing A had a destabilising effect as heat is conducted away from the boundary at a higher rate, whereas increasing B had a stabilising effect, where the coefficients A and B are proportional to the rate at which heat is conducted away from the surface reaction and the rate that the reactant diffuses away from the lower boundary. In our current study we would therefore expect that increasing H , and hence increasing $HA + B$, would have a linearly stabilising effect. Figure 5.2 shows that this is indeed the case and we also notice that increasing H increases the critical Lewis number. Table 5.1 shows that increasing H causes the thermal gradient, β_1 , to be less negative whilst the solutal gradient, β_3 , becomes more positive. These effects compete, however the thermal gradient is here the driving force of convection and thus has a larger effect and therefore, overall increasing H is linearly stabilising.

Similarly, we observe from Table 5.1 that increasing B whilst A , H and ξ are kept constant reduces $|\beta_1|$ and may also decrease β_3 . We would therefore expect increasing B to have a linearly stabilising effect and increase R_c . On the other hand, increasing A increases both $|\beta_1|$ and β_3 (it is easy to prove that this is always the case when $\xi = 0$ using equations (5.7)) and is destabilising.

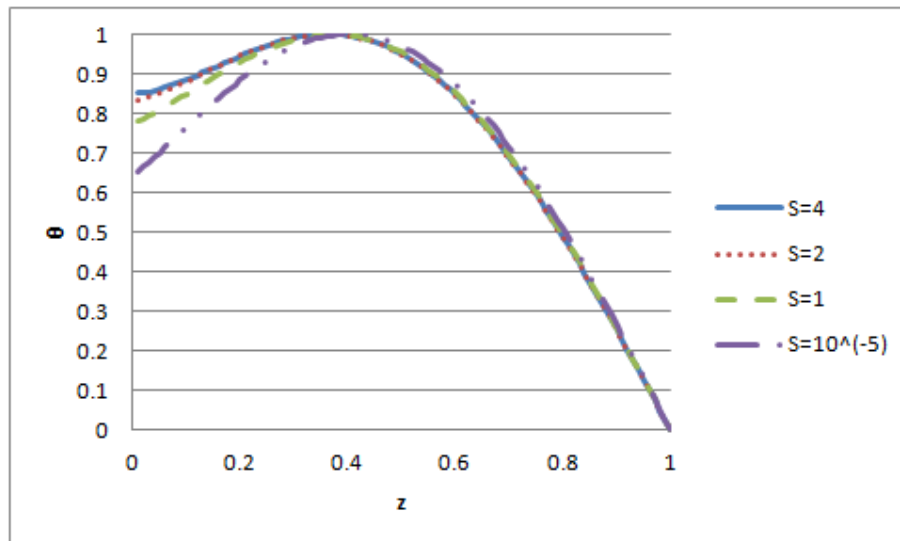


Figure 5.3: Normalised Θ eigenfunction for $A = 1$, $B = 1$, $H = 1$, $\xi = 0.5$, $Le = 0.5$, $M\phi = 1$.

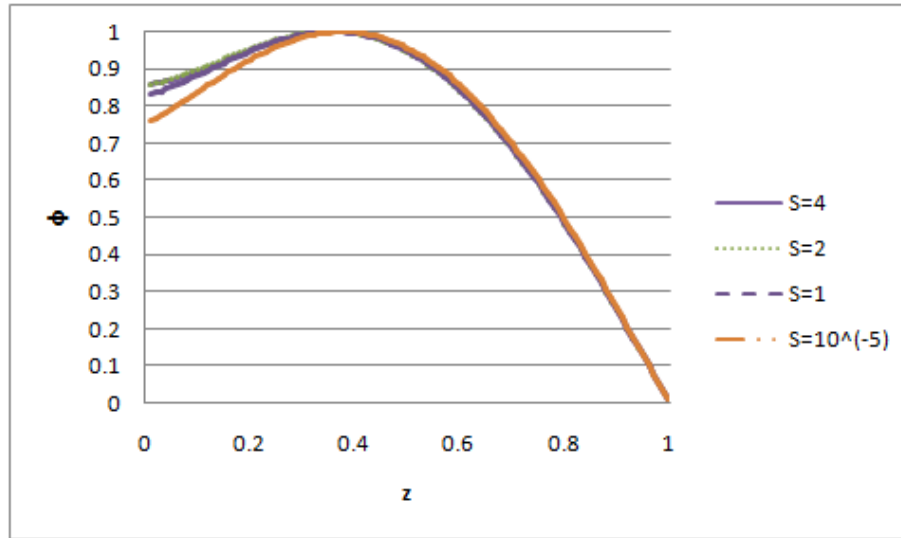


Figure 5.4: Normalised Φ eigenfunction for $A = 1$, $B = 1$, $H = 1$, $Le = 0.5$, $\xi = 0.5$, $M\phi = 1$.

Figures 5.3 and 5.4 show the effect of the Soret coefficient on the Φ and Θ normalised eigenfunctions for $Le = 0.5$ and reaction parameters that yield stationary convection at the onset of instability. The Soret effect has little, if any, effect on the W eigenfunction and this is therefore not presented. The values of the Θ and Φ eigenfunctions at $z = 0, 1$ are found by the boundary conditions (5.8), (5.9). We see from 5.3 and 5.4 that for all Soret numbers $\Theta(1) = \Phi(1) = 0$, but that as S is increased the values of the Θ and Φ normalised eigenfunctions at $z = 0$ increase. We previously discussed that when stationary convection occurs increasing S has an equivalent effect to increasing β_3 . As $\beta_3 + \beta_4 = 1$ this would consequently mean that it has an effect similar to decreasing β_4 . As A , B , H and ξ are positive, boundary conditions (5.9)₂ and (5.9)₃ show that at $z = 0$ the values of $d\Theta/dz$ and $d\Phi/dz$ for the eigenfunctions become closer to zero (the eigenfunctions are normalised to take values between 0 and 1) and therefore the values of the Θ and Φ eigenfunctions at $z = 0$ are large.

Finally, we may see from Tables 5.2 and 5.3 that increasing the Soret coefficient increases the critical wave number and therefore the convection cells become narrower.

Chapter 6

Instability boundaries for a highly porous medium with an exothermic boundary reaction

In the investigations in Chapters 2-5 we have assumed that the porosity of the medium is low to moderate and that the Darcy equation may therefore be employed. However, when the porosity of the medium or fluid viscosity is large higher order derivatives of the velocity become important and it is necessary to use the Brinkman equation, cf. Hill & Carr [34]. In this chapter we will investigate how inclusion of the Brinkman term affects the linear instability of a horizontal porous layer with an exothermic reaction on the lower boundary.

Practical materials which may benefit by use of the Brinkman equation are man-made high porosity metallic forms, such as those based on copper oxide or aluminium, which have a porosity very close to 1. These are currently popular in academic studies as well as in the heat transfer industry, c.f. Zhao *et al* [122], Straughan [107]. The onset of natural convection using the Brinkman model is investigated by Hsu & Cheng [38] in a vertical flat plate of a porous medium and by Goyeau *et al* [33] in a porous cavity. There have been fewer studies incorporating both the Brinkman term and a chemical reaction, however Li *et al* [49] examine the fluid flow of

porous media with a strong endothermic chemical reaction using a Forchheimer-

Brinkman non-thermal equilibrium model.

It has been shown by experimental work that catalytic surface reactions may create large temperature differences, which in turn can drive a convective flow. It is therefore assumed in many studies, for example Merkin & Mahmood [64] and Pop *et al* [81], that changes in concentration create only a small change in density compared to changes created by the varying temperature and thus concentration may be neglected in the density term. In the following work this assumption will be adopted so that $\rho = \rho(T)$, where the variables ρ and T are density and temperature, respectively.

6.1 Basic equations

We begin our study by considering a periodic cell in a horizontal layer of depth h of a porous medium with a catalytic exothermic reaction on the lower wall and fixed temperature and reactant concentration on the upper wall. This is studied by Postelnicu [84] and Scott & Straughan [98], where both assume that the porous medium is of Darcy type. A similar situation is considered in Merkin & Mahmood [64], however the layer is assumed to have infinite depth. For media with a high porosity, ϕ , such as metallic foams as mentioned above with $\phi \approx 1$, sedimentary rocks which may have $\phi \geq 0.65$, or fluids with a high viscosity, higher level derivatives of the velocity, \mathbf{v} , are likely to influence the behaviour of the system. We assume that this is the case and that our porous medium therefore satisfies the Brinkman equation, c.f. Ingham & Pop [39], Nield & Bejan [70], Pop & Ingham [82], Straughan [105], Vadasz [115] and Vafai [117, 118],

$$\nabla p = -\frac{\mu}{K}\mathbf{v} + \lambda\Delta\mathbf{v} - \rho g\mathbf{k}, \quad (6.1)$$

where μ , K and λ are the fluid's dynamic viscosity, the permeability of the porous medium and an effective viscosity, ρ and p are density and pressure, g is gravity acting in the negative z direction, and $\mathbf{k} = (0, 0, 1)$.

The Boussinesq approximation is employed so that changes in the density are assumed to be negligible everywhere except the body force term in (6.1). We also

assume that the density depends linearly on temperature, T , and is independent of the concentration, C , therefore

$$\rho = \rho_0(1 - \alpha(T - T_0)), \quad (6.2)$$

where ρ_0 is the density at the reference temperature, T_0 , and α is the coefficient of thermal expansion. By substituting (6.2) into (6.1) we obtain the momentum equation

$$p_{,i} = -\frac{\mu}{K}v_i + \lambda\Delta v_i - \rho_0(1 - \alpha(T - T_0))gk_i. \quad (6.3)$$

The temperature and concentration fields satisfy, see Ingham & Pop [39], Nield & Bejan [70], Pop & Ingham [82], Straughan [105], Vadasz [115] and Vafai [117,118],

$$\begin{aligned} \frac{1}{M} \frac{\partial T}{\partial t} + v_i \frac{\partial T}{\partial x_i} &= \kappa \Delta T, \\ \phi \frac{\partial C}{\partial t} + v_i \frac{\partial C}{\partial x_i} &= \phi k_c \Delta C, \end{aligned} \quad (6.4)$$

where $M = (\rho_0 c_p)_f / (\rho_0 c)_m$, with $(\rho_0 c)_m = \phi(\rho_0 c_p)_f + (1 - \phi)(\rho c)_s$ and $\kappa = k_m / (\rho_0 c_p)_f$, is the thermal diffusivity of the porous medium, where $k_m = \kappa_s(1 - \phi) + \kappa_f \phi$. The specific heat at constant pressure of the fluid and the specific heat of the solid are c_p and c_s , respectively, and k_c is the diffusivity of the reactant.

The final equation

$$v_{i,i} = 0 \quad (6.5)$$

is found by assuming that the fluid saturating the porous medium is incompressible.

On the upper boundary the temperature and concentration are held constant, there is zero mass flux across the boundary and there is no-slip so that

$$v_i = 0, \quad \frac{\partial v_3}{\partial z} = 0, \quad T = T_U, \quad C = C_U, \quad \text{on } z = h, \quad (6.6)$$

where the condition $\partial v_3 / \partial z = 0$ follows from (6.5) and the fact that $u = 0$, $v = 0$ on $z = h$. A full derivation of the no-slip boundary conditions is provided in Appendix B.

We assume that the lower boundary is catalytic so that an exothermic reaction takes place in which a reactant is converted into an inert product at a rate, r , where

$$r = k_0 C \exp\left(\frac{-E}{R^*T}\right).$$

The parameter k_0 is a rate constant, E is the activation energy of the reaction and R^* is the universal gas constant. The rate of change of temperature with respect to z is proportional to the reaction rate and the heat of the reaction, Q , and inversely proportional to the rate at which heat is conducted away from the surface, k_T . The rate of change of the reactant concentration with respect to z is proportional to the rate at which the reaction occurs and inversely proportional to the porosity and the diffusivity of the reactant. There is no mass flux across the lower boundary and there is no slip. The boundary conditions on the lower wall, $z = 0$, are then

$$\begin{aligned} v_i &= 0, \\ \frac{\partial v_3}{\partial z} &= 0, \\ k_T \frac{\partial T}{\partial z} &= -Qk_0C \exp\left(\frac{-E}{R^*T}\right), \\ \phi k_c \frac{\partial C}{\partial z} &= k_0C \exp\left(\frac{-E}{R^*T}\right) \quad \text{on } z = 0. \end{aligned} \tag{6.7}$$

6.2 Steady state and non-dimensional perturbation equations

We follow the linear method used in Chapter 2 and begin by non-dimensionalising equations (6.3), (6.4) and (6.5) and boundary conditions (6.6) and (6.7) using

$$\begin{aligned} x_i &= hx_i^*, \quad t = \frac{h^2}{\kappa M} t^*, \quad v_i = \frac{\kappa}{h} v_i^*, \\ C &= C_U C^*, \quad T = T_U T^*, \quad p = \frac{\kappa \mu}{K} p^*. \end{aligned}$$

We find the equations

$$\begin{aligned} -v_i + Br \Delta v_i - \frac{Kh}{\kappa \mu} \rho_0 (1 - \alpha T_U (T - T_0)) g k_i &= p_{,i}, \\ v_{i,i} &= 0, \\ \frac{\partial T}{\partial t} + v_i \frac{\partial T}{\partial x_i} &= \Delta T, \\ M \phi \frac{\partial C}{\partial t} + v_i \frac{\partial C}{\partial x_i} &= \frac{1}{Le} \Delta C, \end{aligned} \tag{6.8}$$

where $Br = \lambda K / (h^2 \mu)$ is the Darcy number and $Le = \kappa / (\phi k_c)$, with the boundary conditions

$$v_i = 0, \quad \frac{\partial v_3}{\partial z} = 0, \quad T = 1, \quad C = 1, \quad \text{on } z = 1, \tag{6.9}$$

and

$$\begin{aligned}
v_i &= 0, \\
\frac{\partial v_3}{\partial z} &= 0, \\
\frac{\partial T}{\partial z} &= -AC \exp\left(\frac{-\xi}{T}\right), \\
\frac{\partial C}{\partial z} &= BC \exp\left(\frac{-\xi}{T}\right) \quad \text{on } z = 0,
\end{aligned} \tag{6.10}$$

where

$$A = \frac{Qk_0hC_U}{k_T T_U}, \quad B = \frac{k_0h}{\phi k_c}, \quad \xi = \frac{E}{R^* T_U}$$

are non-dimensional coefficients.

We now assume that the temperature and concentration fields are functions of z only and consider a steady state $(\bar{v}_i, \bar{T}, \bar{C}, \bar{p})$ to exist such that $\bar{v}_i = 0$, $\bar{T}_{,t} = 0$ and $\bar{C}_{,t} = 0$. Equations (6.8) then immediately yield

$$\begin{aligned}
\bar{T} &= \beta_1 z + \beta_2, \\
\bar{C} &= \beta_3 z + \beta_4, \\
\bar{p}_{,i} &= -\frac{Kh}{\kappa\mu} \rho_0 (1 - \alpha T_U (\bar{T} - T_0)) g k_i,
\end{aligned} \tag{6.11}$$

where the β_i depend on the reaction parameters and values for these are given later in this section. We find there that $\beta_1 < 0$ and $\beta_3 > 0$ and therefore the basic solution has a negative thermal gradient and a positive solutal gradient. We would expect this as the reaction on the lower boundary releases heat and consumes the reactant.

Next, we introduce small perturbations u_i, θ, γ, π to the steady state, where

$$\begin{aligned}
v_i &= \bar{v}_i + u_i, \quad T = \bar{T} + \theta, \\
C &= \bar{C} + \gamma, \quad p = \bar{p} + \pi.
\end{aligned} \tag{6.12}$$

Inserting (6.12) into (6.8) and then subtracting the steady state we find

$$\begin{aligned}
-u_i + Br\Delta u_i + R\theta k_i &= \pi_{,i}, \\
\theta_{,t} + u_i \bar{T}_{,i} + u_i \theta_{,i} &= \Delta\theta, \\
M\phi\gamma_{,t} + u_i \bar{C}_{,i} + u_i \gamma_{,i} &= \frac{1}{Le} \Delta\gamma,
\end{aligned} \tag{6.13}$$

where we define the Rayleigh number by $R = Kh\rho_0\alpha T_U g/(\kappa\mu)$. The system is stable if R is less than some critical value, which will be calculated, and so increasing κ or μ or decreasing $K, h, \rho_0, \alpha, T_U$ or g decreases R and is stabilising.

In order to remove the pressure term in (6.13)₁, we take the *curlcurl* and retain only the third component ($i = 3$). We also linearise (6.13) by neglecting terms which are the product of two perturbations and transform the variables using the Fourier transformations (2.15).

The real part of an eigenvalue, also called the growth rate, determines whether or not a perturbation to the basic solution of arbitrary amplitude decays. If the real part of each eigenvalue is negative then the solution will indeed decay as $t \rightarrow \infty$, however if any eigenvalue has a positive real part then the amplitude of the perturbation may grow and the basic solution will be unstable. The critical Rayleigh number, R_c , is the value of R for which instability first occurs. It is found by varying k and investigating the value of R for which the dominant eigenvalue has a real part equal to zero, where the dominant eigenvalue is the eigenvalue with largest real part. We therefore consider a general eigenvalue, σ , and wish to solve the system

$$\begin{aligned} 0 &= (D^2 - k^2)W - Br(D^2 - k^2)^2W + Rk^2\Theta, \\ \sigma\Theta &= (D^2 - k^2)\Theta - \beta_1W, \\ M\phi\sigma\Phi &= \frac{1}{Le}(D^2 - k^2)\Phi - \beta_3W, \end{aligned} \quad (6.14)$$

where $w = u_3$, k is a wave number and $D = d/dz$.

To find the non-dimensional, perturbation boundary conditions we apply (6.12) to (6.9) and (6.10), subtract the steady state and linearise. We then find that

$$W = 0, \quad DW = 0, \quad \Phi = 0, \quad \Theta = 0 \quad \text{on } z = 1, \quad (6.15)$$

and

$$\begin{aligned} W &= 0, \\ DW &= 0, \\ D\Theta &= -A \frac{\beta_4\xi}{\beta_2^2} \exp\left(\frac{-\xi}{\beta_2}\right) \Theta - A \exp\left(\frac{-\xi}{\beta_2}\right) \Phi, \\ D\Phi &= B \frac{\beta_4\xi}{\beta_2^2} \exp\left(\frac{-\xi}{\beta_2}\right) \Theta + B \exp\left(\frac{-\xi}{\beta_2}\right) \Phi \quad \text{on } z = 0. \end{aligned} \quad (6.16)$$

We now obtain expressions that may be solved to find values for the β_i by evaluating the steady state (6.11) on the upper and lower boundaries, (6.9) and

(6.10). These expressions are found to be

$$\begin{aligned}
 1 &= \beta_1 + \beta_2, \\
 1 &= \beta_3 + \beta_4, \\
 \beta_1 &= -A\beta_4 \exp\left(\frac{-\xi}{\beta_2}\right), \\
 \beta_3 &= B\beta_4 \exp\left(\frac{-\xi}{\beta_2}\right)
 \end{aligned} \tag{6.17}$$

and may be solved for given values of A , B and ξ . Some values of β_1 and β_3 for values of A , B and ξ that were chosen to coincide with the values used in Chapter 2 are given in Table 6.1. As mentioned earlier we note that β_1 is negative and β_3 is

Table 6.1: Values of β_1 and β_3 for specified A , B and ξ .

A	B	ξ	β_1	β_3
1	1	0	-0.500000	0.500000
1	1	0.15	-0.474591	0.474591
1	1	0.5	-0.412412	0.412412
0.5	1	0	-0.250000	0.500000
5	1	0	-2.500000	0.500000
1	0.5	0	-0.666667	0.333333
1	5	0	-0.166667	0.833333

positive for the chosen values of A and B and indeed it may be shown that this is always the case. Both the thermal and solutal gradients are therefore destabilising.

6.3 Numerical results and conclusions

We now solve equations (6.14) with the boundary conditions (6.15) and (6.16) for given values of the parameters A , B , Br , ξ and $M\phi$ to find the critical Rayleigh number. To do this we first define a new variable as $\chi = D^2W$. With this substitution

(6.14) becomes

$$\begin{aligned} 0 &= D^2W - \chi \\ 0 &= -(k^2 + Brk^4)W + (1 + 2Brk^2 - BrD^2)\chi + Rk^2\Theta, \\ \sigma\Theta &= (D^2 - k^2)\Theta - \beta_1W, \\ M\phi Le\sigma\Phi &= (D^2 - k^2)\Phi - \beta_3LeW. \end{aligned}$$

We then use the D^2 Chebyshev-tau method as discussed in Appendix A and Dongarra *et al* [20] and the QZ algorithm to find the eigenvalues and then minimise over k to find R_c .

Some of the values of the critical Rayleigh number we obtain are given in Table 6.2. The results are presented graphically in Figures 6.1-6.5, where we show the effect of varying the reaction parameters, A , B , ξ , the Darcy number, Br , and then $M\phi$, respectively.

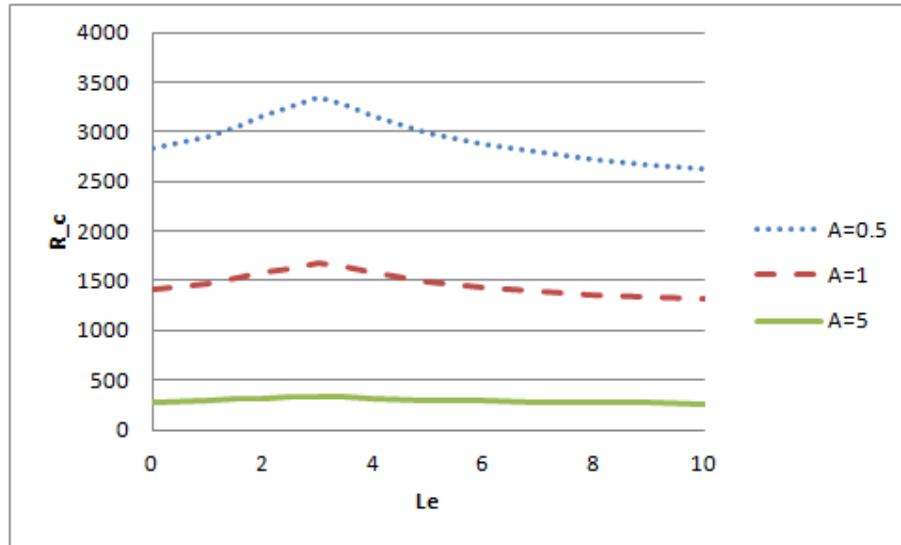


Figure 6.1: Variation of R_c with A , for $B = 1$, $Br = 0.5$, $\xi = 0$ and $M\phi = 1$.

The instability curves in Figures 6.1-6.5 exhibit a similar shape to those in Chapter 2, where $Br = 0$. For fixed A , B , ξ , Br , $M\phi$, increasing the Lewis number from 0 increases the value of the critical Rayleigh number, R_c , which is the smallest Rayleigh number for which instability occurs. The leading eigenvalue, σ_1 , is real and therefore the instability is due to stationary convection. At a critical Lewis number, Le_c , an eigenvalue which has a non-zero imaginary part becomes dominant

Table 6.2: Values of R_c , k_c and $\text{Im}(\sigma_1)$ for varying values of Le , A , B , ξ , Br and $M\phi$.

Br	A	B	ξ	$M\phi$	$Le = 1$			$Le = 2.5$			$Le = 5$			$Le = 10$		
					R_c	k_c	$\text{Im}(\sigma_1)$	R_c	k_c	$\text{Im}(\sigma_1)$	R_c	k_c	$\text{Im}(\sigma_1)$	R_c	k_c	$\text{Im}(\sigma_1)$
0.5	1	1	0	0.25	1471.484	2.753	0.000	1627.929	3.030	0.000	1868.340	3.403	0.000	1555.773	2.381	5.057
0.5	1	1	0	0.5	1471.484	2.753	0.000	1627.929	3.030	0.000	1707.242	2.489	3.054	1389.158	2.387	3.535
0.5	1	1	0	1	1471.484	2.753	0.000	1627.929	3.030	0.000	1494.548	2.478	2.469	1312.586	2.398	2.414
0.5	1	1	0	1	1471.484	2.753	0.000	1627.929	3.030	0.000	1494.548	2.478	2.469	1312.586	2.398	2.414
0.5	1	1	0.15	1	1539.155	2.735	0.000	1693.618	2.999	0.000	1576.211	2.473	2.346	1386.297	2.3950	2.330
0.5	1	1	0.5	1	1741.121	2.693	0.000	1891.385	2.923	0.000	1819.288	2.465	2.039	1605.961	2.390	2.124
0.5	1	0.5	0	1	1069.564	2.675	0.000	1138.366	2.849	0.000	1150.574	2.504	1.560	1026.070	2.446	1.857
0.5	1	1	0	1	1471.484	2.753	0.000	1627.929	3.030	0.000	1494.548	2.478	2.469	1312.586	2.398	2.414
0.5	1	5	0	1	4885.252	2.969	0.000	5406.882	2.599	-3.683	4283.092	2.463	-4.428	3609.636	2.334	3.861
0.5	0.5	1	0	1	2942.969	2.753	0.000	3255.859	3.030	0.000	2989.097	2.478	2.469	2625.172	2.398	2.414
0.5	1	1	0	1	1471.484	2.753	0.000	1627.929	3.030	0.000	1494.548	2.478	2.469	1312.586	2.398	2.414
0.5	5	1	0	1	294.297	2.753	0.000	325.586	3.030	0.000	298.910	2.478	2.469	262.517	2.398	2.414
0.25	1	1	0	1	772.148	2.755	0.000	854.149	3.035	0.000	784.349	2.477	-2.471	688.869	2.396	2.416
0.5	1	1	0	1	1471.484	2.753	0.000	1627.929	3.030	0.000	1494.548	2.478	2.469	1312.586	2.398	2.414
1	1	1	0	1	2870.033	2.752	0.000	3175.375	3.027	0.000	2914.816	2.478	2.468	2559.906	2.398	2.413

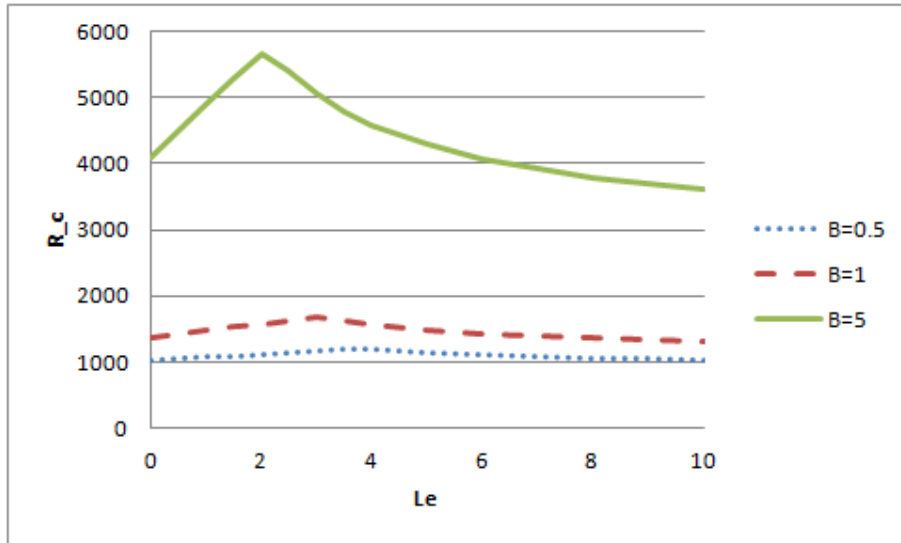


Figure 6.2: Variation of R_c with B , for $A = 1$, $Br = 0.5$, $\xi = 0$ and $M\phi = 1$.

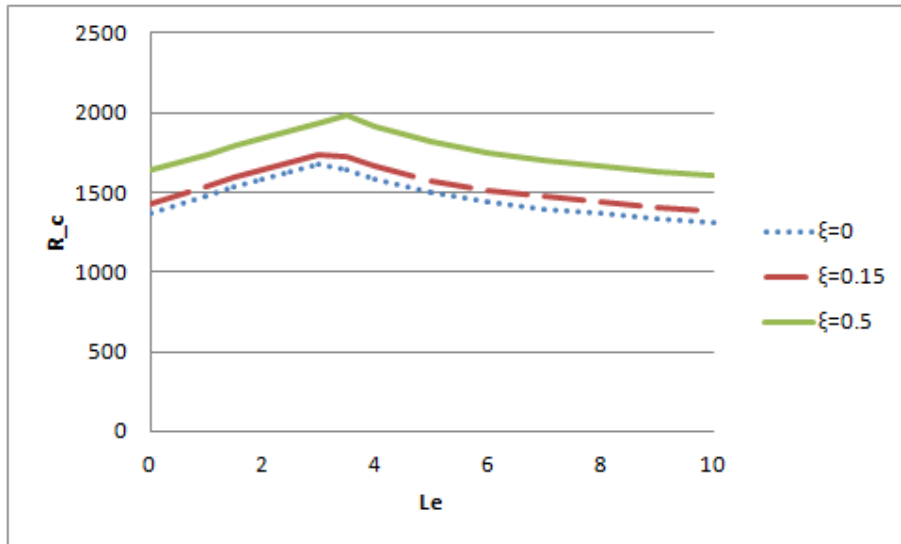


Figure 6.3: Variation of R_c with ξ , for $A = 1$, $B = 1$, $Br = 0.5$ and $M\phi = 1$.

and the critical Rayleigh number reaches a maximum value. If the Lewis number is further increased then the critical Rayleigh number decreases. This part of the instability curve is due to oscillatory convection.

Figure 6.1 shows that increasing A is destabilising and decreases R_c . When $\xi \neq 0$, increasing A increases $|\beta_1|$ and increases β_3 . The parameters β_1 and β_3 are the thermal and solutal gradients and as such an increase in $|\beta_1|$ and increase in β_3 causes a more negative thermal gradient and a more positive solutal gradient. Each of these changes has a destabilising effect, therefore a decrease in R_c would be

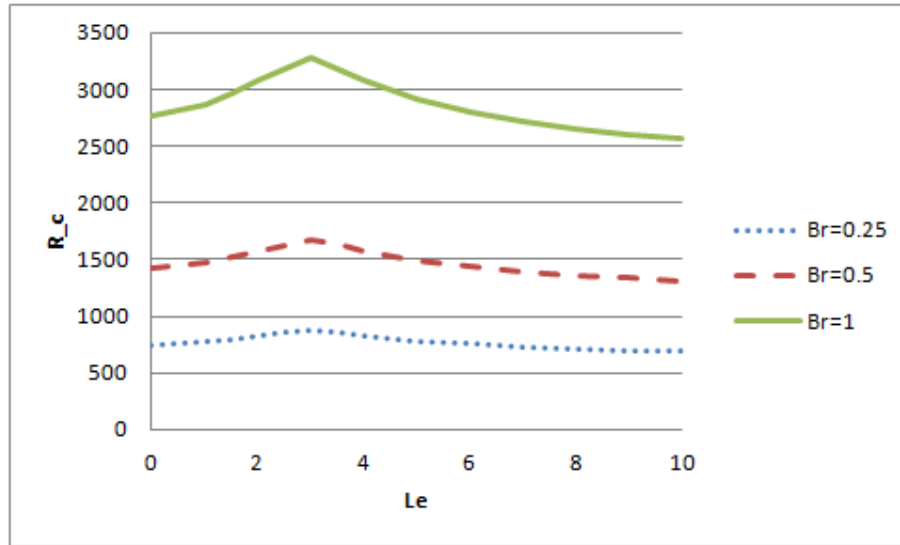


Figure 6.4: Variation of R_c with Br , for $A = 1$, $B = 1$, $\xi = 0$ and $M\phi = 1$.

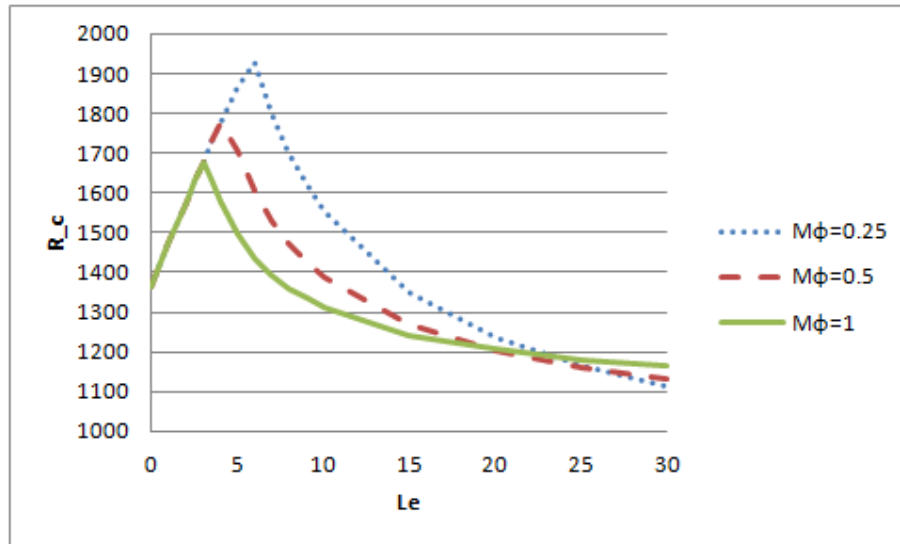


Figure 6.5: Variation of R_c with $M\phi$, for $A = 1$, $B = 1$, $Br = 0.5$ and $\xi = 0$

expected. This may also be noticed by examining the boundary condition (6.10)₃, which indicates the rate that heat is conducted away from the boundary reaction and released into the system. Increasing A means that heat from the reaction is released from the lower boundary at a higher rate, which is destabilising. Table 6.1 indicates that for $\xi = 0$ increasing A by a factor of n increases the absolute value of $|\beta_1|$ by a factor of n and has no effect on the value of β_3 . This is proven by using (6.17) to show that (for $\xi = 0$) $\beta_3 = B/(1 + B)$ and $\beta_1 = -A/(1 + B)$. Close examination of Table 6.2 shows that, when $\xi = 0$, increasing A by a factor of

n decreases the critical Rayleigh number by a factor of n . This is demonstrated in Figure 6.1, and is due to the thermal gradient being n times as large.

In the limit $A \rightarrow 0$, it is seen that $D\Phi \rightarrow 0$. It therefore becomes possible to decouple the concentration field in equations (6.14) and the instability ceases to be double-diffusive, instead becoming single diffusive with the boundary conditions

$$W = 0, \quad DW = 0, \quad \Theta = 0 \quad \text{on } z = 1$$

$$W = 0, \quad DW = 0, \quad D\Theta = 0 \quad \text{on } z = 0,$$

which are of Neumann type. By solving (6.17) for β_1 it is found that

$$\beta_1 = \frac{A \exp\left(\frac{-\xi}{1-\beta_1}\right)}{1 + B \exp\left(\frac{-\xi}{1-\beta_1}\right)},$$

which may be easily rearranged in terms of A . After noting that $\exp[-\xi/(1-\beta_1)] > 0$ and $1 + B \exp[-\xi/(1-\beta_1)] \neq 0$ it is observed that $\beta_1 \rightarrow 0$ as $A \rightarrow 0$. This means that as A decreases the thermal gradient decreases until, in the limit, it is zero. There is then no force to drive convection and the system becomes linearly stable. It is possible to conclude this from the earlier discussion that when $\xi = 0$, R_c increases by a factor of n when A is decreased by a factor of n . This is further demonstrated by Table 6.3. The linear theory used here may only provide information about

Table 6.3: Values of R_c , k_c and $\text{Im}(\sigma_1)$ as $A \rightarrow 0$, for $B = 0.5$, $Br = 0.5$, $\xi = 0$, $M\phi = 1$.

A	β_1	β_3	$Le = 0.1$			$Le = 1$		
			R_c	k_c	$\text{Im}(\sigma_1)$	R_c	k_c	$\text{Im}(\sigma_1)$
0.25	-0.16667	0.33333	4278.250	2.675	0.000	4602.289	2.504	1.560
0.1	-0.06667	0.33333	10695.591	2.675	0.000	11505.690	2.504	1.560
0.05	-0.03333	0.33333	21391.516	2.675	0.000	23011.707	2.504	1.560

instability and therefore in the limit $A \rightarrow 0$ we have no information about the stability of the system. In order to establish stability bounds it is necessary to perform a non-linear analysis, for example the energy analysis in Chapter 3.

Increasing B makes β_1 less negative and β_3 more positive, therefore the thermal gradient becomes less destabilising and the solutal gradient becomes more destabilising. The two changes then have competing effects on R_c , however the convection

is driven by the thermal gradient and it was considered that the thermal gradient is dominant over the solutal gradient. The change in the thermal gradient thus has a much greater effect and it is found that increasing B is stabilising overall, see Figure 6.2.

Similarly, increasing ξ makes β_1 less negative and β_3 less positive, so the thermal and solutal gradients are both less destabilising. Increasing ξ therefore increases R_c , this is demonstrated in Figure 6.3.

Physically, increasing $Br = \lambda K / (h^2 \mu)$ means that the effective viscosity λ is increased, and the higher level derivatives of the velocity have a larger influence, or that the dynamic viscosity μ is decreased. It would be expected that increasing λ would be stabilising as a more viscous fluid is more stable, and this is indeed observed in Figure 6.4. In Chapter 2 we studied a horizontal layer with an exothermic reaction on the lower wall, where we assumed that the Darcy model may be employed. That system is recovered here by setting $Br = 0$, hence it would be expected that R_c should approach the results we found for value from above as $Br \rightarrow 0$. This is demonstrated in Table 6.4, where small values of Br were chosen and the results for R_c , k_c , $\text{Im}(\sigma_1)$ and the corresponding values from Chapter 2 for a chosen value of A , B , ξ and $M\phi$ are given.

Figure 6.5 shows that for Lewis numbers less than Le_c changing $M\phi$ has no effect on R_c . This would be expected as the onset of convection occurs when $\text{Re}(\sigma_1) = 0$, where σ_1 is the dominant eigenvalue. For $Le < Le_c$ the leading eigenvalue is real, therefore the first instance of instability is found by setting $\sigma = 0$. The parameter $M\phi$ now does not appear in (6.14), (6.15) or (6.16) and thus changing it has effect on R_c .

The critical Lewis number is dependent on B , ξ , Br and $M\phi$ but not on A . This is seen in Table 6.2 and Figures 6.1-6.5. It is observed in the table that changing B , ξ , Br or $M\phi$ whilst keeping the other parameters constant changes the imaginary part of the eigenvalue, but changing A has no effect. In particular it is noted that for $Le = 2.5$ when $B = 0.5$ or $B = 1$ then $\text{Im}(\sigma_1)$ is real, however when $B = 5$ then $\text{Im}(\sigma_1) \neq 0$. This implies that increasing B decreases Le_c . Figures 6.2, 6.3 and 6.5 obtain their maximums at different values of B , ξ and $M\phi$, respectively, showing

Table 6.4: Values of R_c , k_c and $\text{Im}(\sigma_1)$ as $Br \rightarrow 0$, for $A = 0.5$, $B = 0.5$, $\xi = 0$, $M\phi = 1$.

Br	$Le = 0.1$			$Le = 1$		
	R_c	k_c	$\text{Im}(\sigma_1)$	R_c	k_c	$\text{Im}(\sigma_1)$
10^{-5}	82.834	2.351	0.000	87.805	2.500	0.000
10^{-7}	82.059	2.344	0.000	87.044	2.493	0.000
10^{-10}	82.046	2.344	0.000	87.031	2.492	0.000
Chapter 2 results, $Br = 0$	81.847	2.342	0.000	86.836	2.490	0.000

Le	$Le = 10$			$Le = 100$		
	R_c	k_c	$\text{Im}(\sigma_1)$	R_c	k_c	$\text{Im}(\sigma_1)$
10^{-5}	84.078	2.255	1.977	74.114	2.185	1.320
10^{-7}	83.357	2.250	1.981	73.617	2.182	1.335
10^{-10}	83.345	2.249	1.981	73.608	2.182	1.335
Chapter 2 results, $Br = 0$	83.160	2.248	1.982	73.484	2.181	1.339

clearly that the values of B , ξ and $M\phi$ influence the critical Lewis number. The value of Br has a much smaller influence on Le_c , which we see both from Figure 6.4 and the fact that the eigenvalues in 6.2 change only slightly.

Chapter 7

Continuous dependence of the Brinkman model on the reaction parameters

In this chapter we aim to establish continuous dependence on the reaction terms for the model considered in Chapter 6. There, the Brinkman model is used to describe a porous medium of high porosity and we consider a horizontal layer with an exothermic reaction on the lower boundary and fixed temperature and reactant concentration on the upper boundary.

The problem of demonstrating continuous dependence on the reaction terms for the Brinkman model is simpler than we found for the Darcy model, Chapter 4. This is due to the existence of a Laplacian velocity term in the momentum equation. This means that all components of the velocity may be specified on the boundary and allows us bound the L^4 velocity norm using the Sobolev inequality.

7.1 The boundary-initial value problem

The porous medium is assumed to occupy a bounded region Ω in \mathbb{R}^3 with boundary Γ sufficiently smooth to allow application of the divergence theorem. Again, the basic variables are velocity, v_i , temperature, T , concentration, C , and pressure, p .

The equations of motion without loss of generality for this class of problem are

$$\begin{aligned}
 v_i - \Delta v_i &= -p_{,i} + g_i T + \tilde{g}_i C, \\
 v_{i,i} &= 0, \\
 T_{,t} + v_i T_{,i} &= \Delta T, \\
 C_{,t} + v_i C_{,i} &= \Delta C,
 \end{aligned} \tag{7.1}$$

on $\Omega \times (0, \mathcal{T})$, for some $\mathcal{T} < \infty$, where Δ is the Laplace operator, g_i, \tilde{g}_i are gravity terms with $|\mathbf{g}| \leq 1, |\tilde{\mathbf{g}}| \leq 1$, and standard indicial notation is employed throughout. Equations (7.1)₃ and (7.1)₄ are transport equations for temperature and concentration, (7.1)₂ expresses incompressibility of the saturating fluid, and (7.1)₁ is the Brinkman equation, cf. Straughan [107], Chapter 1.

Assuming that the reaction is well catalysed and the temperature on the upper boundary is not low, the boundary conditions are

$$v_i = 0, \quad \frac{\partial T}{\partial n} = AC, \quad \frac{\partial C}{\partial n} = -BC, \tag{7.2}$$

on $\Gamma \times [0, \mathcal{T})$, where A, B are positive constants and $\partial/\partial n$ denotes the unit normal derivative pointing out of Γ . The initial conditions to be satisfied are

$$T(\mathbf{x}, 0) = T_0(\mathbf{x}), \quad C(\mathbf{x}, 0) = C_0(\mathbf{x}), \tag{7.3}$$

where T_0 and C_0 are prescribed functions. Let the boundary-initial value problem comprised of (7.1) - (7.3) be denoted by \mathcal{P} .

Before establishing continuous dependence on A and B it is necessary to establish some auxilliary results and some *a priori* estimates for T and C . We find that in creating the necessary estimates equation (7.1)₁ is not used. As this is the only difference between the problem considered here and that in Chapter 4 we here state the results.

Rellich identity

Let ψ be a function defined on $\bar{\Omega}$ and let f_i be a function defined on Γ with

$$f_i n_i \geq f_0 > 0, \quad \text{on } \Gamma,$$

where n_i is the unit outward normal to Γ and f_0 is a constant. Suppose now that $f_{i,i} \leq m_1$ in Ω , $|f_i| \leq m_2$ in Ω , m_1, m_2 positive constants, for example, if $f_i = x_i$, then $f_{i,i} = 3$ and $|f_i|$ is bounded by the geometry of Ω . We find the bound

$$f_0 \oint_{\Gamma} \psi^2 dA \leq \left(m_1 + \frac{m_2}{\alpha}\right) \int_{\Omega} \psi^2 dx + \alpha m_2 \int_{\Omega} \psi_{,i} \psi_{,i} dx. \quad (7.4)$$

Concentration bound

We find that the concentration may be bound by

$$\sup_{\Omega \times [0, \mathcal{T}]} |C| \leq \max_{\Omega} |C_0| \equiv C_m. \quad (7.5)$$

Temperature bound

Finally, we require a bound for the L^4 temperature norm, which we find to be

$$\|T(t)\|_{4 \leq} D_2, \quad (7.6)$$

where D_2 is a known data term.

7.2 Continuous dependence on the boundary reaction terms

We now let (v_i, T, C, p) and (v_i^*, T^*, C^*, p^*) be two solutions to \mathcal{P} for the same initial data but for boundary coefficients (A, B) and (A^*, B^*) in (7.2), respectively, and define the quantities $u_i, \pi, \theta, \phi, a$ and b by

$$\begin{aligned} u_i &= v_i - v_i^*, & \pi &= p - p^*, & \theta &= T - T^*, \\ \phi &= C - C^*, & a &= A - A^*, & b &= B - B^*. \end{aligned}$$

Then, we find that the difference solution (u_i, θ, ϕ, π) satisfies the boundary-initial value problem

$$\begin{aligned} u_i - \Delta u_i &= -\pi_{,i} + g_i \theta + \tilde{g}_i \phi, \\ u_{i,i} &= 0, \\ \theta_{,t} + v_i \theta_{,i} + u_i T_{,i}^* &= \Delta \theta, \\ \phi_{,t} + v_i \phi_{,i} + u_i C_{,i}^* &= \Delta \phi, \end{aligned} \quad (7.7)$$

in $\Omega \times (0, \mathcal{T})$, together with the boundary conditions

$$u_i = 0, \quad \frac{\partial \theta}{\partial n} = aC + A^* \phi, \quad \frac{\partial \phi}{\partial n} = -(bC + B^* \phi),$$

on $\Gamma \times [0, \mathcal{T}]$, and the initial conditions

$$\theta(\mathbf{x}, 0) = 0, \quad \phi(\mathbf{x}, 0) = 0, \quad \mathbf{x} \in \Omega.$$

We begin by multiplying (7.7)₁ by u_i and then integrate over Ω to derive

$$\begin{aligned} \|\mathbf{u}\|^2 + \|\nabla \mathbf{u}\|^2 &= (g_i \theta, u_i) + (\tilde{g}_i \phi, u_i) \\ &\leq \|\theta\|^2 + \frac{1}{4} \|\mathbf{u}\|^2 + \|\phi\|^2 + \frac{1}{4} \|\mathbf{u}\|^2 \end{aligned}$$

where the arithmetic-geometric mean inequality has been employed. From this we see that

$$\frac{1}{2} \|\mathbf{u}\|^2 + \|\nabla \mathbf{u}\|^2 \leq \|\theta\|^2 + \|\phi\|^2. \quad (7.8)$$

Next, we multiply (7.7)₃ by θ and (7.7)₄ by ϕ , then integrate by parts using the boundary conditions to find

$$\begin{aligned} \frac{d}{dt} \frac{1}{2} \|\theta\|^2 &= -(u_i T_{,i}^*, \theta) + (\theta, \Delta \theta) \\ &= (u_i T^*, \theta_{,i}) - \|\nabla \theta\|^2 + a \oint_{\Gamma} C \theta dA + A^* \oint_{\Gamma} \theta \phi dA, \end{aligned} \quad (7.9)$$

and

$$\frac{d}{dt} \frac{1}{2} \|\phi\|^2 = (u_i C^*, \phi_{,i}) - \|\nabla \phi\|^2 - b \oint_{\Gamma} C \phi dA - B^* \oint_{\Gamma} \phi^2 dA. \quad (7.10)$$

To handle the cubic term on the right of (7.10) we use (7.5) and the Cauchy-Schwarz and arithmetic-geometric mean inequalities to find, for $\gamma > 0$ at our disposal,

$$(u_i C^*, \phi_{,i}) \leq C_m \|\mathbf{u}\| \|\nabla \phi\| \leq \frac{C_m^2}{2\gamma} \|\mathbf{u}\|^2 + \frac{\gamma}{2} \|\nabla \phi\|^2. \quad (7.11)$$

Now, we insert (7.11) in (7.10) and use the arithmetic-geometric mean inequality on the C, ϕ boundary term, then also use (7.8), to obtain

$$\begin{aligned} \frac{d}{dt} \frac{1}{2} \|\phi\|^2 &\leq \frac{C_m^2}{\gamma} (\|\theta\|^2 + \|\phi\|^2) - \left(1 - \frac{\gamma}{2}\right) \|\nabla \phi\|^2 \\ &\quad - \left(B^* - \frac{\beta}{2}\right) \oint_{\Gamma} \phi^2 dA + \frac{b^2}{2\beta} \oint_{\Gamma} C^2 dA, \end{aligned} \quad (7.12)$$

where $\beta > 0$ is a constant at our disposal.

To deal with the cubic term in (7.9) we use the Cauchy-Schwarz inequality as follows

$$(u_i T^*, \theta_{,i}) \leq \| \nabla \theta \| \left(\int_{\Omega} u_i u_i (T^*)^2 dx \right)^{\frac{1}{2}} \leq \| \nabla \theta \| \| \mathbf{u} \|_4 \| T^* \|_4 .$$

We employ the Sobolev inequality $\| \mathbf{u} \|_4 \leq \hat{c}_1 \| \nabla \mathbf{u} \|$ and estimates (7.8) and (7.6) to see that

$$(u_i T^*, \theta_{,i}) \leq \hat{c}_1 \| \nabla \theta \| (\| \theta \|^2 + \| \phi \|^2)^{\frac{1}{2}} D_2 . \quad (7.13)$$

After inserting inequality (7.13) into (7.9) and further use the arithmetic-geometric mean inequality with weights $\delta, \epsilon > 0$, we find

$$\begin{aligned} \frac{d}{dt} \frac{1}{2} \| \theta \|^2 &\leq \hat{c}_1 D_2 \| \nabla \theta \| (\| \theta \|^2 + \| \phi \|^2)^{\frac{1}{2}} - \| \nabla \theta \|^2 + \frac{a^2}{2\delta} \oint_{\Gamma} C^2 dA \\ &\quad + \frac{1}{2} (\delta + A^* \epsilon) \oint_{\Gamma} \theta^2 dA + \frac{A^*}{2\epsilon} \oint_{\Gamma} \phi^2 dA . \end{aligned} \quad (7.14)$$

Adding (7.12) and (7.14), and employing inequalities (7.4) and (7.5) we find

$$\begin{aligned} \frac{d}{dt} \frac{1}{2} (\| \theta \|^2 + \| \phi \|^2) &\leq \left(\frac{C_m^2}{\gamma} + \hat{c}_1 D_2 \frac{\xi}{2} \right) (\| \theta \|^2 + \| \phi \|^2) - \left(1 - \frac{\gamma}{2} \right) \| \nabla \phi \|^2 \\ &\quad - \left(1 - \frac{\hat{c}_1 D_2}{2\xi} - \left(\frac{\delta}{2} + \frac{A^* \epsilon}{2} \right) \alpha_2 m_2 \right) \| \nabla \theta \|^2 \\ &\quad - \left(B^* - \frac{\beta}{2} - \frac{A^*}{2\epsilon} \right) \oint_{\Gamma} \phi^2 dA + \left(\frac{a^2}{2\delta} + \frac{b^2}{2\beta} \right) C_m^2 |\Gamma| \\ &\quad + \frac{1}{2f_0} (\delta + A^* \epsilon) \left(m_1 + \frac{m_2}{\alpha_2} \right) \| \theta \|^2 . \end{aligned} \quad (7.15)$$

We now select $\gamma = 2$, $\beta = B^*$, $\epsilon = A^*/B^*$, so that the coefficients of the second and fourth terms on the right of (7.15) are zero. Then we pick $\xi = \hat{c}_1 D_2$, $\delta = 1$, and $\alpha_2 = m_2/(1 + A^{*2}/B^*)$ so that the coefficient of the third term is also zero.

Finally, we define

$$\begin{aligned} \lambda_1 &= \max \left\{ 1, \frac{1}{B^*} \right\} , \\ \lambda_2 &= \lambda_1 C_m^2 |\Gamma| , \\ \lambda_3 &= C_m^2 + \hat{c}_1^2 D_2^2 + \frac{1}{f_0} \left(1 + \frac{(A^*)^2}{B^*} \right) \left(m_1 + 1 + \frac{(A^*)^2}{B^*} \right) \end{aligned}$$

and also define a function $G(t) = \|\theta\|^2 + \|\phi\|^2$. We then observe that from (7.15) the function $G(t)$ satisfies

$$\frac{dG}{dt} \leq \lambda_2(a^2 + b^2) + \lambda_3 G.$$

This inequality easily integrates to find

$$G(t) \leq \frac{\lambda_2}{\lambda_3} e^{\lambda_3 t} (a^2 + b^2). \quad (7.16)$$

Inequality (7.16) demonstrates continuous dependence on the reaction parameters A and B in the measures $\|\theta\|$ and $\|\phi\|$.

Utilising inequality (7.8) we also have continuous dependence in the measures $\|\mathbf{u}\|$ and $\|\nabla \mathbf{u}\|$.

Chapter 8

Non-linear stability results for a vertical porous channel with thermal non-equilibrium

In each of the previous chapters we have used the averaged temperature equation for a porous medium. This was derived in Section 1.3 from the separate solid and fluid temperature equations. We will now turn our attention to the stability of a vertical porous channel in which the fluid and solid components of the porous configuration are in local thermal non-equilibrium. By this we mean that the saturating fluid and the solid it touches may be at different temperatures. This is an area that is gaining much impetus and is of intense research with many applications, see e.g. Banu & Rees [5], Bhadauria & Shilpi [7], Chen *et al* [16], Lee *et al* [48], Malashetty *et al* [60,61], Postelnicu & Rees [85], Rees [90], Rees & Pop [91], Shivakumar *et al* [101,102], Straughan [106] and Sunil *et al* [111,112]. In particular, Straughan [106] proves a rigorous nonlinear stability result for thermal convection which exactly complements the linear analysis of Banu & Rees [5], while Straughan [108] adapts a theory of Green & Naghdi to be applicable to thermal convection in nanofluids.

Another class of problem which has attracted much attention is that where the porous medium occupies a vertical layer subject to differential heating from one side to the other. This clearly has many applications in insulation, such as in buildings. The first proof that a vertical porous slab of Darcy type which is held

at fixed but different temperatures on the vertical walls is stable to perturbations from the equilibrium state was presented by Gill [32]. Gill's [32] analysis is based on a linear theory and studies the two-dimensional case. Straughan [106] analysed the same problem but in three dimensions and treated the fully nonlinear case by means of energy integral techniques. In particular, he derived a threshold on the Rayleigh number which guarantees global stability regardless of how large the initial perturbation may be. However, he also used a generalized energy method employing solution gradients to demonstrate that Gill's [32] result yielding stability for all Rayleigh numbers is true in the fully nonlinear three-dimensional case, but for initial data suitably restricted. Such generalized energy methods have been used in other contexts by Galdi [28], Galdi *et al* [29] and Galdi & Straughan [30, 31]. Some articles that deal with other aspects of convection in a vertical porous slab include Bera & Khalili [6], Kumar *et al* [44, 45], Papanicolaou *et al* [72], Rees [89] and Vadasz [116]. Articles dealing with energy stability techniques in porous vertical convection include Flavin & Rionero [26], Kwok & Chen [46] and Qin & Kalone [86]. These final three are discussed in detail in Straughan [105], pp. 126-134.

Of particular relevance to the problem we discuss in this chapter is the recent work of Rees [90] who treated the Gill [32] problem of thermal convection in a vertical porous medium, but employed the theory of non-local thermal equilibrium, allowing for different fluid and solid temperatures. This analysis again shows that the vertical configuration is always stable according to linear theory, even with the much more complicated local thermal equilibrium theory. In this chapter we will revisit the Rees [90] problem but treat the fully nonlinear three-dimensional situation. It is very important to do this as linear theory provides no information on stability, it merely yields a threshold for instability. It is well known that for many problems a solution may become unstable well below the linear instability threshold due to a large initial data disturbance, giving rise to sub-critical instability. Thus, the following fully nonlinear analysis is important to show whether the linear theory yields any useful information about stability.

In the next section we present the basic equations for thermal convection in a local thermal non-equilibrium porous medium and for the problem of differentially

heated sidewalls in a vertical layer configuration. We then develop an L^2 nonlinear stability analysis which yields fully global (for all initial data) stability provided that the Rayleigh number is below a threshold which we derive. Finally, we show how a generalized energy method may be utilized to yield nonlinear stability for all Rayleigh numbers, provided the initial data is suitably restricted.

8.1 Basic problem

We begin our analysis by considering a vertical channel of a porous medium saturated by an incompressible fluid, which extends infinitely in the vertical, z , direction. We will assume that the Boussinesq approximation is satisfied and that Darcy's Law holds, but the fluid and porous material satisfy different heat transport equations. On the boundaries of the channel, $x = L/2$ and $x = -L/2$, the horizontal velocity is zero, $u = 0$ and the temperature, T , is kept constant at $T^f = T^s = T_h$ and $T^f = T^s = T_c$, respectively, where T_h and T_c are constants with $T_h > T_c$ and the superscripts f and s represent the fluid and solid. A diagram of this model is given in Figure 8.1.

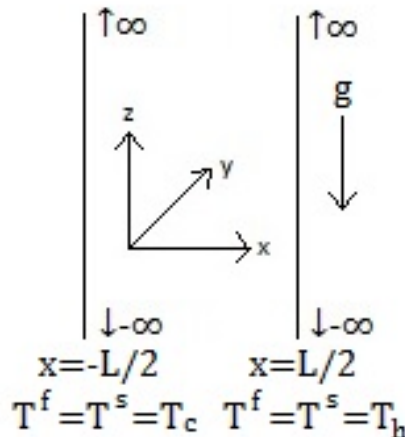


Figure 8.1: Diagram of a vertical porous channel in thermal non-equilibrium and differentially heated on the horizontal walls.

The full three dimensional equations are, c.f. Rees [90],

$$\begin{aligned}
v_{i,i} &= 0, \\
v_i &= -\frac{K}{\mu}p_{,i} + k_i \frac{\rho^f g \beta K}{\mu} (T^f - T^{ref}), \\
\epsilon(\rho c)^f T_{,t}^f + (\rho c)^f v_i T_{,i}^f &= \epsilon k^f \Delta T^f + h(T^s - T^f), \\
(1 - \epsilon)(\rho c)^s T_{,t}^s &= (1 - \epsilon)k^s \Delta T^s - h(T^s - T^f),
\end{aligned} \tag{8.1}$$

where standard indicial notation is employed, $\mathbf{v} = (u, v, w)$ is the velocity of the fluid, K is the permeability of the porous medium, μ is the dynamic viscosity of the fluid, p and ρ are pressure and density, β is the coefficient of thermal expansion, c is the specific heat, k is the diffusivity, $T^{ref} = (T_h + T_c)/2$ is the reference temperature, $\mathbf{k} = (0, 0, 1)$ is a unit vector in the vertical direction and h is the interfacial heat transfer coefficient.

We non-dimensionalise equations (8.1) using the variables

$$\begin{aligned}
x_i &= Lx_i^*, & u_i &= \frac{\epsilon k^f}{(\rho c)^f L} u_i^*, & p &= \frac{\epsilon k^f \mu}{(\rho c)^f K} p^*, \\
T^f &= (T_h - T_c)\theta + T^{ref}, & T^s &= (T_h - T_c)\phi + T^{ref}, & t &= \frac{(\rho c)^f L^2}{k^f} t^*,
\end{aligned}$$

where θ and ϕ represent the temperature of the fluid and solid. This yields the following system

$$\begin{aligned}
v_{i,i} &= 0, \\
v_i &= -p_{,i} + k_i R \theta, \\
\theta_{,t} + v_i \theta_{,i} &= \Delta \theta + H(\phi - \theta), \\
\alpha \phi_{,t} &= \Delta \phi - H\gamma(\phi - \theta),
\end{aligned} \tag{8.2}$$

together with the boundary conditions

$$u \equiv v_1 = 0, \quad \theta = \phi = \pm 1/2 \quad \text{on } x = \pm 1/2. \tag{8.3}$$

The non-dimensional coefficients α , γ , H are defined by

$$\alpha = \frac{(\rho c)^s k^f}{(\rho c)^f k^s}, \quad \gamma = \frac{\epsilon k^f}{(1 - \epsilon)k^s}, \quad H = \frac{L^2 h}{\epsilon k^f} \tag{8.4}$$

and the Rayleigh number, R , is introduced as

$$R = \frac{\rho^f g \beta K L (\rho c)^f (T_h - T_c)}{\mu \epsilon k^f}.$$

The steady solution to system (8.2), (8.3) we are interested in is

$$\bar{u} = \bar{v} = 0, \quad \bar{w} = Rx, \quad \bar{\theta} = x, \quad \bar{\phi} = x, \quad (8.5)$$

where $\mathbf{v} = (u, v, w)$ and an overbar indicates the steady state. To study stability we introduce perturbations $\mathbf{u} = (\hat{u}, \hat{v}, \hat{w}), \pi, \hat{\theta}, \hat{\phi}$ around this steady solution to system (8.2), (8.3), and then derive the equations governing the perturbation variables as

$$\begin{aligned} u_{i,i} &= 0, \\ u_i &= -\pi_{,i} + k_i R \theta, \\ \theta_{,t} + u_i \theta_{,i} + u + Rx \theta_{,z} &= \Delta \theta + H(\phi - \theta), \\ \alpha \phi_{,t} &= \Delta \phi - H\gamma(\phi - \theta), \end{aligned}$$

with boundary conditions

$$u = \theta = \phi = 0 \quad \text{on } x = \pm 1/2, \quad (8.6)$$

where we have dropped the $\hat{\cdot}$ symbol from all parameters to simplify notation.

8.2 Non-linear energy stability; L^2 analysis

We now define a convection cell, V , in which $-1/2 < x < 1/2$ and, as standard for this type of problem, the solution is assumed to be periodic in y and z . This periodicity is due to the fact that the model extends infinitely in the y and z directions. As throughout this thesis we then let $\|\cdot\|$ and (\cdot, \cdot) be the norm and inner product on $L^2(V)$, e.g.

$$\|f\|^2 = \int_V f^2 dV \quad \text{and} \quad (f, g) = \int_V fg dV.$$

Next, equation (8.6)₂ is multiplied by u_i , (8.6)₃ by θ and (8.6)₄ by ϕ before integrating over V . We integrate by parts and utilise the boundary conditions to find

$$\begin{aligned} 0 &= -\|\mathbf{u}\|^2 + R(\theta, w), \\ \frac{1}{2} \frac{d}{dt} \|\theta\|^2 &= -\|\nabla \theta\|^2 + H(\phi - \theta, \theta) - (u, \theta) - R \int_V x \theta \theta_{,z} dV, \\ \frac{\alpha}{2} \frac{d}{dt} \|\phi\|^2 &= -\|\nabla \phi\|^2 - \gamma H(\phi - \theta, \phi). \end{aligned} \quad (8.7)$$

Due to periodic boundary conditions in the y and z directions and (8.6) we may remove the final term on the right hand side of (8.7)₂ by

$$\int_V x\theta\theta_{,z} dV = \frac{1}{2} \int_V \frac{\partial}{\partial z}(x\theta^2) dV = 0.$$

We choose coupling parameters $\lambda > 0$, $\gamma > 0$ and create the combination $\lambda(8.7)_1 + \gamma(8.7)_2 + (8.7)_3$ to arrive at the equation

$$\begin{aligned} \frac{1}{2} \frac{d}{dt}(\gamma\|\theta\| + \alpha\|\phi\|^2) &= -\lambda\|\mathbf{u}\|^2 - \gamma\|\nabla\theta\|^2 - \|\nabla\phi\|^2 + R\lambda(\theta, w) \\ &\quad - \gamma(u, \theta) - \gamma H\|\phi - \theta\|^2. \end{aligned} \quad (8.8)$$

Next we use the arithmetic-geometric inequality $2ab \leq \xi a^2 + b^2/\xi$, with parameters $\xi, \eta > 0$ at our disposal on the (u, θ) and (θ, w) terms in (8.8). As $\theta = \phi = 0$ on the boundary we may now use Poincaré's inequality, $\|\nabla\theta\|^2 \geq \pi^2\|\theta\|^2$, $\|\nabla\phi\|^2 \geq \pi^2\|\phi\|^2$, and further use the fact that $\|\mathbf{u}\|^2 = \|u\|^2 + \|v\|^2 + \|w\|^2$ to find

$$\begin{aligned} \frac{1}{2} \frac{d}{dt}(\gamma\|\theta\| + \alpha\|\phi\|^2) &\leq -\left(\lambda - \frac{\gamma\xi}{2}\right)\|u\|^2 - \left(\lambda - \frac{R\lambda\eta}{2}\right)\|w\|^2 \\ &\quad - \lambda\|v\|^2 - \pi^2\|\phi\|^2 \\ &\quad - \left(\gamma\pi^2 - \frac{R\lambda}{2\eta} - \frac{\gamma}{2\xi}\right)\|\theta\|^2 - \gamma H\|\phi - \theta\|^2. \end{aligned} \quad (8.9)$$

In order to show that the perturbation decays we now require

$$\lambda - \frac{\gamma\xi}{2} \geq 0, \quad \lambda - \frac{R\lambda\eta}{2} \geq 0 \quad \text{and} \quad \gamma\pi^2 - \frac{R\lambda}{2\eta} - \frac{\gamma}{2\xi} \geq 0$$

and therefore choose

$$\xi = \frac{2\lambda}{\gamma}, \quad \eta = \frac{2}{R} \quad \text{and} \quad 0 < \lambda_- < \lambda < \lambda_+$$

where, after substituting for ξ and η ,

$$\lambda_{\pm} = \frac{2\gamma\pi^2}{R^2} \pm \frac{\gamma}{R^2} \sqrt{4\pi^2 - R^2}. \quad (8.10)$$

In order for (8.10) to have to real solutions for λ we require that $R < 2\pi$. If we assume that this holds, inequality (8.9) may be reduced to

$$\frac{1}{2} \frac{d}{dt}(\gamma\|\theta\| + \alpha\|\phi\|^2) \leq -\pi^2\|\phi\|^2 - \left(\gamma\pi^2 - \frac{R\lambda}{2\eta} - \frac{\gamma}{2\xi}\right)\|\theta\|^2. \quad (8.11)$$

We now define an energy E by

$$E(t) = \frac{\gamma}{2} \|\theta\|^2 + \frac{\alpha}{2} \|\phi\|^2,$$

and then observe that

$$\frac{d}{dt} E \leq -cE \tag{8.12}$$

with

$$c = \min \left(\frac{2\pi^2}{\alpha}, \frac{2\omega}{\alpha} \right),$$

where

$$\omega = \gamma\pi^2 - \frac{R\lambda}{2\eta} - \frac{\gamma}{2\xi}.$$

Inequality (8.12) is easily integrated to see that

$$E(t) \leq e^{-ct} E(0). \tag{8.13}$$

From inequality (8.13) we deduce that both θ and ϕ decay at least exponentially in L^2 measure. Also, use of the Cauchy-Schwarz inequality on equation (8.7)₁ allows us to deduce

$$\|\mathbf{u}\|^2 \leq \frac{R^2}{2} \|\theta\|^2 + \frac{1}{2} \|w\|^2$$

and therefore, remembering that $\|\mathbf{u}\|^2 = \|u\|^2 + \|v\|^2 + \|w\|^2$,

$$\|\mathbf{u}\|^2 \leq R^2 \|\theta\|^2. \tag{8.14}$$

We then see that \mathbf{u} likewise decays at least exponentially in the L^2 norm.

We conclude that if $R < 2\pi$ then the steady solution is stable to perturbations of any amplitude. In order to derive restrictions to the initial conditions such that the steady solution is stable for any Rayleigh number we now introduce a generalized energy involving gradient terms, c.f. Galdi [28] and Galdi & Straughan [31].

8.3 Non-linear stability for all Rayleigh numbers

We now demonstrate stability for any Rayleigh number, provided the initial disturbances are small enough. To do this we begin by taking curl curl of equation (8.6)₁ to obtain

$$-\Delta u_i = Rk_j \theta_{,ij} - k_i R \Delta \theta$$

and then retain only the 1st component to find

$$-\Delta u = R\theta_{,xz}. \quad (8.15)$$

We multiply (8.6)₂ by $-\Delta\theta$ and (8.6)₃ by $-\Delta\phi$, and integrate each term over V . Then, after integrating by parts, we obtain the separate identities

$$\begin{aligned} \frac{1}{2} \frac{d}{dt} \|\nabla\theta\|^2 &= -\|\Delta\theta\|^2 + \int_V u_i \theta_{,i} \Delta\theta \, dV + \int_V u \Delta\theta \, dV \\ &\quad - H \int_V (\phi - \theta) \Delta\theta \, dV + R \int_V x \theta_{,z} \Delta\theta \, dV, \end{aligned} \quad (8.16)$$

and

$$\frac{\alpha}{2} \frac{d}{dt} \|\nabla\phi\|^2 = -\|\Delta\phi\|^2 + \gamma H \int_V (\phi - \theta) \Delta\phi \, dV. \quad (8.17)$$

Again integrating by parts, utilising the boundary conditions and (8.15) we find that the third and final terms of (8.16) cancel, since

$$\begin{aligned} R \int_V x \theta_{,z} \Delta\theta \, dV &= -R \int_V x \theta \Delta\theta_{,z} \, dV \\ &= \frac{R}{2} \int_V \frac{\partial}{\partial z} x |\nabla\theta|^2 \, dV + R \int_V \theta \nabla x \nabla\theta_{,z} \, dV \\ &= R \int_V \theta \theta_{,xz} \, dV \\ &= - \int_V \Delta u \theta \, dV = - \int_V u \Delta\theta \, dV. \end{aligned}$$

We proceed by bounding the non-linear cubic term in (8.16) using the estimate

$$\int_V u_i \theta_{,i} \Delta\theta \, dV \leq \sup_V |\mathbf{u}| \cdot \|\nabla\theta\| \|\Delta\theta\|,$$

c.f. Galdi [28] and Galdi & Staughan [31], and create the combination $\gamma(8.16)+(8.17)$, where $\gamma > 0$, to find

$$\begin{aligned} \frac{1}{2} \frac{d}{dt} (\gamma \|\nabla\theta\|^2 + \alpha \|\nabla\phi\|^2) &\leq -\gamma \|\Delta\theta\|^2 - \|\Delta\phi\|^2 - \gamma H \|\nabla(\theta - \phi)\|^2 \\ &\quad + \gamma \sup_V |\mathbf{u}| \cdot \|\nabla\theta\| \|\Delta\theta\|. \end{aligned} \quad (8.18)$$

If we additionally impose the condition that $u_i n_i = 0$ on the lateral cell boundary then it is shown in Galdi & Straughan [31] that there exists a constant C that depends on the shape of the domain such that $\sup_V |\mathbf{u}| \leq C \|\Delta\mathbf{u}\|$. In order to

bound $\|\Delta \mathbf{u}\|$ we square (8.15) and use the fact that the boundary condition $\theta = 0$ on $x = \pm 1/2$ implies that $\theta_{,z} = 0$ on $x = \pm 1/2$ to derive

$$\begin{aligned}\|\Delta \mathbf{u}\|^2 &= R^2(\|\Delta \theta\|^2 - \|\theta_{,zz}\|^2 - \|\theta_{,xz}\|^2 - \|\theta_{,yz}\|^2) \\ &\leq R^2\|\Delta \theta\|^2.\end{aligned}$$

Inserting this inequality into (8.18) we find that

$$\begin{aligned}\frac{1}{2} \frac{d}{dt} F &\leq -\gamma(1 - CR\|\nabla \theta\|)\|\Delta \theta\|^2 - \|\Delta \phi\|^2 - \gamma H\|\nabla(\theta - \phi)\|^2 \\ &\leq -\gamma(1 - CR\|\nabla \theta\|)\|\Delta \theta\|^2 - \|\Delta \phi\|^2,\end{aligned}\tag{8.19}$$

where we have defined a function

$$F = \gamma\|\nabla \theta\|^2 + \alpha\|\nabla \phi\|^2,$$

which we assume to be continuous, and have dropped the non-positive H term.

To proceed, we now estimate $\|\nabla \theta\|$ as follows,

$$\|\nabla \theta\| = (\|\nabla \theta\|^2)^{1/2} \leq \left(\|\nabla \theta\|^2 + \frac{\alpha}{\gamma} \|\nabla \phi\|^2 \right)^{1/2} \leq \frac{1}{\sqrt{\gamma}} F^{1/2}.\tag{8.20}$$

We then insert inequality (8.20) into (8.19) and rearrange to obtain

$$\frac{1}{2} \frac{dF}{dt} = \frac{1}{2} \dot{F} \leq -\|\Delta \phi\|^2 - \gamma\|\Delta \theta\|^2 \left(1 - \frac{CR}{\sqrt{\gamma}} F^{1/2} \right).\tag{8.21}$$

We must now consider two cases, namely $\alpha \leq 1$ and $\alpha > 1$. In the first case

$$-\|\Delta \phi\|^2 \leq -\alpha\|\Delta \phi\|^2$$

and therefore from (8.21)

$$\begin{aligned}\frac{1}{2} \dot{F} &\leq -\alpha\|\Delta \phi\|^2 - \gamma\|\Delta \theta\|^2 \left(1 - \frac{CR}{\sqrt{\gamma}} F^{1/2} \right) \\ &\leq -(\alpha\|\Delta \phi\|^2 + \gamma\|\Delta \theta\|^2) \left(1 - \frac{CR}{\sqrt{\gamma}} F^{1/2} \right).\end{aligned}\tag{8.22}$$

If we now suppose that

$$F^{1/2}(0) < \frac{\sqrt{\gamma}}{CR}\tag{8.23}$$

then either $F(t) < \gamma/C^2R^2, \forall t > 0$, or $\exists \tau > 0$ such that

$$F(\tau) = \frac{\gamma}{C^2R^2}.\tag{8.24}$$

We will assume that the latter is true. By integration by parts and use of the boundary conditions we may show that

$$\begin{aligned}\|\nabla\theta\|^2 &= -(\theta, \Delta\theta) \\ &\leq \|\theta\|\|\Delta\theta\|\end{aligned}$$

where in the last line the Cauchy-Schwarz inequality has been employed. Further use of Poincaré's inequality allows us to deduce

$$\begin{aligned}\|\nabla\theta\|^2 &\leq \pi^{-1}\|\nabla\theta\|\|\Delta\theta\| \\ &\leq \frac{1}{2}\|\nabla\theta\|^2 + \frac{1}{2\pi^2}\|\Delta\theta\|^2\end{aligned}$$

from which we derive

$$\pi^2\|\nabla\theta\|^2 \leq \|\Delta\theta\|^2. \quad (8.25)$$

We next suppose $t \in [0, \tau)$ and then employing inequality (8.25) and the analogue for ϕ we see from inequality (8.22) that

$$\dot{F} \leq -2\pi^2 F \left(1 - \frac{CR}{\sqrt{\gamma}} F^{1/2} \right). \quad (8.26)$$

F' is then strictly decreasing on $[0, \tau)$, and thus by continuity, $F(\tau) < F(0)$. This contradicts assumption (8.24) and so from inequality (8.26) $F(t) \leq F(0)$, for all t . We may then replace $F^{1/2}(t)$ in (8.26) by $F^{1/2}(0)$. With the constant b defined by

$$b = 1 - \frac{CR F^{1/2}(0)}{\sqrt{\gamma}} > 0,$$

inequality (8.26) yields

$$F' \leq -2bF$$

which may be integrated to find

$$F(t) \leq F(0) \exp(-2bt).$$

Thus, provided (8.23) holds $\|\nabla\theta\|$ and $\|\nabla\phi\|$ decay at least exponentially in L^2 norm and from Poincaré's inequality likewise $\|\theta\|$ and $\|\phi\|$ decay. Additionally the argument leading to (8.14) applies and so $\|\mathbf{u}\|^2$ also decays.

In the case where $\alpha > 1$ we again begin by substituting (8.20) into (8.19) to obtain

$$\frac{1}{2}\dot{F} \leq -\|\Delta\phi\|^2 - \gamma\|\Delta\theta\|^2 + CR\sqrt{\gamma}F^{1/2}\|\Delta\theta\|^2. \quad (8.27)$$

Now, if $\alpha > 1$ then $1/\alpha < 1$ and (8.27) becomes

$$\begin{aligned} \frac{1}{2}\dot{F} &\leq -\frac{1}{\alpha} (\alpha\|\Delta\phi\|^2 + \gamma\|\Delta\theta\|^2) + \frac{CR}{\sqrt{\gamma}}F^{1/2} (\alpha\|\Delta\phi\|^2 + \gamma\|\Delta\theta\|^2) \\ &= -\left(\frac{1}{\alpha} - \frac{CR}{\sqrt{\gamma}}F^{1/2}\right) (\alpha\|\Delta\phi\|^2 + \gamma\|\Delta\theta\|^2). \end{aligned}$$

A similar argument to that for the case $\alpha \leq 1$ can now be applied to deduce that F decays exponentially, and hence there is non-linear stability, provided now

$$F^{1/2}(0) < \frac{\sqrt{\gamma}}{\alpha CR}.$$

8.3.1 Physical value for α

From the definition (8.4) of α we know $\alpha = \kappa^f/\kappa^s$, where $\kappa = k/\rho c$ denotes thermal conductivity and the superscripts f and s represent the fluid and solid respectively. If, for example, we consider a porous medium composed of glass beads with the saturating fluid being water at room temperature, then from Lide [50], pages 1-37, 6-9 and 15-36 we find $\kappa^s \approx 6.7 \times 10^{10} - 8.4 \times 10^{10} \text{ mW m}^{-1} (\text{°K})^{-1}$ and $\kappa^f \approx 580 \text{ mW m}^{-1} (\text{°K})^{-1}$. Therefore, for a typical laboratory porous medium α is clearly very small and we have the situation $\alpha < 1$.

Chapter 9

Conclusions

In Chapter 2 we investigated how the linear instability of a horizontal Darcy porous layer is affected by the presence of an exothermic reaction on the lower boundary. It was assumed that the density depends linearly on temperature and is independent of the concentration of the reactant, this was in line with literature on similar models. We found that both stationary and oscillatory convection occur and that the critical Rayleigh number, R_c , which is the Rayleigh number, R , at the onset of instability, increases as some parameters of the reaction are increased and decreases as others are increased. A simple modification to this work would be to allow the density to also depend on the reactant concentration.

The instability boundaries obtained in Chapter 2 show that the model is unstable above this boundary, however provide no information about the instability or stability below it. It was therefore natural to consider this area separately and in Chapter 3 we used a non-linear energy method to show that a region of stability does exist. Between these two regions we have no information about stability and sub-critical instabilities may occur. We also showed that the parameter $M\phi$ has no influence on the stability boundary obtained. In order to do the energy analysis we restricted the reactions to those for which are well catalysed so that $\xi = E/R^*T_U \approx 0$, where E is the activation energy, R^* is the universal gas constant and T_U is the temperature on the upper boundary and therefore we may set $\exp(-\xi/T) = 1$. This is a necessary assumption to be able to keep the equations fully non-linear throughout the analysis. Further analysis could be carried out in order to find regions of non-linear

stability for all values of ξ .

Chapter 4 considered the model studied in Chapter 2, but allows the density to depend on the reactant concentration and shows that it is continuously dependent on the reaction coefficients. Again, in order to complete the analysis it was necessary to restrict the model to $\xi \approx 0$ and the work could be extended to relax this assumption.

The influence of including the Soret effect on the linear instability of the Darcy model was considered in Chapter 5. We found that stationary convection may only occur for small Lewis numbers as increasing the Soret effect causes the Lewis number at which the dominant type of convection switches from stationary to oscillatory to decrease. When it does occur the critical Rayleigh number is greater for stronger Soret effects, this is because increasing the Soret number acts equivalently to increasing the destabilising concentration field.

In Chapters 6 and 7 we considered a horizontal highly porous layer with an exothermic reaction on the lower boundary. In this case higher derivatives of the velocity may have a significant impact on stability and we therefore employed the Brinkman model. This model includes a Laplacian velocity term and in Chapter 6 we investigated the influence of this term on linear instability, finding that increasing the coefficient greatly increases the critical Rayleigh number. Continuous dependence on the reaction parameters was established in Chapter 7, where we again let the density depend on the reactant concentration and assumed $\xi \approx 0$.

Finally, in Chapter 8 we turned our attention to a vertical porous layer. We allowed the solid and fluid components to be in thermal non-equilibrium, i.e. they may locally be at different temperatures, and developed two non-linear stability results. The first is that the model is stable given any initial disturbance from the steady state provided that $R < 2\pi^2$. The second is that the model is stable for any Rayleigh number provided that the initial disturbance is smaller than a given value. It is found that the value in this second case is dependent on the porous medium.

9.1 Further work

We will now discuss some more potential extensions to the work in this thesis.

It was shown in Chapter 6 that increasing the Brinkman coefficient greatly increased the critical Rayleigh number and thus the region below the instability curve with unknown stability became much larger. A non-linear energy method similar to that employed in Chapter 3 could be used here to obtain a stability boundary. It may also be possible to develop a non-linear method that allows the restriction that $\xi = 0$ to be removed.

Another interesting opportunity to extend this work is to study a porous layer saturated by a fluid and overlaid by the same fluid, with a reaction occurring on the lower boundary of the porous layer. There are many applications of multi-layer convection problems and a few of these include melt-water formations above and below ice-sheets, see e.g. Bogorodskii & Nagurnyi [9] and Carr [12], and flow in underground channels or streambeds, see e.g. Ewing *et al* [25], El-Habel *et al* [21], Boana *et al* [8]. There have recently been a large number of multi-layer models proposed including those of McKay [62], Nield [69], Payne & Straughan [76] and Chen & Chen [15]. A number of other applications and references to many more studies may be found in Chapter 6 of Straughan [107].

A further possibility is to allow the density of the fluid to take a form that is non-linear in the temperature dependence. An example of such a fluid is water, which attains its maximum density at 4°C. If the temperature on the upper boundary is greater than the temperature at which the fluid attains its maximum, T_0 , and the temperature on the lower boundary lower than T_0 then there is a stabilised layer over a potentially unstable layer. It is known that if instabilities occur in the lower layer then these may penetrate into the upper stabilised layer, this is discussed in detail in Moore & Weiss [66]. Applications for penetrative convection are wide ranging, for example Straughan [105] discusses geophysical applications, Zhang & Schubert [121] provide applications in astrophysics and Bogorodskii & Nagurnyi [9] study how it may affect the speed at which ice sheets melt. A possible model for us to consider is a porous layer that is saturated by water, in which there is a salt dissolved, and with the salt undergoing a chemical reaction on the lower boundary.

Bibliography

- [1] G. Ahmadi. Stability of a micropolar fluid layer heated from below. *Int. J. Eng. Sci.*, 14:81–89, 1976.
- [2] M.S. Alam, M.M. Rahman, and M.A. Sattar. Effects of chemical reaction and thermophoresis on magneto-hydrodynamic mixed convective heat and mass transfer flow along an inclined plate in the presence of heat generation and (or) absorption with viscous dissipation and Joule heating. *Canadian J. Physics*, 86:1057–1066, 2011.
- [3] J.T.H. Andres and S.S.S. Cardoso. Onset of convection in a porous medium in the presence of chemical reaction. *Phys. Rev. E*, 83:046312, 2011.
- [4] E. Aulisa, L. Bloshanskaya, L. Hoang, and A. Ibragimov. Analysis of generalized Forchheimer flows of compressible fluids in porous media. *J. Math. Phys.*, 50:103102, 2009.
- [5] N. Banu and D.A.S. Rees. The onset of Darcy-Bénard convection using a thermal nonequilibrium model. *Int. J. Heat Mass Transfer*, 45:2221–2228, 2002.
- [6] P. Bera and A. Khalili. Influence of Prandtl number on stability of mixed convective flow in a vertical channel filled with a porous medium. *Phys. Fluids*, 18:124103, 2006.
- [7] B.S. Bhadauria and A. Shilpi. Convective transport in a nanofluid saturated porous layer with thermal non equilibrium model. *Transport in Porous Media*, 88:107–131, 2011.

- [8] F. Boana, R. Revelli, and L. Ridolfi. Bedform-induced hyporheic exchange with unsteady flows. *Advances in Water Resources*, 30:148–156, 2007.
- [9] P.V. Bogorodskii and A.P. Nagurnyi. Under-ice meltwater puddles: a factor of fast sea ice melting in the arctic. *Doklady Earth Sciences*, 373:885–887, 2000.
- [10] D. Bourne. Hydrodynamic stability, the Chebyshev tau method and spurious eigenvalues. *Continuum Mech. Thermodyn.*, 15:571–579, 2003.
- [11] F. Capone and S. Rionero. Nonlinear stability of a convective motion in a porous layer driven by a horizontally periodic temperature gradient. *Continuum Mech. Thermodyn.*, 15:529–538, 2003.
- [12] M. Carr. A model for convection in the evolution of under-ice melt ponds. *Continuum Mech. Thermodyn.*, 15:45–54, 2003.
- [13] A.O. Celebi, V.K. Kalantarov, and D. Ugurlu. On continuous dependence on coefficients of the Brinkman-Forchheimer equations. *Appl. Math. Letters*, 19:801–807, 2006.
- [14] S. Chandrasekhar. *Hydrodynamic and Hydromagnetic Stability*. Oxford, 1961.
- [15] F. Chen and C.F. Chen. Onset of finger convection in a horizontal porous layer underlying a fluid layer. *J. Heat Transfer*, 110:403–409, 1988.
- [16] X. Chen, S. Wang, J. Tao, and W. Tan. Stability analysis of thermosolutal convection in a horizontal porous layer using a thermal non-equilibrium model. *Int. J. Heat Fluid Flow*, 32:78–87, 2011.
- [17] D.G. Christopherson. Note on the vibration of membranes. *Quart. J. Math.*, 11:63–65, 1940.
- [18] R. Courant and D. Hilbert. *Methods of Mathematical Physics, Volume I*. Interscience Publishers, New York, 1953.
- [19] P.A. Domenico. Transport phenomena in chemical rate processes in sediments. *Ann. Rev. Earth Planet Sci.*, 5:287–317, 1977.

- [20] J.J. Dongarra, B. Straughan, and D.W. Walker. Chebyshev-tau-QZ algorithm methods for calculating spectra of hydrodynamic stability problems. *App. Num. Math.*, 22:399–434, 1996.
- [21] F. El-Habel, C. Mendoza, and A.C. Bagtzoglou. Solute transport in open channel flows and porous streambeds. *Advances in Water Resources*, 25:455–469, 2002.
- [22] I.A. Eltayeb, Hamza E.A., Jervase J.A., Krishan E.V., and Loper D.E. Compositional convection in the presence of a magnetic field. I. a single interface. *Proc. Roy. Soc. London A*, 460:3505–3528, 2004.
- [23] I.A. Eltayeb, Hamza E.A., Jervase J.A., Krishan E.V., and Loper D.E. Compositional convection in the presence of a magnetic field. II. cartesian plume. *Proc. Roy. Soc. London A*, 461:2605–2633, 2005.
- [24] G. Evans. *Practical Numerical Integration*. Wiley, Chichester, 1993.
- [25] R.E. Ewing, O.P. Iliev, and R.D. Lazarov. Numerical simulation of contaminant transport due to flow in liquid and porous media. *Manuscript*, 1994.
- [26] J.N. Flavin and S. Rionero. Nonlinear stability for a thermofluid in a vertical porous slab. *Cont. Mech. Thermodyn.*, 11:173–179, 1999.
- [27] F. Franchi and B. Straughan. Continuous dependence and decay for the Forchheimer equations. *Proc. Roy. Soc. London A*, 459:3195–3202, 2003.
- [28] G.P. Galdi. Nonlinear stability of the magnetic Bénard problem via a generalized energy method. *Arch. Rational Mech. Anal.*, 87:167–186, 1985.
- [29] G.P. Galdi, L.E. Payne, M.R.E. Proctor, and B. Straughan. Convection in thawing subsea permafrost. *Proc. Roy. Soc. London A*, 414:83–102, 1987.
- [30] G.P. Galdi and B. Straughan. Exchange of stabilities, symmetry and nonlinear stability. *Arch. Rational Mech. Anal.*, 89:211–228, 1985.
- [31] G.P. Galdi and B. Straughan. A nonlinear analysis of the stabilizing effect of rotation in the Bénard problem. *Proc. R. Soc. London*, 402:257–283, 1985.

- [32] A.E. Gill. A proof that convection in a porous vertical slab is stable. *J. Fluid Mech.*, 35:545–547, 1969.
- [33] B. Goyeau, J.P. Songbe, and D. Gobin. Numerical study of double-diffusive natural convection in a porous cavity using the Darcy-Brinkman formulation. *Int. J. of Heat and Mass Transfer*, 39:1363–1378, 1996.
- [34] A.A. Hill and M. Carr. Sharp global nonlinear stability for a fluid overlying a highly porous material. *Proc. Roy. Soc. London A*, 466:127–140, 2010.
- [35] A.A. Hill, S. Rionero, and B. Straughan. Global stability for penetrative convection with throughflow in a porous material. *J. Appl. Math.*, 72:635–643, 2007.
- [36] M. W. Hirsch and S. Smale. *Differential equations, dynamical systems, and linear algebra*. Academic Press, New York, 1974.
- [37] L. Hoang and A. Ibragimov. Structural stability of generalized Forchheimer equations for compressible fluids in porous media. *Nonlinearity*, 24:1–41, 2011.
- [38] C.T. Hsu and P. Cheng. The Brinkman model for natural convection about a semi-infinite vertical flat plate in a porous medium. *Int. J. of Heat and Mass Transfer*, 28:683–697, 1985.
- [39] D.B. Ingham and I. Pop. *Transport Phenomena in Porous Media III*. Elsevier, Oxford, 2005.
- [40] D. Joseph. On the stability of the Boussinesq equations. *Arch. Rational Mech. Anal.*, 20:59–71, 1965.
- [41] D. Joseph. Nonlinear stability of the Boussinesq equations by the method of energy. *Arch. Rational Mech. Anal.*, 22:163–184, 1966.
- [42] D. Joseph and S. Carmi. Subcritical convective instability. part 2. spherical shells. *Arch. Rational Mech. Anal.*, 26:769–777, 1966.
- [43] D. Joseph and C. Shir. Subcritical convective instability. part 1. fluid layers. *J. Fluid Mech.*, 26:753–768, 1966.

- [44] A. Kumar, P. Bera, and A. Khalili. Influence of inertia and drag terms on the stability of mixed convection in a vertical porous-medium channel. *Int. J. Heat Mass Transfer*, 53:23–24, 2010.
- [45] A. Kumar, P. Bera, and J. Kumar. Non-Darcy mixed convection in a vertical pipe filled with porous medium. *Int. J. Thermal Sciences*, 50:725–735, 2011.
- [46] L. Kwok and C. Chen. Stability of thermal convection in a vertical porous layer. *J. Heat Transfer*, 109:889–893, 1987.
- [47] P.A. Lakshmi Narayana and P.V.S.N. Murthy. Soret and Dufour effects on free convection heat and mass transfer from a horizontal flat plate in a darcy porous medium. *J. Heat Transfer*, 130:104504–1, 2008.
- [48] J. Lee, I.S. Shivakumara, and A.L. Mamatha. Effect of nonuniform temperature gradients on thermogravitational convection in a porous layer using a thermal nonequilibrium model. *J. Porous Media*, 14:659–669, 2011.
- [49] M. Li, Y. Wu, Y. Tian, and Y. Zhai. Non-thermal equilibrium model of the coupled heat and mass transfer in strong endothermic chemical reaction system of porous media. *Int. J. of Heat and Mass Transfer*, 50:2936–2943, 2007.
- [50] D.R. Lide. *Handbook of Chemistry and Physics*. CRC Press, Boca Raton, 72nd edition, 1991.
- [51] C. Lin and L.E. Payne. Structural stability for a Brinkman fluid. *Math. Meth. Appl. Sci.*, 30:567–578, 2007.
- [52] C. Lin and L.E. Payne. Structural stability for the Brinkman equations of flow in double diffusive convection. *J. Math. Anal. Appl.*, 325:1479–1490, 2007.
- [53] C. Lin and L.E. Payne. Continuous dependence on the Soret coefficient for double diffusive convection in Darcy flow. *J. Math. Anal. Appl.*, 342:311–325, 2008.

- [54] Y. Liu. Convergence and continuous dependence for the Brinkman - Forchheimer equations. *Math. Computer Modelling*, 49:1401–1415, 2009.
- [55] Y. Liu, Y. Du, and C. Lin. Convergence results for Forchheimer’s equations for fluid flow in porous media. *J. Math. Fluid Mech.*, 12:576–593, 2010.
- [56] Y. Liu, Y. Du, and C.H. Lin. Convergence and continuous dependence results for the Brinkman equations. *Applied Mathematics and Computation*, 215:4443–4455, 2010.
- [57] A. Mahdy. Effect of chemical reaction and heat generation or absorption on double diffusive convection from a vertical truncated cone in porous media with variable viscosity. *Int. Communications in Heat and Mass Transfer*, 37:548–554, 2010.
- [58] M.S. Malashetty and B.S. Biradar. The onset of double diffusive convection in a binary Maxwell fluid saturated porous layer with cross-diffusion effects. *Physics of Fluids*, 23:064109, 2011.
- [59] M.S. Malashetty and B.S. Biradar. The onset of double diffusive reaction-convection in an anisotropic porous layer. *Phys. Fluids*, 23:064102, 2011.
- [60] M.S. Malashetty, I.S. Shivakumara, and K. Sridhar. The onset of convection in an anisotropic porous layer using a thermal nonequilibrium model. *Transport in Porous Media*, 60:199–215, 2005.
- [61] M.S. Malashetty, I.S. Shivakumara, and K. Sridhar. The onset of Lapwood-Brinkman convection using a thermal nonequilibrium model. *Int. J. Heat Mass Transfer*, 48:1155–1163, 2005.
- [62] G. McKay. Onset of buoyancy-driven convection in superposed reacting fluid and porous layers. *J. Engng. Math.*, 33:31–46, 1998.
- [63] C.L. McTaggart and B. Straughan. Chemical surface reactions and nonlinear stability by the method of energy. *SIAM J. Math. Anal.*, 17:342–351, 1986.

- [64] J.H. Merkin and T. Mahmood. Convective flows on reactive surfaces in porous media. *Transport in Porous Media*, 33:279–293, 1998.
- [65] C.B. Moler and G.W. Stewart. An algorithm for generalized matrix eigenproblems. *SIAM J. Numer. Anal.*, 10:241–256, 1973.
- [66] D.R. Moore and N.O. Weiss. Nonlinear penetrative convection. *J. Fluid Mech.*, 61:553–581, 1973.
- [67] G. Mulone and S. Rionero. On the nonlinear stability of the rotating Bénard problem via the lyapunov direct method. *J. Math. Anal. and Appl.*, 144:109–127, 1998.
- [68] H.D. Nguyen, S. Paik, R.W. Douglass, and I. Pop. Unsteady non-darcy reaction-driven flow from an anisotropic cylinder in porous media. *Chem. Eng. Science*, 51:4963–4977, 1996.
- [69] D.A. Nield. Onset of convection in a fluid overlaying a layer of a porous medium. *J. Fluid Mech.*, 81:513–522, 1977.
- [70] D.A. Nield and A. Bejan. *Convection in Porous Media*. Springer, New York, 3rd edition, 2006.
- [71] Y. Ouyang and L. Yang. A note on the existence of a global attractor for the Brinkman - Forchheimer equations. *Nonlinear Analysis, Theory, Methods and Applications*, 70:2054–2059, 2009.
- [72] N.C. Papanicolaou, C. Christov, and P.M. Jordan. The influence of thermal relaxation on the oscillatory properties of two-gradient convection in a vertical slot. *European J. Mech. B - Fluids*, 30:68–75, 2011.
- [73] L. E. Payne and H. F. Weinberger. New bounds for solutions of second order elliptic partial differential equations. *Pacific J. Math.*, 8:551–573, 1958.
- [74] L.E. Payne, J.C. Song, and B. Straughan. Continuous dependence and convergence results for Brinkman and Forchheimer models with variable viscosity. *Proc. Roy. Soc. London A*, 455:2173–2190, 1999.

- [75] L.E. Payne and B. Straughan. Stability in the initial-time geometry problem for the Brinkman and Darcy equations of flow in porous media. *J. Math. Pures et Appl.*, 75:225–271, 1996.
- [76] L.E. Payne and B. Straughan. Analysis of the boundary condition at the interface between a viscous fluid and a porous medium and related modelling questions. *J. Math. Pures et Appl.*, 77:317–354, 1998.
- [77] L.E. Payne and B. Straughan. Structural stability for the Darcy equations of flow in porous media. *Proc. Roy. Soc. London A*, 454:1691–1698, 1998.
- [78] L.E. Payne and B. Straughan. Convergence and continuous dependence for the Brinkman - Forchheimer equations. *Stud. Appl. Math.*, 102:419–439, 1999.
- [79] L.E. Payne and B. Straughan. A naturally efficient technique for porous convection stability with non-trivial boundary condition. *Int. J. Numer. Anal. Geomech.*, 24:815–836, 2000.
- [80] R. Piazza and A. Guarino. Soret effect in interacting micellar solutions. *Phys. Rev. Lett.*, 88:208302, 2002.
- [81] I. Pop, T. Grosan, and R. Cornelia. Effect of heat generated by an exothermic reaction on the fully developed mixed convection flow in a vertical channel. *Comm. in Nonlinear Sc. and Num. Simulation*, 15:471–474, 2009.
- [82] I. Pop and D.B. Ingham. *Convective Heat Transfer: Mathematical and Computational Modeling of Viscous Fluids and Porous Media*. Pergamon, Oxford, 2001.
- [83] A. Postelnicu. Influence of chemical reaction on heat and mass transfer by natural convection from vertical surfaces in porous media considering Soret and Dufour effects. *Heat Mass Transfer*, 43:595–602, 2006.
- [84] A. Postelnicu. Onset of convection in a horizontal porous layer driven by catalytic surface reaction on the lower wall. *Int. J. Heat and Mass Transfer*, 52:2466–2470, 2009.

- [85] A. Postelnicu and D.A.S. Rees. The onset of Darcy-Brinkman convection in a porous medium using a thermal nonequilibrium model. part 1. stress-free boundaries. *Int. J. Energy Research*, 27:961–973, 2003.
- [86] Y. Qin and P.N. Kaloni. A nonlinear stability problem of convection in a porous vertical slab. *Phys. Fluids A*, 5:2067–2069, 1993.
- [87] M.M. Rahman and M. Al-Lawatia. Effects of higher order chemical reaction on micropolar fluid flow on a power law permeable stretched sheet with variable concentration in a porous medium. *Canadian J. Chem. Eng.*, 88:23–32, 2010.
- [88] K.R. Rajagopal. On a hierarchy of approximate models for flows of incompressible fluids through porous solids. *Models Meth. Appl. Sci.*, 17:215–252, 2007.
- [89] D.A.S. Rees. The stability of Prandtl-Darcy convection in a vertical porous layer. *Int. J. Heat Mass Transfer*, 31:1529–1534, 1988.
- [90] D.A.S. Rees. The effect of local thermal nonequilibrium on the stability of convection in a vertical porous channel. *Trans. Porous Med.*, 87:459–464, 2011.
- [91] D.A.S. Rees and I. Pop. Free convective stagnation point flow in a porous medium using a thermal nonequilibrium model. *Int. Comm. Heat Mass Transfer*, 26:945–954, 1999.
- [92] S. Rionero and L. Vergori. Long-time behaviour of fluid motions in porous media according to the Brinkman model. *Acta Mechanica*, 210:221–240, 2010.
- [93] A.M. Salem. Thermal-diffusion and diffusion-thermo effects on convective heat and mass transfer in a visco-elastic fluid flow through a porous medium over a stretching sheet. *Comm. Numerical Methods in Biomedical Engineering*, 22:955–966, 2006.
- [94] N.L. Scott. Convection in a horizontal layer of high porosity with an exothermic surface reaction on the lower boundary. *Int. J. Thermal Sc.*, 56:70–76, 2012.

- [95] N.L. Scott. Convection in a saturated Darcy porous medium with an exothermic chemical surface reaction and Soret effect. *Int. Comm. Heat and Mass Transfer*, 39:1331–1335, 2012.
- [96] N.L. Scott. Continuous dependence on boundary reaction terms in porous medium of Darcy type. *J. Math. Anal. Appl.*, 399:667–675, 2013.
- [97] N.L. Scott. Non-linear stability bounds for a horizontal layer of a porous medium with an exothermic reaction on the lower boundary. *Int. J. Non-Linear Mech.*, 57:163–167, 2013.
- [98] N.L. Scott and B. Straughan. Convection in a porous layer with a surface reaction. *Int. J. Heat and Mass Transfer*, 43:5653–5657, 2011.
- [99] N.L. Scott and B. Straughan. A nonlinear stability analysis of convection in a porous vertical channel including local thermal nonequilibrium. *J. Math. Fluid Mech.*, 15:171–178, 2013.
- [100] N.L. Scott and B. Straughan. Continuous dependence on the reaction terms in porous convection with surface reactions. *Quarterly of Applied Mathematics*, <http://dx.doi.org/10.1090/S0033-569X-2013-01289-X>.
- [101] I.S. Shivakumara, J. Lee, A.L. Mamatha, and M. Ravisha. Boundary and thermal non-equilibrium effects on convective instability in an anisotropic porous layer. *J. Mechanical Science Technology*, 25:911–921, 2011.
- [102] I.S. Shivakumara, J. Lee, A.L. Mamatha, and M. Ravisha. Effects of thermal nonequilibrium and non-uniform temperature gradients on the onset of convection in a heterogeneous porous medium. *Int. Communications Heat Mass Transfer*, 38:906–910, 2011.
- [103] C. Soret. Sur l'état d'équilibre que prend au point vue de sa concentration une dissolution saline primitivement homogène dont deux parties sont portées a des températures différentes. *Arch. Sci. Phys. Nat.*, 2:48–61, 1879.
- [104] B. Spain. *Tensor Calculus*. Oliver & Boyd; Interscience Publishers, New York, 1960.

- [105] B. Straughan. *The energy method, stability, and nonlinear convection*, volume 91 of *Applied Mathematical Sciences*. Springer, New York, second edition, 2004.
- [106] B. Straughan. Global nonlinear stability in porous convection with a thermal non-equilibrium model. *Proc. Roy. Soc. London A*, 462:409–418, 2006.
- [107] B. Straughan. *Stability and wave motion in porous media*, volume 165 of *Applied Mathematical Sciences*. Springer, New York, 2008.
- [108] B. Straughan. Green-Naghdi fluid with non-thermal equilibrium effects. *Proc. Roy. Soc. London A*, 466:2021–2032, 2010.
- [109] B. Straughan. Continuous dependence on the heat source in resonant porous penetrative convection. *Studies in Applied Mathematics*, 127:302–314, 2011.
- [110] B. Straughan and K. Hutter. A priori bounds and structural stability for double diffusive convection incorporating the Soret effect. *Proc. Roy. Soc. London A*, 455:767–777, 1999.
- [111] Sunil, P. Sharma, and A. Mahajan. Onset of Darcy-Brinkman double-diffusive convection in a magnetized ferrofluid layer using a thermal non-equilibrium model: a nonlinear stability analysis. *J. Geophys. Engng.*, 7:417–430, 2010.
- [112] Sunil, P. Sharma, and A. Mahajan. Onset of Darcy-Brinkman ferroconvection in a rotating porous layer using a thermal non-equilibrium model: A nonlinear stability analysis. *Transport in Porous Media*, 88:421–439, 2011.
- [113] B.C. Tai and M.I. Char. Soret and Dufour effects on free convection flow of non-Newtonian fluids along a vertical plate embedded in a porous medium with thermal radiation. *Int. Comm. Heat and Mass Transfer*, 37:480–483, 2010.
- [114] D. Ugurlu. On the existence of a global attractor for the Brinkman - Forchheimer equations. *Nonlinear Analysis, Theory, Methods and Applications*, 68:1986–1992, 2008.

- [115] P. Vadasz. *Emerging Topics in Heat and Mass Transfer in Porous Media*. Springer, New York, 2008.
- [116] P. Vadasz. Basic natural convection in a vertical porous layer differentially heated from its sidewalls subject to lack of local thermal equilibrium. *Int. J. Heat Mass Transfer*, 54:2387–2396, 2011.
- [117] K. Vafai. *Handbook of Porous Media*. Taylor & Francis, New York, 2nd edition, 2005.
- [118] K. Vafai. *Porous Media: Applications in Biological Systems and Biotechnology*. CRC Press, 2010.
- [119] G. Veronis. Motions at subcritical values of the Rayleigh number in a rotating fluid. *J. Fluid Mech.*, 24:545–554, 1966.
- [120] B. Wang and S. Lin. Existence of global attractors for the three-dimensional Brinkman-Forchheimer equation. *Math. Meth. Appl. Sci.*, 31:1479–1495, 2008.
- [121] K.K. Zhang and G. Schubert. From penetrative convection to teleconvection. *Astrophys. J.*, 572:461–476, 2002.
- [122] C.Y. Zhao, T.J. Lu, and H.P. Hodson. Thermal radiation in ultralight foams with open cells. *Int. J. Heat and Mass Transfer*, 47:2927–2939, 2004.

Appendix A

Chebyshev-tau numerical method

Throughout this thesis we have used the Chebyshev-tau method to numerically solve eigenvalue problems and find values for the critical Rayleigh number. In this appendix we will describe how this method works and derive some useful identities that apply at the boundaries of the domain. We will then show how the technique may be applied to a specific system.

A.1 Chebyshev polynomials

We begin by defining Chebyshev polynomials of the n^{th} degree, $T_n : [-1, 1] \rightarrow [-1, 1]$ by

$$T_n(\cos(\theta)) = \cos(n\theta), \quad (\text{A.1.1})$$

where $n \in \{0, 1, 2, 3, \dots\}$. The first two polynomials, of degrees 0 and 1, may be found by simply setting n equal to 0 or 1 in (A.1.1). We then find that

$$T_0 = \cos(0) = 1,$$

$$T_1 = \cos(\theta).$$

For the polynomials of degree 2 and greater we use the well known trigonometric identity

$$\cos(A + B) = \cos(A)\cos(B) - \sin(A)\sin(B). \quad (\text{A.1.2})$$

Setting $A = n\theta$ and first $B = m\theta$ then $B = -m\theta$ we find the two relations

$$\cos((n + m)\theta) = \cos(n\theta)\cos(m\theta) - \sin(n\theta)\sin(m\theta) \quad (\text{A.1.3})$$

and

$$\begin{aligned}\cos((n-m)\theta) &= \cos(n\theta)\cos(-m\theta) - \sin(n\theta)\sin(-m\theta) \\ &= \cos(n\theta)\cos(m\theta) + \sin(n\theta)\sin(m\theta).\end{aligned}\tag{A.1.4}$$

Adding (A.1.3) and (A.1.4) we find

$$\cos((n+m)\theta) + \cos((n-m)\theta) = 2\cos(n\theta)\cos(m\theta),$$

which in terms of the Chebyshev polynomials is

$$T_{n+m}(\cos(\theta)) + T_{|n-m|}(\cos(\theta)) = 2T_n(\cos(\theta))T_m(\cos(\theta)).\tag{A.1.5}$$

We find the polynomials of degree 2 and higher by writing $T_n = T_{1+m}$, where $m \in \{1, 2, 3, \dots\}$ and set $n = 1$ in (A.1.5) to obtain the recurrence relation

$$T_{m+1}(\cos(\theta)) + T_{m-1}(\cos(\theta)) = 2\cos(\theta)T_m(\cos(\theta)).$$

The known polynomials T_0 and T_1 are now used to calculate the full set of Chebyshev polynomials, where we set $x = \cos(\theta)$, and we find

$$\begin{aligned}T_0(x) &= 1, \\ T_1(x) &= x, \\ T_2(x) &= 2x^2 - 1, \\ T_3(x) &= 4x^3 - 3x, \\ T_4(x) &= 8x^4 - 8x^2 + 1, \\ &\text{etc.}\end{aligned}\tag{A.1.6}$$

A.1.1 Orthogonality of the Chebyshev polynomials

The Chebyshev-tau method uses the fact that the Chebyshev polynomials are orthogonal and will therefore demonstrate this fact here.

The weighted inner product of two general Chebyshev polynomials is defined by

$$\begin{aligned}\int_{-1}^1 \frac{T_n(x)T_m(x)}{\sqrt{1-x^2}} dx &= \int_0^\pi T_n(\cos(\theta))T_m(\cos(\theta))d\theta \\ &= \frac{1}{2} \int_0^\pi \cos((n+m)\theta) + \cos(|n-m|\theta) d\theta\end{aligned}\tag{A.1.7}$$

We now consider three cases; $n \neq m$, $n = m = 0$ and $n = m \neq 0$.

Case 1: $n \neq m$

In this first case we may immediately integrate (A.1.7) to find

$$\begin{aligned} \int_0^\pi T_n(\cos(\theta))T_m(\cos(\theta))d\theta &= \frac{1}{2} \int_0^\pi [\cos((n+m)\theta) + \cos(|n-m|\theta)] d\theta \\ &= \frac{1}{2} \left[\frac{\sin((n+m)\theta)}{n+m} + \frac{\sin(|n-m|\theta)}{|n-m|} \right]_0^\pi \\ &= 0. \end{aligned}$$

Case 2: $n = m = 0$

In this case to avoid dividing by zero after integration we must first simplify both the second first and second terms of (A.1.7). We then find

$$\begin{aligned} \int_0^\pi T_n(\cos(\theta))T_m(\cos(\theta))d\theta &= \frac{1}{2} \int_0^\pi [1 + 1] d\theta \\ &= [\theta]_0^\pi \\ &= \pi. \end{aligned}$$

Case 3: $n = m \neq 0$

In the final case we must simplify only the second term, we then integrate to find

$$\begin{aligned} \int_0^\pi T_n(\cos(\theta))T_m(\cos(\theta))d\theta &= \frac{1}{2} \int_0^\pi [\cos((n+m)\theta) + 1] d\theta \\ &= \frac{1}{2} \left[\frac{\sin((n+m)\theta)}{n+m} + \theta \right]_0^\pi \\ &= \frac{\pi}{2}. \end{aligned}$$

Together, these three cases clearly demonstrate that the Chebyshev polynomials are orthogonal with respect to the weighted inner product (A.1.7).

A.2 Chebyshev boundary identities

We now show some useful identities for representing the boundary conditions of a given function in terms of Chebyshev polynomials.

The Chebyshev polynomials are defined on the interval $x \in (-1, 1)$ and so we assume that the boundary conditions given are on $x = -1$ and $x = 1$, or equivalently on $\theta = 0$ and $\theta = \pi$.

Using (A.1.1) we quickly find the identities

$$T_n(\pm 1) = (\pm 1)^n.$$

Next, by differentiating (A.1.6) with respect to x we find that

$$\begin{aligned} \frac{dT_n}{dx} &= \frac{dT_n}{d\theta} \cdot \frac{d\theta}{dx} \\ &= \frac{n \sin(n\theta)}{\sin(\theta)}. \end{aligned} \tag{A.2.8}$$

In order to evaluate this at the boundaries we must first use L'Hopital's rule and then find that

$$T'_n = n^2(\pm 1)^{n+1}.$$

A.3 The Chebyshev differentiation matrices

In this section we will derive the coefficients of the Chebyshev differentiation matrix, **D**.

We begin by assuming that we may express a continuously differentiable function f , defined on the interval $(-1, 1)$, by a series of Chebyshev polynomials such that

$$f(x) = \sum_{n=0}^{\infty} f_n T_n(x), \tag{A.3.9}$$

where f_n are coefficients of the expansion. It will later be assumed that the function may be approximated by truncating this series at $n = N$. Suppose that the derivatives of f take similar forms to (A.3.9) for example

$$f'(x) = \sum_{n=0}^{\infty} f_n^{(1)} T_n(x),$$

or in general,

$$f^{(k)}(x) = \sum_{n=0}^{\infty} f_n^{(k)} T_n(x),$$

where $f^{(k)}$ is the k^{th} derivative of f and $f_n^{(k)}$ are coefficients relating to the Chebyshev expansion of the k^{th} derivative.

From (A.2.8) we now obtain a recurrence relation for T'_n , where

$$\frac{1}{n+1}T'_{n+1}(x) = 2T_n(x) + \frac{1}{n-1}T'_{|n-1|}(x) \quad \text{for } n \geq 2. \quad (\text{A.3.10})$$

When $n = 0$ we find

$$T'_1(x) = 2T_0(x) - T'_1(x) \quad (\text{A.3.11})$$

and when $n = 1$ we first multiply by $n - 1$ (A.3.10) before finding

$$0 = T'_0(x). \quad (\text{A.3.12})$$

Use of (A.1.6) shows that (A.3.11) and (A.3.12) are true and hence that the relation (A.3.10) is in fact valid for $n \geq 0$.

A.3.1 First differentiation matrix

It is now possible to write the coefficients f_n in terms of $f_n^{(1)}$ by

$$\begin{aligned} \frac{d}{dx} \sum_{n=0}^{\infty} f_n T_n(x) &= \sum_{n=0}^{\infty} f_n^{(1)} T_n(x) \\ &= \frac{1}{2} \left(\sum_{\substack{n=0 \\ n \neq 1}}^{\infty} \left[\frac{1}{n+1} T'_{n+1} - \frac{1}{n-1} T'_{|n-1|} \right] + \frac{1}{2} f_1^{(1)} T'_2 \right) \\ &= \frac{1}{2} \frac{d}{dx} \left(\sum_{\substack{n=0 \\ n \neq 1}}^{\infty} \left[\frac{1}{n+1} T_{n+1} - \frac{1}{n-1} T_{|n-1|} \right] + \frac{1}{2} f_1^{(1)} T_2 \right) \\ &= \frac{1}{2} \frac{d}{dx} \left(T_1 \left(2f_0^{(1)} - f_2^{(1)} \right) + \frac{T_2}{2} \left(f_1^{(1)} - f_2^{(3)} \right) + \frac{T_3}{3} \left(f_2^{(1)} - f_4^{(1)} \right) + \dots \right), \end{aligned}$$

where in the first step we have used (A.3.10) and the fact that $T'_0(x) = 0$. By equating coefficients of $T_i(x)$ we find that

$$\begin{aligned} 2f_0 &= 0, \\ 2f_1 &= 2f_0^{(1)} - f_2^{(1)}, \\ 2f_2 &= \frac{1}{2} \left(f_1^{(1)} - f_3^{(1)} \right), \\ 2f_3 &= \frac{1}{3} \left(f_2^{(1)} - f_4^{(1)} \right), \end{aligned}$$

etc

which leads to the recurrence relation

$$2jf_j = c_{j-1}f_{j-1}^{(1)} - f_{j+1}^{(1)} \quad \text{for } j \geq 1, \quad (\text{A.3.13})$$

where $c_0 = 2$ and $c_j = 1$ for $j \geq 1$

We now continue by summing both sides of (A.3.13) over j from $j - 1 = n$ to infinity, where $n \geq 0$ to find

$$\begin{aligned} 2 \sum_{j=n+1}^{\infty} jf_j &= \sum_{j=n+1}^{\infty} c_j f_{j-1}^{(1)} - f_{j+1}^{(1)} \\ &= \left(c_n f_n^{(1)} - f_{n+2}^{(1)} \right) + \left(c_{n+1} f_{n+1}^{(1)} - f_{n+3}^{(1)} \right) + \left(c_{n+2} f_{n+2}^{(1)} - f_{n+4}^{(1)} \right) + \\ &\quad + \left(c_{n+3} f_{n+3}^{(1)} - f_{n+5}^{(1)} \right) + \left(c_{n+4} f_{n+4}^{(1)} - f_{n+6}^{(1)} \right) + \dots \\ &= c_n f_n^{(1)} + f_{n+1}^{(1)} \end{aligned}$$

where we have used the fact that only $c_0 \neq 1$. This is a useful check when calculating the coefficients of the Chebyshev differentiation matrix, however it is more useful to instead consider the sum of (A.3.13) over j from $j = n + 1$ to infinity, but with the condition $j + n = \text{odd}$. From this we obtain a infinite series for $f_n^{(1)}$ alone in terms of the $f_j^{(1)}$ where

$$\begin{aligned} 2 \sum_{\substack{j=n+1 \\ j+n=\text{odd}}}^{\infty} jf_j &= \sum_{\substack{j=n+1 \\ p+n=\text{odd}}}^{\infty} c_j f_{j-1}^{(1)} - f_{j+1}^{(1)} \\ &= \left(c_n f_n^{(1)} - f_{n+2}^{(1)} \right) + \left(c_{n+2} f_{n+2}^{(1)} - f_{n+4}^{(1)} \right) + \left(c_{n+4} f_{n+4}^{(1)} - f_{n+6}^{(1)} \right) + \dots \\ &= c_n f_n^{(1)}, \end{aligned}$$

from which we find that

$$f_n^{(1)} = \frac{2}{c_n} \sum_{\substack{j=n+1 \\ j+n=\text{odd}}}^{\infty} jf_j.$$

The $f_n^{(1)}$ are therefore given by

$$\begin{aligned} f_0^{(1)} &= f_1 + 3f_3 + 5f_5 + \dots \\ f_1^{(1)} &= 4f_2 + 8f_4 + 12f_6 + \dots \\ f_2^{(1)} &= 6f_3 + 10f_5 + 14f_7 + \dots \\ f_3^{(1)} &= 8f_4 + 12f_6 + 16f_8 + \dots \end{aligned}$$

etc

and in general we have that

$$f_n^{(k)} = \frac{2}{c_n} \sum_{\substack{j=n+1 \\ j+n=\text{odd}}}^{\infty} j f_j^{(k-1)}. \quad (\text{A.3.14})$$

The Chebyshev expansion of $f^{(k)}(x)$ is now truncated at the $j = N$ term so that we may write

$$f^{(k)}(x) = \sum_{n=0}^N f_n^{(k)} T_n(x) + e_{N+1}(x)$$

where e_{N+1} is the error term. We assume that this error is small and that there exists a function $\hat{f}^{(k)}(x) = \sum_{n=0}^N \hat{f}_n T_n$ that approximates $f^{(k)}$. We then define a vector $\hat{\mathbf{f}}^{(k)} = (\hat{f}_0^{(k)}, \hat{f}_1^{(k)}, \dots, \hat{f}_N^{(k)})^T$ and then by substituting this vector into (A.3.14) we find that

$$\hat{f}_n^{(k)} = \frac{2}{c_n} \sum_{\substack{j=n+1 \\ j+n=\text{odd}}}^N j f_j^{(k-1)}.$$

We may then construct an upper triangular matrix \mathbf{D} of dimension $(N+1) \times (N+1)$ given by

$$\mathbf{D} = \begin{pmatrix} 0 & 1 & 0 & 3 & 0 & 5 & 0 & \dots \\ 0 & 0 & 4 & 0 & 8 & 0 & 12 & \dots \\ 0 & 0 & 0 & 6 & 0 & 10 & 0 & \dots \\ 0 & 0 & 0 & 0 & 8 & 0 & 12 & \dots \\ 0 & 0 & 0 & 0 & 0 & 10 & 0 & \dots \\ 0 & 0 & 0 & 0 & 0 & 0 & 12 & \dots \\ \dots & \dots \end{pmatrix},$$

where $\hat{\mathbf{f}}^{(k)} = \mathbf{D}\hat{\mathbf{f}}^{(k-1)}$.

A.3.2 Second differentiation matrix

If we define a second differentiation matrix \mathbf{D}^2 by $\hat{f}^{(k)} = \mathbf{D}^2 \hat{f}^{(k-2)}$ we expect that by matrix multiplication

$$\mathbf{D}^2 = \mathbf{D} \times \mathbf{D} = \begin{pmatrix} 0 & 0 & 4 & 0 & 32 & 0 & 108 & \dots \\ 0 & 0 & 0 & 24 & 0 & 120 & 0 & \dots \\ 0 & 0 & 0 & 0 & 48 & 0 & 192 & \dots \\ 0 & 0 & 0 & 0 & 0 & 80 & 0 & \dots \\ \dots & \dots \end{pmatrix}. \quad (\text{A.3.15})$$

We shall now verify this by starting with (A.3.14) to find

$$\begin{aligned} f_n^{(k)} &= \frac{2}{c_n} \sum_{\substack{j=n+1 \\ j+n=\text{odd}}}^{\infty} j f_j^{(k-1)} \\ &= \frac{2}{c_n} \sum_{\substack{j=n+1 \\ j+n=\text{odd}}}^{\infty} j \left(\frac{2}{c_j} \sum_{\substack{i=j+1 \\ i+j=\text{odd}}}^{\infty} i f_i^{(k-2)} \right) \\ &= \frac{4}{c_n} \sum_{\substack{j=n+1 \\ j+n=\text{odd}}}^{\infty} j \left((j+1) f_{j+1}^{(k-2)} + (j+3) f_{j+3}^{(k-2)} + (j+5) f_{j+5}^{(k-2)} + \dots \right) \\ &= \frac{4}{c_n} \sum_{\substack{j=n+2 \\ j+n=\text{even}}}^{\infty} j f_j^{(k-2)} \sum_{\substack{i=n+1 \\ i+n=\text{odd}}}^{j-1} i, \end{aligned} \quad (\text{A.3.16})$$

where we have used the fact that $c_j = 1$ for $j \geq 1$. We may rewrite the second sum as

$$\begin{aligned} \sum_{\substack{i=n+1 \\ i+n=\text{odd}}}^{j-1} i &= (n+1) + (n+3) + (n+5) + \dots + (j-1) \\ &= \sum_{k=0}^{\frac{1}{2}(j-n)-1} (n+1+2k) \\ &= (n+1) \sum_{k=0}^{\frac{1}{2}(j-n)-1} 1 + 2 \sum_{k=0}^{\frac{1}{2}(j-n)-1} k \\ &= \frac{1}{2}(j-n)(n+1) + \left(\frac{1}{2}(j-n) - 1 \right) \frac{1}{2}(j-n) \\ &= \frac{1}{2}(j-n) \left[(n+1) + \left(\frac{1}{2}(j-n) - 1 \right) \right] \\ &= \frac{1}{4}(j^2 - n^2). \end{aligned}$$

Inserting this back into (A.3.16) we find that

$$f_n^{(k)} = \frac{1}{c_n} \sum_{\substack{j=n+2 \\ j+n=\text{even}}}^{\infty} j(j^2 - n^2) f_j^{(k-2)}. \quad (\text{A.3.17})$$

From here we find that

$$f_0^{(k)} = 4f_2^{(k-2)} + 32f_4^{(k-2)} + 108f_6^{(k-2)} + \dots$$

$$f_1^{(k)} = 24f_3^{(k-2)} + 120f_5^{(k-2)} + \dots$$

$$f_2^{(k)} = 48f_4^{(k-2)} + 192f_6^{(k-2)} + \dots$$

$$f_3^{(k)} = 80f_5^{(k-2)} + \dots$$

etc

Following the truncation method used to find the first differentiation matrix we find that (A.3.17) is compatible with the matrix (A.3.15).

Using this technique it is possible to calculate higher order derivative matrices such as the \mathbf{D}^4 matrix. The coefficients of this matrix have a large growth rate, and as a consequence the method may suffer from large round off errors. The \mathbf{D}^2 and \mathbf{D} Chebyshev matrices have smaller growth rates, but require larger matrices and hence a longer computing time. A detailed discussion of the merits of each of the methods may be found in Dongarra *et al* [20].

A.4 Approximation of functions

In the previous section we assumed that we may approximate our function $f(x)$ by $\hat{f}(x)$, where

$$\hat{f}(x) = \sum_{n=0}^N \hat{f}_n T_n(x).$$

We will now show how the coefficients \hat{f}_n may be calculated using a summary of Clenshaw-Curtis quadrature, see e.g. Evans [24].

We begin by considering that, for an integer k ,

$$\begin{aligned} \sum_{n=0}^N d_n \hat{f} \left(\cos \left(\frac{n\pi}{N} \right) \right) \cos \left(\frac{kn\pi}{N} \right) &= \sum_{n=0}^N d_n \left[\sum_{m=0}^N \hat{f}_m T_m \left(\cos \left(\frac{n\pi}{N} \right) \right) \right] \cos \left(\frac{kn\pi}{N} \right) \\ &= \sum_{n=0}^N d_n \left[\sum_{m=0}^N \hat{f}_m \cos \left(\frac{mn\pi}{N} \right) \right] \cos \left(\frac{kn\pi}{N} \right). \end{aligned}$$

Using standard orthogonality results we then find that

$$\sum_{n=0}^N d_n \hat{f}\left(\cos\left(\frac{n\pi}{N}\right)\right) \cos\left(\frac{kn\pi}{N}\right) = \hat{f}_k d_k$$

where $d_k = N$ if $k = 0$ or $k = N$ and $d_k = N/2$ otherwise. This is then easily rearranged to find \hat{f}_k .

A.5 Application of the Chebyshev-tau method to a simple system

We will now demonstrate how the \mathbf{D}^2 Chebyshev-tau method may be applied to the simple case of Bénard convection in a horizontal layer with $z \in (-1, 1)$, discussed in Chapter 1. We find that the equations for both the linear instability and non-linear stability boundaries

$$\begin{aligned} W''(z) - k^2 W(z) &= Rk^2 \Theta(z), \\ \Theta''(z) - k^2 \Theta(z) &= -RW(z) \end{aligned} \tag{A.5.18}$$

with the boundary conditions

$$W(-1) = W(1) = \Theta(-1) = \Theta(1) = 0,$$

where W is the vertical velocity perturbation, Θ is the temperature, k is the wave number and R is the Rayleigh number. We consider R to be the eigenvalue of the system and aim to find R_c , the least positive eigenvalue.

We assume that W and Θ may be expanded as infinite series of Chebyshev polynomials by

$$\begin{aligned} W(z) &= \sum_{n=0}^{\infty} W_n T_n(z), & W''(z) &= \sum_{n=0}^{\infty} W_n^{(2)} T_n(z), \\ \Theta(z) &= \sum_{n=0}^{\infty} \Theta_n T_n(z), & \Theta''(z) &= \sum_{n=0}^{\infty} \Theta_n^{(2)} T_n(z), \end{aligned}$$

where W_n and Θ_n are coefficients of the expansion. These expansions are now truncated at the $n = N$ term to provide approximations for the functions, where

$$\begin{aligned} \hat{W}(z) &= \sum_{n=0}^N W_n T_n(z), & \hat{W}''(z) &= \sum_{n=0}^N W_n^{(2)} T_n(z), \\ \hat{\Theta}(z) &= \sum_{n=0}^N \Theta_n T_n(z), & \hat{\Theta}''(z) &= \sum_{n=0}^N \Theta_n^{(2)} T_n(z), \end{aligned}$$

Using these approximations equations (A.5.18) become

$$\begin{aligned}\hat{W}^{(2)}(z) - k^2\hat{W}(z) - Rk^2\hat{\Theta}(z) &= \tau_1T_{N-1} + \tau_2T_N, \\ \hat{\Theta}^{(2)}(z) - k^2\hat{\Theta}(z) + R\hat{W}(z) &= \tau_3T_{N-1} + \tau_4T_N,\end{aligned}\tag{A.5.19}$$

where τ_i are errors resulting from the approximation. The weighted inner product of (A.5.19) with T_i for $i = 0, 1, \dots, N - 2$ is taken to remove the τ_i 's and provide $2(N - 1)$ equations. We then create the vectors $\hat{\mathbf{W}} = (W_0, W_1, \dots, W_N)^T$ and $\hat{\mathbf{\Theta}} = (\Theta_0, \Theta_1, \dots, \Theta_N)^T$ and make the substitutions $\hat{\mathbf{W}}^{(2)} = \mathbf{D}^2\hat{\mathbf{W}}$ and $\hat{\mathbf{\Theta}}^{(2)} = \mathbf{D}^2\hat{\mathbf{\Theta}}$. We add two rows of zeros to the bottom of \mathbf{D}^2 to make the matrix square and may then write our system in the form

$$\begin{aligned}\mathbf{D}^2\hat{\mathbf{W}} - k^2\hat{\mathbf{W}} &= Rk^2\hat{\mathbf{\Theta}}, \\ \mathbf{D}^2\hat{\mathbf{\Theta}} - k^2\hat{\mathbf{\Theta}} &= -R\hat{\mathbf{W}}.\end{aligned}$$

The rows of zeros are overwritten by the boundary conditions, using the identities obtained in Section A.2 these are found to be

$$\sum_{n=0}^N W_n = 0, \quad \sum_{n=0}^N (-1)^n W_n = 0, \quad \sum_{n=0}^N \Theta_n = 0, \quad \sum_{n=0}^N (-1)^n \Theta_n = 0.$$

The system is now in the form of a generalised eigenvalue problem $\mathbf{A}\mathbf{p} = R\mathbf{B}\mathbf{p}$ with

$$\mathbf{A} = \begin{pmatrix} \mathbf{D}^2 - k^2\mathbf{I} & 0 \\ 1, 1, \dots, 1 & 0, 0, \dots, 0 \\ -1, 1, \dots, (-1)^N & 0, 0, \dots, 0 \\ 0 & \mathbf{D}^2 - k^2\mathbf{I} \\ 0, 0, \dots, 0 & 1, 1, \dots, 1 \\ 0, 0, \dots, 0 & -1, 1, \dots, (-1)^N \end{pmatrix},$$

$$\mathbf{B} = \begin{pmatrix} 0 & k^2\mathbf{I} \\ 0, 0, \dots, 0 & 0, 0, \dots, 0 \\ 0, 0, \dots, 0 & 0, 0, \dots, 0 \\ -\mathbf{I} & 0 \\ 0, 0, \dots, 0 & 0, 0, \dots, 0 \\ 0, 0, \dots, 0 & 0, 0, \dots, 0 \end{pmatrix},$$

where \mathbf{I} is the standard identity matrix, and

$$\mathbf{p} = (W_0, W_1, \dots, W_N, \Theta_0, \Theta_1, \dots, \Theta_N)^T. \quad (\text{A.5.20})$$

This may be solved using the QZ algorithm developed in Moler & Stewart [65].

Further examples of implementing the Chebyshev-tau method including discussions of reducing fourth order problems to second order problems may be found in Bourne [10] and Dongarra *et al* [20].

Appendix B

Derivation of no-slip and stress-free boundary conditions

In Chapters 6 and 7 we assume that the porous medium is of high porosity and satisfies the Brinkman equation. In the previous chapters we employ the Darcy model; this contains no velocity derivative terms and requires only one velocity boundary condition, namely the prescription of the normal component. In contrast the Brinkman equation contains second order velocity derivatives and we therefore require two boundary conditions for the velocity. We will here derive both stress-free and no-slip boundary conditions, although in Chapters 6 and 7 we only use the no-slip conditions as they are more physically realistic.

We begin by considering a horizontal layer of a porous medium that is saturated by an incompressible fluid and satisfies the Brinkman equation, cf. Straughan [107],

$$0 = -\frac{\mu}{K}\mathbf{v} - \rho g\mathbf{k} + \nabla \cdot (\lambda\mathbf{d} - p) \quad (\text{B.0.1})$$

in the domain Ω , with boundary Γ . Here, $\mathbf{v} = (u, v, w)$ is the pore averaged velocity of the fluid, μ , K and λ are the fluid's dynamic viscosity, the permeability of the porous medium and the Brinkman coefficient, ρ and p are density and pressure, g is gravity acting in the negative z direction, $\mathbf{k} = (0, 0, 1)$ and $\mathbf{d} = \frac{1}{2}(v_{i,j} + v_{j,i})$.

The third term in (B.0.1) is the derivative of the stress vector, t_{ij} , where

$$t_{ij} = -p\delta_{ij} + 2\lambda d_{ij}. \quad (\text{B.0.2})$$

As the fluid is incompressible we know, by conservation of mass, that

$$\frac{\partial v_i}{\partial x_i} = \frac{\partial u}{\partial x} + \frac{\partial v}{\partial y} + \frac{\partial w}{\partial z} = 0 \quad \text{in } \Omega$$

and therefore by continuity

$$\frac{\partial u}{\partial x} + \frac{\partial v}{\partial y} + \frac{\partial w}{\partial z} = 0 \quad \text{on } \Gamma, \quad (\text{B.0.3})$$

where $\Omega \in \mathbb{R}^3$ is a three-dimensional domain bounded by horizontal surfaces $z = 0, d$ which define Γ .

B.1 No-slip boundary

To derive the no-slip boundary conditions we assume that the fluid cannot cross the boundary and that there is no slip. This means that the fluid has zero velocity relative to the boundary, i.e. that $\mathbf{v} = 0$ on Γ , or

$$\begin{aligned} u &= 0, \\ v &= 0, \\ w &= 0, \quad \text{on } \Gamma. \end{aligned} \quad (\text{B.1.4})$$

By differentiating (B.1.4)₁ and (B.1.4)₂ along the x and y axes respectively we find that

$$\frac{\partial u}{\partial x} = 0 \quad \text{and} \quad \frac{\partial v}{\partial y} = 0 \quad \text{on } \Gamma.$$

After inserting these into (B.0.3) we find that the no slip boundary conditions for w are

$$\begin{aligned} w &= 0, \\ \frac{\partial w}{\partial z} &= 0 \quad \text{on } \Gamma. \end{aligned} \quad (\text{B.1.5})$$

B.2 Stress-free boundary

The stress-free boundary conditions are developed by again assuming that there is no mass flux across the boundary, $w = 0$ on Γ , but now that the stress vector is zero on the boundary, $t_i = n_j t_{ij} = 0$ on Γ .

We desire the boundary conditions for w and so set $i = 3$ in (B.0.2). Then with $j = 1$ and $j = 2$ we find

$$t_{31} = -p\delta_{31} + 2\lambda \left(\frac{\partial u}{\partial z} + \frac{\partial w}{\partial x} \right) = 0 \quad \text{on } \Gamma \quad (\text{B.2.6})$$

and

$$t_{32} = -p\delta_{32} + 2\lambda \left(\frac{\partial v}{\partial z} + \frac{\partial w}{\partial y} \right) = 0 \quad \text{on } \Gamma. \quad (\text{B.2.7})$$

As $w = 0$ on Γ , we find by differentiation that $\partial w/\partial x = 0$ and $\partial w/\partial y = 0$ on Γ . Inserting these into (B.2.6) and (B.2.7) and, using the fact that $\delta_{ij} = 0$ if $i \neq j$, we see that

$$\begin{aligned} \frac{\partial u}{\partial z} &= 0, \\ \frac{\partial v}{\partial z} &= 0. \end{aligned} \quad (\text{B.2.8})$$

We now differentiate (B.0.3) with respect to z to find

$$\frac{\partial^2 u}{\partial x \partial z} + \frac{\partial^2 v}{\partial y \partial z} + \frac{\partial^2 w}{\partial z^2} = 0 \quad \text{on } \Gamma. \quad (\text{B.2.9})$$

Finally, inserting (B.2.8) into (B.2.9) yields $\partial^2 w/\partial z^2 = 0$.

The stress-free boundary conditions for w are therefore

$$\begin{aligned} w &= 0, \\ \frac{\partial^2 w}{\partial z^2} &= 0 \quad \text{on } \Gamma. \end{aligned}$$